IMMUNOREGULATORY ACTIVITIES OF NANOPARTICLE-FORMING OLIGODEOXYNUCLEOTIDES

A THESIS SUBMITTED TO
THE DEPARTMENT OF MOLECULAR BIOLOGY AND GENETICS
AND THE INSTITUTE OF ENGINEERING AND SCIENCE OF
BILKENT UNIVERSITY
IN PARTIAL FULFILLMENT OF THE REQUIREMENTS FOR
THE DEGREE OF MASTER OF SCIENCE

BY

KUTAY KARATEPE

AUGUST 2009

I certify that I have read this thesis and that in my opinion it is fully adequate, in scope and in quality, as a thesis for the degree of Master of Science.

Assoc. Prof. Dr. İhsan Gürsel

I certify that I have read this thesis and that in my opinion it is fully adequate, in scope and in quality, as a thesis for the degree of Master of Science.

Assist. Prof. Dr. Tamer Yağcı

I certify that I have read this thesis and that in my opinion it is fully adequate, in scope and in quality, as a thesis for the degree of Master of Science.

Assoc. Prof. Dr. Cansın Saçkesen

Approved for the Institute of Engineering and Science

Director of Institute of Engineering and Science
Prof. Dr. Mehmet Baray

ABSTRACT

IMMUNOREGULATORY ACTIVITIES OF NANOPARTICLE-FORMING OLIGODEOXYNUCLEOTIDES

Kutay Karatepe
M.Sc. in Molecular Biology and Genetics
Supervisor: Assoc. Prof. Dr. İhsan Gürsel
August 2009, 99 pages

Innate immune system is activated by a wide range of microbial by products leading to an immediate immune activation primarily designed to neutralize and control the invading insult. The cells of the innate immune system also instruct the development of antigen-specific adaptive immunity. While TLR9 is triggered by bacterial DNA, extended and over-exuberant immune response poses a threat since it may exacerbate cell and tissue destruction leading to organ failure. Telomeric TTAGGG conserved motifs are previously reported to antagonize TLR mediated events. The down-regulatory effect of these motifs may help to restore the desired homeostatic balance of the immune system. While CpG ODN patterned after bacterial DNA can be harnessed in different clinical settings to provide an advantage to host to resist infectious diseases, control tumor growth or alleviate allergic symptoms, the immunosuppressive telomeric motifs could be effectively applied in controlling systemic anti-inflammatory or autoimmune related disorders.

Several challenges exist in the utilization of synthetic ODNs in the clinic. The first challenge is that conventional classes of synthetic ODNs exhibit different properties. K-type ODNs are more effective in proliferation and activation of B cells and DC. D-type ODNs are in nanoparticle forms, lead to anti-viral type I IFN production and mature monocytes into DCs. Of note, the efficacy of these synthetic ODNs is reduced under physiological conditions due to premature clearance and low levels of internalization. Moreover, D-ODNs as one of the most potent IFNα inducing TLR9 ligands possess a large-scale production problem due to 3'polyG-runs, which hamper their entry into the clinic.

We have designed a novel class of ODN, designated as ODN420, devoid of polyGs that can undergo nanoparticle formation necessary for its IFNα induction. *Ex vivo* stimulation of mouse splenocytes and *in vivo* administration of ODN420 have revealed that this ODN exhibits higher immunostimulatory potential and is more stable than most commonly used ODNs due to its nanoparticle-forming ability. Another interesting finding is that ODN420 with the natural phosphodiester (PO) backbone is at least as potent as its more stable counterpart with the modified phosphorothioate backbone. Furthermore, it combines superior properties of conventional classes of K and D-ODNs. These results have been reproduced in human peripheral blood mononuclear cells by various assays.

Next, we have analyzed whether this ODN could be utilized as a vaccine adjuvant and an anti-cancer agent with two independent experiments. Our immunization results demonstrate that ODN420 induces a higher level of Th1-mediated response than conventional ODNs and is a promising candidate as a vaccine adjuvant. This response is hampered when ODN420 is used in combination with ODN-A151. In the tumor xenograft model, ODN420 has promoted partial remission of the tumors or delayed the tumor growth. This knowledge will pave the way for more effective immunotherapeutic approaches.

Keywords: TLR, immunomodulatory DNA, nanoparticle, anti-cancer immunotherapy, vaccine

ÖZET

NANOPARÇACIK OLUŞTURAN OLİGODEOKSİNÜKLEOTİDLERİN İMMÜNMODÜLATÖR ETKİLERİ

Kutay Karatepe
Moleküler Biyoloji ve Genetik Yüksek Lisans
Danışman: Doç. Dr. İhsan Gürsel
Ağustos 2009, 99 sayfa

Doğal bağışıklık sistemi öncelikle değişik mikroorganizmaların yan ürünlerini tanıyarak mikroorganizmanın yayılmasını kontrol edecek mekanizmaları harekete geçirir. Bağışıklık sisteminin bu kolundaki hücreler aynı zamanda antijene özgü kazanılmış bağışıklık sistemi hücrelerini de uyarır.

CpG-motifleri taşıyan bakteriyel DNA TLR9 almaçı tarafından tanınır. Ancak bağışıklık sisteminin uzun ve aşırı bir şekilde aktif halde olması organ hasarına kadar gidebilecek hücre ve doku yıkımına sebep olabilir. Memeli genomundaki korunmuş TTAGGG motiflerinin TLR almaçlarının sinyal yolaklarını bastırdığı daha önceden ispat edilmiştir. Bu baskılayıcı etki bağışıklık sisteminde homeostatik dengeyi tekrar eski haline getirir. Bakteriyel DNA'lardan esinlenmiş CpG-motifleri taşıyan sentetik DNA'lar bulaşıcı hastalıklar, kanser veya alerji gibi çeşitli klinik durumlarda kullanılabilirken, bağışıklık sistemini bastırıcı DNA parçacıkları antiinflamatuar etki gerektiren sistemik otoimmün hastalıklar için çözüm vaat etmektedir.

Sentetik DNA parçacıklarının (ODN) klinikte kullanılmasının önünde çeşitli engeller bulunmaktadır. Şu ana kadar kullanılmakta olan ODN'ler ait oldukları alt sınıfa göre farklı etkilere yol açarlar. K-tipi ODN'ler B hücrelerinin ve dendritik hücrelerinin çoğalması ve aktivasyonunda daha etkilidir. D-tipi ODN'ler ise nanoparçacık yapısında olup anti-viral tip I interferon üretimini ve monositlerin dendritik hücrelere farklılaşmasını tetikler. Ayrıca bu sentetik ODN'lerin hücre içine alınmadan nükleazlar tarafından parçalanması bunların fizyolojik koşullardaki etkinliğini azatmaktadır. Son olarak, interferon-alfa üretimini tetikleyen D-tipi ODN'ler poli-G uçları içerdiğinden farkı büyüklükte parçacıklar oluşturur. Heterojen yapılar oluşturan D-tipi ODN'lerin büyük ölçekli üretimi ve klinikte kullanımı problemlidir.

Biz poli-G ucu içermeyen, interferon-alfa üretimini tetikleyebilecek homojen nanoparçacıklar oluşturan ODN420 adını verdiğimiz yeni bir sınıf ODN geliştirdik. Fare dalak hücrelerinin *ex vivo* uyarımı ve bu ODN'lerin *in vivo* enjeksiyonu sonucunda elde ettiğimiz sonuçlar ODN420'nin daha önceden kullanılan ODN'lere göre bağışıklık sistemini daha yüksek seviyede tetiklediğini ve nanoparçacık yapısından ötürü eksonükleazlara göre daha dirençli olduğunu gösterdi. Aynı zamanda bu ODN'nin doğal fosfodiester iskelet içeren halinin daha stabil olan modifiye edilmiş fosforotioat iskeletli haliyle benzer aktivite gösterdiğini bulduk. Ayrıca, bu ODN'nin K ve D-tipi ODN'lerin üstün özelliklerini taşıdığını gösterdik. Bu sonuçlar insan kanından izole edilmiş bağışıklık sistemi hücrelerinde de tekrar gösterildi.

Sonra iki farklı hayvan deneyinde bu ODN'nin aşı adjuvanı ve anti-kanser ajanı olarak potansiyelini inceledik. Aşı deneyindeki sonuçlar ODN420'nin şu anda kullanılan ODN'lere göre daha etkin bir antijene özgü Th1 etkisi yarattığını ve bu etkinin ODN-A151 tarafından azaltıldığını bulduk. Tümör modelinde ise ODN420, tümörün büyümesini tersine çevirdi veya geciktirdi. Bu bulgular bağışıklık sisteminin manipülasyonuyla daha etkin tedavi yöntemleri bulunmasına ışık tutacaktır.

Anahtar kelimeler: TLR, immunomodülatör DNA, nanoparçacık, anti-kanser terapi, aşı

ACKNOWLEDGEMENTS

I would like to express my deepest appreciation to my advisor, Assoc. Prof. Dr. İhsan Gürsel. Not only is he an excellent supervisor and scientist but he is also a great mentor. I would like to thank him for his invaluable guidance, support, teaching and patience during my studies. He has always helped me to push my limits and he is one of the few faculty members, who work in the lab on the bench next to his students.

I would like to thank my laboratory mates Fuat, Gizem, Erdem and Tamer as wells as former lab mates Hande and Rashad for their help, precious friendship and support. I have been working in Ihsan Gursel lab for almost four years now and I can only wish I work in such exceptionally friendly academic environments, where lab feels like "home".

Another exceptional person, who has contributed to this thesis and my personal development as a young scientist, is Assoc. Prof. Dr. Mayda Gursel. She has never hesitated to give me a hand whenever I had a problem.

Moreover, I would like to thank to my dearest friends Emre, Elif, Nilüfer, Gurbet, Bala, Zeynep, Sumru, Ceren, Ceyhan, Ayça and Ender for their support and for always being there whenever I needed. Also, I would like to thank my roommates, Burçin and Egemen, for reminding me that I need to eat while writing this thesis. I am also thankful to Balım for her careful review of my thesis.

I would also like to thank Burcu for her help, support and patience during animal experiments and "Abdullah Abi" for solving every technical problem I have encountered.

My sincere thanks go to MBG Family for their guidance, companionship and assistance. It has been six years since I entered this department as an undergraduate student. I have learned a lot from every member of this department.

I would also like to thank to The Scientific and Technological Research Council of Turkey (TÜBİTAK) for their financial support throughout my master studies.

Without my family, none of the exceptional things in my life would have been possible. I would like to express my love and gratitude for their everlasting support in life.

TABLE OF CONTENTS

LIST OF TABLES

LIST OF FIGURES

ABBREVIATIONS

AFM	Atomic Force Microscopy
APC	Antigen presenting cell
AVA	Anthrax vaccine adsorbed
bp	Base pairs
BCG	Bacille Calmette Guerin of Mycobacterium bovis
BCR	B-cell receptor
BSA	Bovine serum albumin
CD	Cluster of differentiation
cDNA	Complementary Deoxyribonucleic Acid
CFA	Complete Freund's adjuvant
CFSE	Carboxyfluorescein Diacetate Succinimidyl Ester
CMV	Cytomegalovirus
CpG	Unmethylated cytosine-phosphate-guaniosine motifs
CCR	Receptor specific for CC chemokine
CRP	C-reactive protein
CXCL	CXC-chemokine ligand
DC	Dendritic cell
DMEM	Dulbecco's Modified Eagle's Medium
DNA	Deoxyribonucleic acid
dsRNA	Double-stranded RNA
ELISA	Enzyme Linked-Immunosorbent Assay
ER	Endoplasmic reticulum
ERGIC	Endoplasmic reticulum-Golgi intermediate compartment
FACS	Fluorescence Activated Cell Sorting
FBS	Fetal Bovine Serum
HBV	Hepatitis-B Virus
HIV	Human Immunodeficiency Virus
HMGB	High mobility group box
Ig	Immunoglobulin

IκK	Inhibitor kappa B kinase
IL	Interleukin
iNOS	Inducible nitric oxide synthase
IFN	Interferon
IRAK	IL-1 receptor-associated kinase
IRF3	Interferon-regulatory factor 3
LBP	LPS-binding protein
LPS	Lipopolysaccharide
LRR	Leucine-rich repeats
LTA	Lipotheicoic acid
MALP	Mycoplasmal lipopeptide
MAP	Mitogen-activated protein
MAPK	Mitogen-activated protein kınase
MCMV	Murine cytomegalovirus
MCP	Monocyte chemoattractant protein
MDP	Muramyl dipeptide
MHC	Major histocompatibility complex
MIP	Macrophage inflammatory protein
mDC	Myeloid dendritic cells
MSR	Macrophage scavenger receptor
MyD-88	Myeloid differentiation primary response gene 88
NF-κB	Nuclear factor-kappa B
NK	Natural killer
NLR	Nucleotide-binding oligomerization domain like proteins or receptors
NO	Nitric oxide
NOD	Nucleotide-binding oligomerization domain
ODN	Oligodeoxynucleotide
OVA	Ovalbumin
PAMP	Pathogen associated molecular pattern
PBMC	Peripheral blood mononuclear cell

PBS	Phosphate buffered saline
PCR	Polymerase chain reaction
pDC	Plasmacytoid dendritic cells
PGN	Peptidoglycan
PHA	Phytohemagglutinin
pI:C	Polyriboinosinic polyribocytidylic acid
PNPP	Para-nitrophenyl pyro phosphate
PRR	Pattern recognition receptors
PO	Phosphodiester
PS	Phosphorothioate
RIH	RIG-like helicase
RIP	Receptor-interacting protein
RNA	Ribonucleic acid
RPMI	Roswell Park Memorial Institute
RT	Reverse transcriptase
SA-AKP	Streptavidin alkaline-phosphatase
SAP	Serum amyloid protein
SLE	Systemic lupus erythematosus
SSCL	Sterically stabilized cationic liposomes
ssRNA	Single-stranded RNA
TCR	T-cell receptor
T_H	T-helper
Th1	Cellular immunity
Th2	Humoral immunity
TIR	Toll/IL-1 receptor
TIRAP	Toll/IL1 receptor-associated protein
TLR	Toll-like receptor
TNF	Tumor necrosis factor
TRAF	TNF-associated factor
TRAM	TRIF-related adaptor molecules
TRIF	TIR domain containing adaptor inducing IFN-β

1. INTRODUCTION

1.1. Immune System

All vertebrates constantly encounter potentially harmful foreign substances, known as “antigens”. In order to protect the body from foreign antigens by distinguishing them from the organism’s normal cells and tissues, the cells of the immune system are in a state of constant surveillance.

The first line of defense is formed from the physical barriers provided by our skin and mucosa. If this primary defense of line cannot prevent pathogens from entering the organism, the innate immune system is activated by the “danger signal”. According to the “danger signal” principle, cells of the innate arm of the immune system detect a specific signature molecule commonly expressed on a large verity of pathogens. These molecules, also known as Pathogen Associated Molecular Patters (PAMP) are absent on the host’s own cells and are recognized by germline encoded Pattern Recognition Receptors (PRR) of the cells of innate immunity. Upon an encounter with the “danger signal”, these cells mount a robust increase in the production of inflammatory molecules so that the invading infectious organism can be contained and eradicated. In most cases, encounters between antigens and immune cells pass by unnoticed, due to the effective protective mechanisms provided by these primary lines of defense.

In certain cases, these lines of defense are breached and the innate immune system cannot contain the infection. This results in the activation of the adaptive immune system and the cooperation between the innate immune system and adaptive immune system allows the clearance of the pathogen. This thesis focuses on manipulation of the innate immune system for therapeutic purposes and thus, the details regarding the function of the adaptive immune system are beyond the scope of this study. Therefore, briefly, adaptive immunity is mainly characterized by clonally expanded T cells and B cells. These cells make use of highly specific antigen receptors -T cell receptor (TCR) and B cell receptor (BCR), respectively- to individual antigenic peptide molecules. Furthermore, unlike the cells of the innate immune system, they are able to retain memory for a previously encountered antigen.

Antigen presenting cells (APCs), including dendritic cells (DCs), macrophages and B cells, are found in their immature state throughout the body at the possible entry sites of pathogens such as mucosal surfaces and skin. Upon recognition of pathogens, DCs phagocytose and process the microbial antigens to their peptide content. These antigens are loaded onto major histocompatibility complex (MHC) class I and II molecules for presentation to $CD8^+$ and $CD4^+$ T cells, respectively. During this maturation process, DCs upregulate the chemokine receptor CCR7 and migrate towards the draining lymph node, the site of antigen presentation. Additionally, the expression of co-stimulatory molecules (i.e. CD80 and CD86) and cytokines required for effective activation of T cells is up-regulated and MHC molecules are translocated from the intracellular vesicles to plasma membrane. In the lymph node, upon proper antigen recognition, naïve lymphocytes become activated (Janeway, 2001; Lee and Iwasaki, 2007). When the strong and specific response generated by the adaptive immune system is dysregulated, however, it becomes responsible for allergy and autoimmunity. Adaptive immunity is also responsible for tissue rejection cases in transplantation surgeries. The major differences between innate immune system and adaptive immune system are given in Table 1.

Table 1. The cardinal features of innate and adaptive immunity. (Janeway and Medzhitov, 2002)

Property	Innate immune system	Adaptive immune system
Receptors	Fixed in genome Rearrangement is not necessary	Encoded in gene segments Rearrangement necessary
Distribution	Non-clonal All cells of a class identical	Clonal All cells of a class distinct
Recognition	Conserved molecular patterns (LPS, LTA, mannans, glycans)	Details of molecular structure (proteins, peptides, carbohydrates)
Self-Nonself discrimination	Perfect: selected over evolutionary time	Imperfect: selected in individual somatic cells
Action time	Immediate activation of effectors	Delayed activation of effectors
Response	Co-stimulatory molecules Cytokines (IL-1β, IL-6) Chemokines (IL-8)	Clonal expansion or anergy IL-2 Effector cytokines: (IL-4, IFNγ)

1.2. Innate Immune System

The innate immune system recognizes and responds to pathogens in a non-specific manner. Due to the generic mechanisms activated by innate immune system, it does not accommodate long-lasting or protective immunity to the host (Alberts, 2008). The major functions of the vertebrate innate immune system include:

- Recruitment of immune cells to sites of infection and inflammation through the production of cytokines,
- Activation of the complement cascade to identify bacteria, activate cells and to promote clearance of dead cells or antibody complexes,
- Identification and removal of foreign substances present in organs, tissues, blood and lymph by specialized white blood cells,
- Activation of the adaptive immune system through a process known as antigen presentation. (Murphy et al., 2008)

Major cell types in the innate immune system are natural killer (NK) cells, mast cells, eosinophils, basophils and phagocytes (i.e. neutrophils, monocytes/macrophages, DCs). NK cells destroy infected cells in a process known as "missing self". As MHC I molecule, located on the surface of all hosts cells, tags the cells as "self", the downregulation or absence of this molecule activates NK cells for killing. Such is the case of virally infected hosts cells that down regulate cell-surface MHC I molecules (Murphy et al., 2008). NK cells also attack tumor cells by various mechanisms (Raulet and Guerra, 2009).

Mast cells release characteristic granules rich in histamine and heparin, along with various hormonal mediators and chemokines. Histamine promotes dilation of blood vessels, a characteristic sign of inflammation, and recruits other immune cells to sites of infection. Although mast cells are primarily responsible for wound healing and defense against pathogens, they are also associated with allergy and anaphylaxis. (Murphy et al., 2008)

Basophils and eosinophils are known as granulocytes along with neutrophils due to the presence of granules in their cytoplasm. Basophils release histamine and eosinophils release a variety of toxic proteins. These products are effective in killing

pathogens. They are, however, also responsible for tissue damage during allergic reactions such as asthma (Macfarlane et al., 2000).

Phagocytes of the innate immune system include neutrophils, macrophages and DCs. Neutrophils are the most abundant type of phagocytes and comprise approximately 50-60% of total circulating leukocytes. Neutrophils are usually the first cells to arrive at the site of an infection. Their granules contain toxic substances that kill or inhibit growth of bacteria and fungi. Upon binding of bacterial molecules to receptors on neutrophils, neutrophils activate a "respiratory burst" causing the generation of reactive oxygen species such as hydrogen peroxide (H_2O_2). Macrophages are another type of cell that utilizes a similar "respiratory burst". They are the most efficient phagocytes and can phagocytose a substantial number of pathogens. The precursors of these tissue-resident macrophages are blood circulating monocytes. As mentioned previously, DCs are the major cell type responsible for antigen presentation. Hematopoietic bone marrow progenitor cells transform into immature dendritic cells characterized by high endocytic activity and low T-cell activation potential. Immature DCs circulate throughout the body and upon pathogen recognition, they phagocytose pathogens, process antigenic molecules into peptides and present them to T cells, thereby activating adaptive immune system (Banchereau and Steinman, 1998). In addition to their antigen presentation function, macrophages and DCs also induce a number of cytokines and chemokines, which allow recruitment of other immune cells to sites of infection, during the onset of innate immune activation. The properties of major cytokines and chemokines are given in Table 2 and Table 3.

Table 2. Cytokines affect behavior of target cells. (Janeway, 2005; Murphy et al., 2008)

Cytokines	Produced by	Function
IL-1β	Mf, keratinocytes	Fever, induction of acute-phase protein secretion, T cell and Mf activation
TNFα	Mf, DC, NK and T cells	Local inflammation and endothelial activation
IL6	Mf, DC	Fever, T and B cell growth and differentiation
IL-12	Mf, DC	Activation of NK cells, induction of CD4 T-cells to differentiate into T_H1
IL-15	Many non-T cells	CD8 memory T cell survival, stimulation of NK and T cell growth
IL-18	Activated Mf	Induction of IFNγ secretion via NK and T cells, favors T_H1 immunity
IFNα	DC	Anti-viral immunity, induction of MHC I expression
IFNγ	T cells, NK cells	Suppression of T_H2 immunity, Mf activation, increased expression of antigen processing components

Mf: Macrophages, T: T cells, DC: Dendritic cells, NK: Natural Killer cells

Table 3. Chemokines recruit target cells to sites of infection. (Janeway, 2005; Murphy et al., 2008)

Chemokines	Produced by	Attracted cells	Major effect
CXCL8 (IL-8)	Monocytes, Mf, DC	Neutrophils, naïve T cells	Mobilization, activation and degranulation of neutrophils
CCL3 (MIP-1α)	Monocytes, T, Mast cells, fibroblasts	Monocyte,NK, T, basophil, DC	Promotes T_H1, antiviral defense, competes with HIV-1
CCL4 (MIP-1β)	Monocytes, Mf, Neutrophils, endothelium	Monocyte, NK, T, DC	Competes with HIV-1
CCL2 (MCP-1)	Monocyte, Mf, fibroblast, keratinocyte	Monocyte, NK, T, basophil, DC	Promotes T_H2, activate Mf, histamine release from basophils
CXCL10 (IP10)	T, fibroblast, endothelial, monocyte, keratinocyte	Resting T cells, NK, monocytes	Promotes T_H1, antiangiogenic, immunostimulant

1.2.1. Pathogen Recognition Receptors (PRR)

While T cell and B cell receptors are formed by rearrangements in gene segments and can recognize an infinite variety of antigens, the receptors of innate immune system are germline-encoded pattern recognition receptors (PRR). These receptors recognize certain signature patterns on pathogens termed as pathogen-associated molecular patterns (PAMP). These include viral nucleic acids, components of bacterial and fungal cell walls and many more. For a long time, innate immunity has been considered as a non-specific immune response characterized by engulfment and digestion of microorganisms and foreign substances by phagocytic cells (Akira et al., 2001). The discovery of PRRs, the specificity of response generated by these cells and the notion that their ligands, PAMPs, can be utilized as adjuvants has fueled interest in the previously underestimated field of innate immunity.

PRRs share common properties among themselves. First, PAMPs recognized by PRRs are essential for the survival of the microorangism and are therefore difficult for the microorganism to modify. Second, PRRs are expressed constitutively in the host and detect the pathogens regardless of their life-cycle stage. Third, PRRs are germline encoded, nonclonal and expressed on all members of a given cell type. Furthermore, cells carrying these receptors lack immunologic memory. Finally, the basic components of innate immunity are highly conserved among species, from plants and fruit flies to mammals (Akira et al., 2006).

There are different PRR families and these are outlined in Table 4. Mannan-binding lectin (MBL), C-reactive protein (CRP), and serum amyloid protein (SAP) are secreted PRRs produced by the liver during the acute phase response at the early stages of infection. While CRP and SAP are members of the pentraxin family, MBL is a member of the collectin family. CRP and SAP bind to phosphorylcholine on bacterial surfaces and opsonize microorganisms leading to their phagocytosis. MBL binds specifically to terminal mannose residues, which are abundant on the surface of many microorganisms, it initate the lectin pathway of complement by cleaving C2 and C4 proteins.

In addition to these extracellular PRRs, many PRRs reside on the plasma membrane. One family of PRRs, which is located on the plasma membrane, is scavenger

receptors. Macrophage scavenger receptor (MSR) has a broad specificity to a variety of ligands, such as double-stranded RNA (dsRNA), LPS, and LTA. Another scavenger receptor expressed on macrophages is MARCO, which binds to bacterial cell walls and LPS, and also mediates phagocytosis of bacterial pathogens (Janeway and Medzhitov, 2002).

NOD-like receptors (NLRs) and RIG-like helicases (RIHs) are two major families of PRRs found in the cytoplasm. NOD1 and NOD2 detect bacterial peptidoglycan, drive activation of mitogen-activated protein kinases (MAPKs) and NF-kB. The minimal structural requirement for activation of NOD2 is muramyl dipeptide, a structure present in both Gram-positive and Gram-negative bacteria. NALP proteins such as NALP1, NALP2 and NALP3 also belong to NLR family of PRRs. They have a cruicial role in activation of proinflammatory caspases through formation of a complex called the inflammasome. Retinoic-acid-inducible gene I (RIG-I) and melanoma-differentiation-associated gene 5 (MDA5) are two members of RIH family. They are activated by dsRNA during a viral infection and trigger the activation of NF-kB and IRF3/7, which cooperate in induction of antiviral type I IFNs (Meylan et al., 2006).

Table 4. PRR families in mammalian cells and their associated ligands. (Lee and Kim, 2007)

Family	Member (major ligand)
TLRs	TLR1 (triacyl lipopeptides), TLR2 (LTA[a], zymosan, lipopeptides), TLR3 (dsRNA, polyI:C), TLR4 (LPS), TLR5 (flagellin), TLR6 (diacyl lipopeptides), TLR7 (ssRNA, R848), TLR8 (ssRNA, R848), TLR9 (CpG-DNA), TLR11 (profillin-like molecule)
C-type lectin receptors	Mannose receptor (ligands bearing mannose, fucose, or N-acetyl glucosamine), DC-SIGN (ICAM-2/3, HIV gp120, *Mycobacterium tuberculosis* ManLAM), Dectin-1 (zymosan, β-glucans from fungi)
Scavenger receptors	Scavenger receptor A (modified LDL, apoptotic cells), CD36 (oxidized LDL, apoptotic cells), MARCO (modified LDL)
Complement receptors	Integrins [CR3 (iC3b, β-glucan, fibrinogen), CR4 (iC3b, β-glucan, fibrinogen)], gC1qR (C1q), C5aR (C5a)
IFN-inducible proteins	PKR (dsRNA), OASs (dsRNA)
CARD helicases	RIG-I (uncapped 5'-triphosphate RNA), MDA5 (polyI:C, dsRNA from EMCV)
NOD-like receptors	NOD1 (iE-DAP), NOD2 (MDP), 14 NALPs [NALP1 (cell rupture), NALP1b (anthrax lethal toxin), NALP3 (bacterial mRNA, R848, extracellular ATP, uric acid crystals)], IPAF (*Salmonella* flagellin), NAIP5 (*Legionella* flagellin)
Complement	C3 (carbohydrates and proteins on microbial surfaces), C1q (immune complexes, apoptotic cells)
Pentraxins	SAP (LPS, C1q, apoptotic cells), CRP (PC, C1q, apoptotic cells), PTX3 (galactomannan, C1q, zymosan, apoptotic cells)
Collectins	MBL (LPS, LTA, HIV gp120)

1.2.1.1. Toll-like Receptors (TLRs)

The main focus in this study is toll-like receptors (TLR), which are the most extensively studied and characterized family of PRRs. Mammalian TLRs are homologous to the *Drosophila* Toll receptor (Medzhitov et al., 1997). These evolutionarily conserved receptors belong to the IL-1R superfamily, characterized by an extracellular leucine-rich repeats (LRR) and an intracellular Toll/IL-1 receptor like (TIR) domain (Medzhitov, 2001). Members of TLR family differ from each other in their ligand specificities, expression patterns, and the downstream signaling pathways.

TLRs in the innate immune system serve an essential role not only in recognition of pathogen, but also in directing the course and type of innate immune response generated following an exposure to foreign antigen (Takeda et al., 2003). TLRs have been demonstrated to have a wide array of functions including initiation of proinflammatory responses and antiviral responses, up-regulation of costimulatory molecules on antigen presenting cells (APC), release of chemokines to induce migration of responder cells to the site of infection and cross-priming of T cells by DCs (Takeda and Akira, 2005). TLRs are responsible for the adjuvant activity that is required to initiate immune responses both in natural infection and in vaccine responses (Lien and Golenbock, 2003). TLRs also have an essential role in shaping adaptive immune responses to pathogen. The signals for activation of adaptive immunity are mostly provided by DCs. TLR-mediated recognition of pathogens by DCs induces the expression of costimulatory molecules such as CD80/CD86 required for the effective activation of T cells and production of inflammatory cytokines such as IL-12 (Akira et al., 2001). DC subsets can induce cellular immunity (Th1) and humoral immunity (Th2). Activation of TLR9 in DCs induces production of IL-12, thereby changing the helper T cell (Th) differentiation toward Th1 type. LPS stimulates TLR4 signaling pathway and allows DCs to support both Th1 and Th2 cell differentiation (Kaisho et al., 2002). Additionally, some pathogen-derived adjuvants such as Complete Freund's Adjuvant (CFA), Bacille Calmette Guerin of Mycobacterium bovis (BCG) are recognized by TLRs; TLR9 and TLR2, TLR4 respectively, which may explain the involvement of TLRs in adaptive immunity (Akira et al., 2003).

Human TLR4 is the first characterized mammalian Toll-like receptor. It is expressed in a variety of cell types, most predominantly in the cells of the immune system, including macrophages and DCs (Medzhitov et al., 1997). TLRs can be classified according to their localization in the cells. While TLR1, 2, 4, 5, 6 and 10 are localized on the plasma membrane and recognize mainly extracellular bacterial products, TLR3, 7, 8 and 9 are located in the intracellular endosomal and/or ER compartments and recognize viral or bacterial nucleic acids (Iwasaki and Medzhitov, 2004; Latz et al., 2004). Subcellular localizations and ligands of TLRs are given in detail in Figure 1.

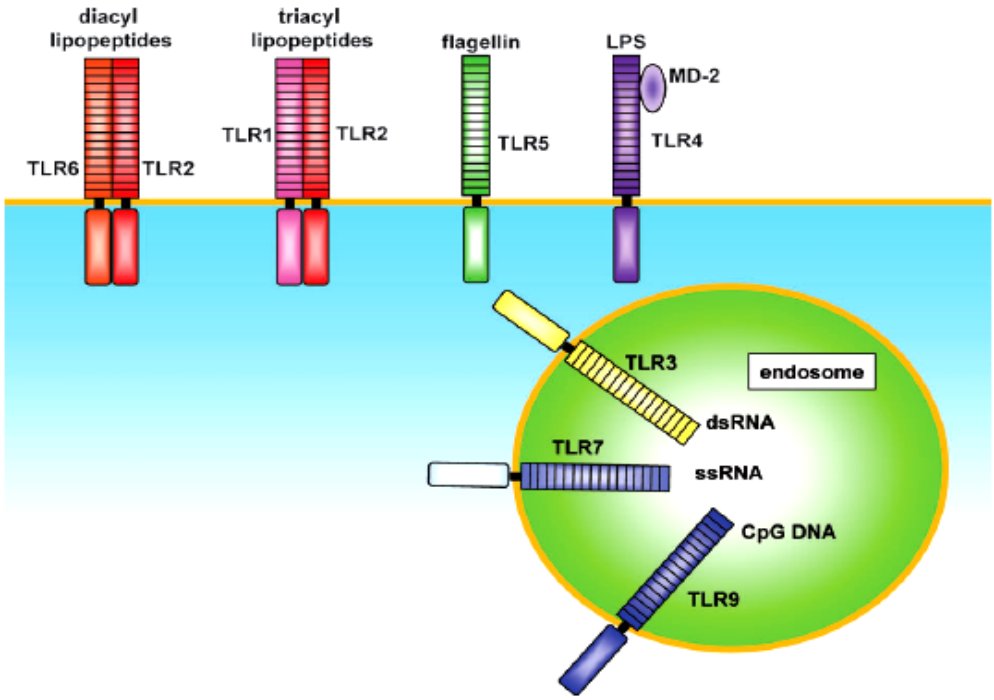

Figure 1. TLR family members and their subcellular localizations (Takeda and Akira, 2005).

1.2.1.1.1. TLR 1, TLR2 and TLR6

TLR2 responds to various microbial products, including lipoproteins, Gram-positive bacterial PGN and LTA, lipoarabinomannan from mycobacteria, glycosylphosphatidylinositol anchors from a protozoan Trypanosoma cruzi, a phenol-soluble modulin from Staphylococcus epidermis, zymosan from fungi (Takeda and Akira, 2005). The wide spectrum recognition of microbial components by TLR2 is due to its

ability to form heterodimers with other TLRs such as TLR1 and TLR6. Inflammatory response to mycoplasma-derived triacyl and diacyl lipopeptides is deficient in TLR6 and TLR1 deficient mice, respectively. This proves that TLR1 and TLR6 functionally associate with TLR2 to discriminate between diacyl or triacyl lipopeptides. TLR2 has also shown to functionally collaborate with other distinct types of receptors such as dectin-1, a lectin family receptor for the fungal cell wall component β-glucan (Sato et al., 2000).

1.2.1.1.2. TLR3

TLR3 is located in endosomal compartments. It recognizes double-stranded RNA, which is produced by most viruses during their replication. This discovery led to the notion that TLRs may have a key role in the host defense against viruses by enhancing NF-kB and interferon (IFN)-regulatory factor 3 (IRF3) pathways (Alexopoulou et al., 2001). Upon dsRNA recognition, type I interferons (IFNα/β), which exert anti-viral and immunostimulatory activities, are induced. NK cells are the major players in anti-viral immunity and express TLR3. They are activated directly in response to synthetic dsRNA, polyriboinosinic polyribocytidylic acid (poly I:C) (Schmidt et al., 2004). Also, myeloid DCs produce IL-12 and IFN-β upon TLR3 activation (Ito et al., 2002b).

1.2.1.1.3. TLR4

As mentioned above TLR4 is the first identified mammalian Toll. This extracellular TLR is expressed in variety of cell types, most predominantly in macrophages and DCs (Medzhitov et al., 1997). The major ligand of TLR4 is lipopolysaccharide (LPS), a major component of the outer membrane of Gram-negative bacteria (Hoshino et al., 1999). Recognition of LPS by TLR4 is complex and requires several accessory molecules. LPS is first bound to a serum protein, LPS-binding protein (LBP), which functions by transferring LPS monomers to CD14 (Wright et al., 1989). Another component of the LPS receptor complex is MD-2 (Shimazu et al., 1999). Although its precise function is not known, MD-2 is also required for LPS recognition (Schromm et al., 2001).

1.2.1.1.4. TLR5

TLR5 recognizes flagellin, the protein subunits that make up bacterial flagella. TLR5 is expressed on the basolateral side of the intestinal epithelium, where it can sense flagellin from pathogenic bacteria, such as Salmonella. Flagellin induces lung epithelial cells to induce inflammatory cytokine production (Hawn et al., 2003).

1.2.1.1.5. TLR7 and TLR8

Both TLR 7 and 8 are structurally highly conserved proteins. Although both of these TLRs are expressed in mice, mouse TLR8 appears to be nonfunctional (Akira et al., 2006). It has been revealed that murine and human TLR7, but not murine TLR8, recognizes synthetic compounds, imidazoquinolines (R848), which are clinically used for treatment of genital warts associated with viral infection (Hemmi et al., 2002). Murine TLR7 and human TLR8 recognize guanosine or uridine-rich single-stranded RNA (ssRNA) from viruses such as HIV, vesicular stomatitis virus and influenza virus. ssRNA is abundant in host but the endosomal localization of TLR7 and TLR8 prevent access of these receptors to self ssRNA (Lund et al., 2004).

1.2.1.1.6. TLR9

One of the most known TLRs, TLR9 is the receptor for bacterial genomic DNA, which is rich in unmethylated CpG motifs. TLR9 is primarily expressed in B cells, DCs and macrophages although its expression pattern differs between mice and humans. Human cells have a more restricted expression of TLR9 (Table 5). A single nucleotide substitution or methylation of a cytosine residue within the CpG motif completely abrogates the immunostimulatory property of bacterial DNA (Krieg et al., 1995). There are different types of synthetic CpG-DNA and their therapeutic potentials are discussed in detail in subsequent sections.

In addition to recognition of bacterial and viral CpG DNA, TLR9 is presumably involved in pathogenesis of autoimmune disorders. The immunoglobulin-G_{2a} (IgG_{2a}) is bound and internalized by the B cell receptor, and the chromatin, including hypomethylated CpG motifs, is then able to engage TLR9, thereby inducing rheumatoid

factor. Chloroquine, a chemical which blocks TLR9 dependent signaling, is widely used for treatment of autoimmune diseases such rheumatoid arthritis and systemic lupus erythematosus (SLE) (Boule et al., 2004). Proposed role of TLR9 in SLE is illustrated in Figure 2.

Table 5. TLR9 expression varies among mice and human (Krieg, 2006).

	B-cells	**pDC**	**mDC**	**monocyte/Mf**
Human	yes	yes	no	no
Mouse	yes	yes	yes	yes

pDC: plasmacytoid DC; mDC: myeloid DC; Mf: macrophage

1.2.1.2. TLR Signaling Pathways

Activation of TLRs by PAMPs leads to induction of various genes involved in host defense. These induced genes include inflammatory cytokines, chemokines, MHC molecules and co-stimulatory molecules. Mammalian TLRs also induce multiple effector molecules such as inducible nitric oxide synthase (iNOS) and antimicrobial peptides, which can directly eliminate microbial pathogens. Although both TLRs and IL-1Rs rely on TIR domains to activate NF-κB and MAP kinases and share some target genes, a growing body of evidence points to several differences in signaling pathways activated by individual TLRs. All TLR family members use a common MyD88 adaptor, except for TLR3, which recruits TRIF. TLR4 is the only family member that activates both MYD88-dependent and TRIF-dependent signal transduction pathways (Barton and Kagan, 2009).

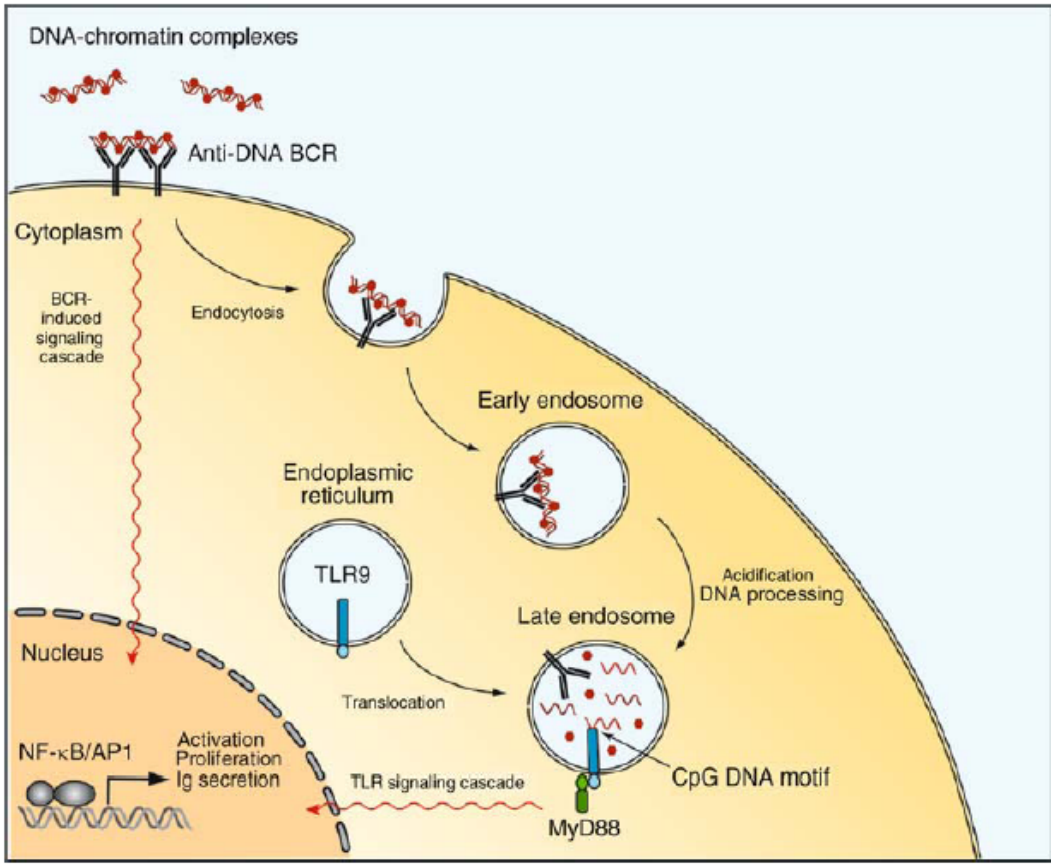

Figure 2. Self-DNA containing immune complexes is recognized by TLR9 and lead to the autoimmune disorder, SLE. (Rahman and Eisenberg, 2006)

.

Furthermore, activation of specific TLRs leads to slightly different patterns of gene expression profiles. While activation of TLR3 and TLR4 signaling pathways results in induction of type I IFNs (Doyle et al., 2002), TLR2- and TLR5-mediated pathways do not induce these anti-viral IFNs (Hoshino et al., 2002). TLR7, TLR8 and TLR9 signaling pathways also lead to induction of type I IFNs in a different manner (Ito et al., 2002a).

1.2.1.2.1. MyD88-Dependent Pathway

MyD88, comprised of a C-terminal TIR domain and an N-terminal death domain, associates with the TIR domain of TLRs. After stimulation, MyD88 recruits IL-1 receptor-associated kinase-4 (IRAK-4) to TLRs through the interaction of the death domains of both molecules. Following this, it facilitates IRAK-4-mediated phosphorylation of IRAK-1. Activated IRAK-1 then associates with TRAF6, leading to the activation of two distinct signaling pathways. One pathway leads to activation of AP-

1 transcription factors through activation of MAP kinases. Another pathway activates the TAK1/TAB complex, which enhances activity of the Inhibitor kappa B kinase (IkK) complex. Once activated, the IkK complex induces phosphorylation and subsequent degradation of IkB, which leads to nuclear translocation of transcription factor NF-kB (Klinman, 2004; Takeda and Akira, 2004). MyD88-deficient mice do not show production of inflammatory cytokines such as TNF-α and IL-12p40 in response to any TLR ligand (Takeuchi et al., 2000). This once again proves that MyD88 is essential for inflammatory cytokine production through all TLRs. MyD88-deficient macrophages, show impaired inflammatory cytokine production in response to TLR4 and TLR2 ligands in contrast to TLR3, TLR5, TLR7 and TLR9 ligands (Yamamoto et al., 2002a).

1.2.1.2.2. MyD88-Independent/TRIF-Dependent Pathway

While TLR4 ligand-induced production of inflammatory cytokines is not observed in MyD88-knock-out macrophages, delayed NF-κB expression is observed. This shows that although TLR4 signaling relies on MyD88-dependent pathways, a MyD88-independent component exists in TLR4 signaling. TLR4-induced activation of IRF-3 leads to production of IFN-β, which in turn activates Stat1 and induces several IFN-inducible genes, like TLR3 (Alexopoulou et al., 2001; Yoneyama et al., 1998). TRIF-deficient mice exhibit impaired expression of IFN-β and IFN-inducible genes in response to TLR3 and TLR4 ligands (Yamamoto et al., 2002b). Studies with other TRIF-related adaptor molecules TRAM/TICAM-2 showed that TRAM is involved in TLR4-mediated, but not TLR3-mediated, activation of IRF-3 and induction of IFN-β and IFN-inducible genes (Yamamoto et al., 2003). Key molecules that mediate IRF-3 activation have been revealed to be non-canonical IkKs, Tank binding kinase-1 (TBK1) and IkKi/IkKe (Fitzgerald et al., 2003). It has been recently reported that complete MyD88 and TRIF expression is required for the effective cooperation, resulting in the induction of IL-12, IL6, and IL-23 but not of TNF-α and IP-10 upon MyD88- and TRIF-dependent TLR stimulation. Downstream of MyD88, TRIF and IRF5 are identified as essential transcription factors for the synergism of IL6, IL-12, and IL-23 gene expression (Ouyang et al., 2007). TRAF6 associates with the N terminal portion of TRIF and the C-terminal portion of TRIF associates with receptor-interacting protein-1 (RIP1), thereby leading to NF-kB activation (Gohda et al., 2004; Meylan et al., 2004).

1.3. A Deeper Insight into Immunostimulatory DNA Particles and TLR9 Activation

TLR9 is the only known member of TLR family that can recognize specific DNA motifs. Five years after the identification of CpG motifs, Hemmi et. al. reported that TLR9 is responsible for the recognition of CpG DNA in mice. They showed that splenocytes, lymph node cells, dendritic cells, and macrophages from TLR9-deficient mice do not respond to CpG motif expressing oligodeoxynucleotides (CpG ODN), evident from the loss of pro-inflammatory cytokine production or cell surface maturation marker downregulation. Moreover, these mice are resistant to harmful side effects of CpG ODN (Hemmi et al., 2000). It has later been shown that human TLR9 is also prerequisite for bacterial DNA/CpG DNA-dependent immunostimulation in both primary cells and TLR9-transfected cell lines (Bauer et al., 2001; Takeshita et al., 2001). Later findings challenged the idea that recognition of foreign DNA is restricted to CpG motifs. Non-CpG phosphodiester ODNs (PO-ODNs), which are delivered into endosomes via DOTAP complexation, and self chromatin DNA/IgG autoantibody complexes have been shown to be recognized via TLR9 (Boule et al., 2004; Yasuda et al., 2006). Recently, TLR9 has been shown to recognize 2'-deoxyribose sugar backbone (base-free) of phophodiester DNA -but not phosphorothioate (PS) modified 2'-deoxyribose, PS or PO modified 2'-ribose backbones- and activate cytokine secretion. Immunostimulatory activity and TLR9 affinity is increased further, when bases and CpG motifs are added to this backbone. PolyG addition (24 extra guanosines at 3'end) or DOTAP complexations are used here to target sugar backbone or PO-ODN into endosomes. PS-modified sugar backbones exhibit higher affinity to TLR9 and TLR7 than PO-modified counterparts both *in vitro and in vivo* (Haas et al., 2008).

In unstimulated cells, TLR9 is localized to endoplasmic reticulum, which is transported to early endosomes and then lysosomes upon CpG stimulation (Latz et al., 2004). It has been suggested that the transfer from ER to endosomes is mediated by UNC93B1 protein (Kim et al., 2008). Two independent studies reveal that the ER to endosome docking is mediated by endosomal localization motifs present on TLR9 which are on opposite locations on ER and endosomes (Barton et al., 2006; Leifer et al., 2006). There exist other controversial data on TLR9 translocation from ER to endosomes. Latz

et al. reported that this translocation is mediated by non-secretory pathway (Latz et al., 2004), while Chockalingam et al. reported that secretory pathway is involved and TLR9 passes through Golgi on the way to endosomes (Chockalingam et al., 2009). In endosomes, TLR9 exists as homodimers and the ligand unbound form represents the inactive conformation of the receptor. Upon ligand binding, seperate TIR domains gets closer and recruit MyD88 for initiation of signaling cascade (Latz et al., 2007). Fitting with this idea, it has been shown that only aggregated, multimeric forms of ODNs are stimulatory. As concentration of multimeric forms increases in ODN solution, the immunostimulatory activity is enhanced (Wu et al., 2004).

Interaction of TLR9 with bacterial/viral DNA in endosomes of wild-type cells seems to prevent recognition of self-DNA. Expression of TLR9 on the plasma membrane by generating a chimeric protein (TLR9/TLR4) makes mammalian DNA stimulatory. Viral DNA becomes inactive in this case possibly due to the coat around the DNA. Mammalian DNA with phosphodiester backbone exhibits parallelism with PO-ODNs, which become more stimulatory against surface expressed TLR9, in sensitivity to DNase (Barton et al., 2006). This finding challenges previous notion that CpG motifs are critical factors in of self/non-self discrimination. Recently, TLR9 has been shown to become activated after proteolytic cleavage of carboxy terminal fragment at endosomes via cathepsin proteases (Ewald et al., 2008; Park et al., 2008). This explains the previous observation that TLR9 signaling is blocked by inhibition of endosomal acidification (Ahmad-Nejad et al., 2002). This acidification is required for optimal activity of TLR9-cleaving proteases. These recent findings strengthen the hypothesis that self/non-self discrimination is mainly achieved by TLR9 compartmentalization as it is functional in endosomes.

1.3.1. Accessory Molecules Involved in TLR9 Activation

LL37: LL37 is an endogenous antimicrobial peptide expressed highly in psoriatic skin. During physical injury, disease condition worsens, self-DNA is released and pDC activation occurs. LL37 forms complexes with self-DNA. These complexes are delivered to early endosomes in pDC and IFNα is induced. Otherwise, self-DNA is inactive since it cannot colocalize with TLR9 in endosomes (Lande et al., 2007).

HMBG1 and RAGE: HMBG1 (High-mobility group box 1) is another DNA-binding protein. It is involved in bending of double-helix to increase affinity of DNA to transcription factors. HMGB1 interacts and preassociates with TLR9 in the endoplasmic reticulum-Golgi intermediate compartment (ERGIC), and hastens TLR9's redistribution to early endosomes in response to CpG DNA (Ivanov et al., 2007). Recent work shows that HMBG1 forms complexes with A/D-type ODN (but not B/K-type ODN), thereby increasing B cell activating and IFNα-inducing potential of pDC. This stimulation also depends on the interaction of RAGE (receptor for advanced glycation end-products), a multi-ligand receptor of immunoglobulin superfamily, with HMBG1-TLR9 complex. The critical roles of HMBG1 and RAGE in IFNα induction by DNA-containing immune complexes have also been shown in lupus patients (Tian et al., 2007).

Cathepsin-K: Cathepsin-K is an osteoclast-specific protease which is involved in degradation of bone matrices. It is seen as a therapeutic target to treat diseases, such as osteoporosis and autoimmune arthritis, in which osteoclast activity abnormally increases. Recently, specific inhibition of Cathepsin-K by pharmacological inhibitor in dendritic cells, has been shown to reduce TLR9-mediated, but not TLR2 or TLR4-mediated, production of IL-12, IL-23 and upregulation of maturation markers such as CD40, CD80 and CD86 in a dose-dependent manner. Moreover, cathepsin $K^{-/-}$ mice are found to be not responsive to stimulation with CpG ODNs (Asagiri et al., 2008).

UNC93B1: Missense mutation in *Unc93b1* gene is called 3d mutation because of the impaired signalling via TLR3, 7 and 9. Mice with 3d mutation show increased susceptibility to murine cytomegalovirus (MCMV) infection (Tabeta et al., 2006). UNC93B1 functions in delivery of TLRs from endoplasmic reticulum to endosomes. Mice with artificially expressed TLR9 on plasma membrane are not affected from 3d mutation and can respond to CpG motifs (Kim et al., 2008).

1.3.2. Different Classes of Synthetic CpG-ODNs

Oligodeoxynucleotide (ODN) sequences designed for antisense therapy have first been shown to be immunostimulatory in 1992 (Yamamoto et al., 1992). Some antisense

ODNs containing palindromic sequences have induced strong type I and/or type II IFN production and led to profound interferon mediated NK cell killing activity. Later, this activation has been attributed to the presence of unmethylated CpG motifs, which are nearly 20 times more frequently expressed in microbial DNA than mammalian DNA (Krieg et al., 1995). CpG motif expressing ODNs stimulate murine B-cell proliferation and IgM production significantly. Meanwhile, control ODNs in which cytosines are methylated or CpG is inverted to GpC does not exhibit any stimulatory effects. Minimum ODN length for stimulatory effect has been shown 8 bp. CpG ODNs stimulate BALB/c mice spleen cells to produce IL6, IL-12 and IFNγ. If a sequence contains multiple CpG motifs over a single strand, the stimulatory activity is enhanced (Klinman et al., 1996). CpG ODN also stimulates human PBMC to release TNFα, IL12, IL6 and upregulate monocyte and B-cell activation markers (Bauer et al., 1999). They induce polyclonal activation and differentiation of memory B cells into plasma cells without B-cell receptor signaling or T cell help. This makes CpG ODNs candidates as powerful adjuvant for induction of humoral immunity. However, BCR signaling is critical for activation of naive B cells (Bernasconi et al., 2002). Overall response to CpG ODNs is Th1-polarized. The immunization of mice with CpG ODN plus an antigen induces Th1 associated IFNγ, IL-12 and antigen specific IgG2a and suppresses Th2 associated IL-5 production (Chu et al., 1997).

Central hexameric sequence is Pu-Pu-C-G-Py-Py for mice and Pu-Py-C-G-Pu-Py for humans in optimal sequences. Substituting a Purine (Pu) for a Pyramidine (Py), or vice versa, significantly reduces or eliminates ODN activity (Krieg et al., 1995; Verthelyi et al., 2001). CpG ODNs designed to date can be grouped into i) A/D-type CpG, ii) B/K-type CpG, and iii) C-type CpG. Additional less well-characterized sequences, which do not fit in any of these three groups, are also covered below.

1.3.2.1. A/D-type CpG ODNs

This group of CpG ODNs is named as A-ODN by some groups and D-ODN by others. It will be referred to as D-ODN hereafter. D-ODNs contain a mixed backbone of phosphodiester and phosphorothiote linkages. Generally, a single CpG motif is present in the middle of a palindromic sequence with phosphodiester (PO) backbone. The

palindromic sequence is capped by G-runs at both ends. The linkage between the G pairs at both ends have phosphorothioate (PS) backbones, which confer increased resistance to nucleases. Minimum length of an active D-ODN is 18 bp. Representative sequences are given below:

D19:	5`-GGtgcatcgatgcagGGGGG-3`
D29:	5`-GGtgcacggtgcagGGGG-3`
D35:	5`-GGtgcatcgatgcaggggGG-3`
D no poly(G):	5`-GGtgcttcgatgcaaaaaAA-3`
D3CG:	5`-GGtcgatcgatcgaggggGG-3`
ODN 2216:	5'-GGgggacgatcgtcggggGG-3'

Please note that lowercase letters indicate phophodiester (PO) linkages between bases, whereas uppercase letters indicate phosphorothioate (PS) linkages between bases. Underlined bases represent unmethylated CpG dinucleotides.

Any inversion, replacement, or methylation of the CpG abolishes the stimulatory activity completely. The polyG ends and central palindromic region of the ODN also contribute to D-type activity significantly (Verthelyi et al., 2001). D-ODN has a high tendency to spontaneously assemble into higher-order structures, heterogenous particles mainly composed of globular (~50nm size) and linear structures (~100nm size), under physiological concentration. This structure formation is dependent on the presence of poly(G) motifs and on the palindromic region (Costa et al., 2004). Kerkmann suggests that monomeric D-ODN forms a duplex via Watson-Crick base pairing from its palindromic regions. Moreover, the poly(G) ends, of which there are four, of the two duplexes are linked together via a non Watson-Crick base pairing. This is an interaction established between guanosines and is known as "Hoogstein Base Pairing". The interaction between the planar four Gs is called "G-tetrads" and multiple forms of these G-tetrads are named as G-quadruplexes. The formation of this structure is given in detail in Figure 3. Exposure of G-tetrads to high temperature leads back to formation of their monomeric molecules (Kerkmann et al., 2005).

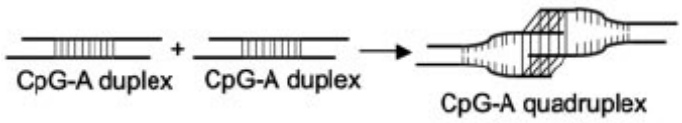

Figure 3. G-tetrad links four D-ODN strands for higher-order structure formation (Kerkmann et al., 2005).

D-ODN induces high amounts of IFN-α/β directly from pDCs and IFN-γ from PBMCs. Maximum activity is reached at 3 μM. They also indirectly induce IFN-γ, IP-10 from PBMC and NK cell activation strongly. NK cell-mediated IFN-γ production by D-ODN is IFNα/β–dependent, and IL12-independent (Krug et al., 2001; Verthelyi et al., 2001). Moderate levels of costimulatory molecules CD80, CD86 and HLA-DR on pDC and B cells are induced. This induction is lower than that of K/B type CpG ODNs (Krug et al., 2001). D-ODN stimulates monocytes to mature into $CD83^{+}/CD86^{+}$ DCs in an IFN-α-dependent manner (Gursel et al., 2002b). NK cell-mediated cytolytic activity, which is a very critical part of innate immunity against intracellular pathogens, also increases considerably (Krug et al., 2001). D-type ODN stimulates mouse splenocytes to produce moderate IL6, IL-12 and high levels of IFNγ. Interestingly, IFNγ induction by D-type ODN reaches maximal activity at 1μg/ml and this activity is reduced at higher concentrations (Vollmer et al., 2004). The therapeutic potentials of D-type ODNs are hampered by the fact that G-rich containing sequences are problematic during synthesis. PolyG-based ODNs lack pharmaceutical attributes due to unpredictable secondary structure formation depending on the experimental conditions and nonsequence-specific protein binding (Wang et al., 2009).

1.3.2.2. K/B-type CpG ODNs

This CpG ODN class is referred to as B or K-type ODNs by different groups. It will be referred to as K-ODN hereafter. These are full phosphorothioate backbone ODNs with at least one CpG motif. This motif is highly active in humans when it is located closer to 5' end of the sequence and at least one more base upstream of the 5`-CpG motif is required. Thymidine in the immediate 5' position is the most favorable for humans (ODN2006). For active CpG ODNs in mice, CpG motif does not have to be at the very 5'

end (ODN1555, ODN1826). Minimum length of ODN should be 12 bases for sustained immune activation (Verthelyi et al., 2001). This type lacks poly-G tails and is believed to remain as single stranded linear sequences under physiological conditions (Costa et al., 2004). Optimal K-ODN sequences are given below:

1. ODN1826: 5`-TCCATGACGTTCCTGACGTT-3`
2. ODN1555: 5`-GCTAGACGTTAGCGT-3`
3. ODN2006: 5`-TCGTCGTTTTGTCGTTTTGTCGTT-3`
4. K23: 5`-TCGAGCGTTCTC-3`

K-ODNs trigger IL6 and IgM secretion from B-cells and induce their proliferation. They also activate $CD19^{+}$ B cells by upregulating CD69 (early activation marker) and CD25 (late activation marker) (Gursel et al., 2002a). These ODNs are superior for pDC maturation and induction of proinflammatory cytokines from pDCs than D-type ODNs (Krug et al., 2001). They can also synergize with GM-CSF and activate the maturation markers of dendritic cells; MHC II, CD40, and CD83 (Hartmann et al., 1999). Poor IFNα induction from pDCs is also characteristic of this type of ODNs, whereas it is reported that even this trace amount of IFNα is sufficient enough to induce MHC-I cross presentation in DCs (Gray et al., 2007). K-ODN induced IFNγ, IP10 secretion from PBMC is little also if compared to other ODN types. Spleen cells also secrete very high amounts of IL6 and IL-12 in response to K-type ODNs (Krug et al., 2001; Verthelyi et al., 2001). Mouse-active K-type ODN induces much higher levels of nitric oxide (NO) from mouse-macrophage cell line (RAW264.7) in comparison with D-type ODN (Utaisincharoen et al., 2002).

1.3.2.3. C-type CpG ODNs

C-type ODNs have fully phosphorothioate backbone with 5' CpG sequences ('TCGTCG motif') and a 12-16 bp palindromic sequence at 3' end for most optimal activity (Vollmer et al., 2004). TCG at 5' end is necessary for ODN activity and IFNα-induction capacity is reduced when this motif is shifted towards 3'. Immunostimulatory activity of C-ODN depends on the ODN length, the base content and a 5'-TCG. Minimum length requirement for optimal activity is 22 bp, where adding poly-T to the 3' end of shorter sequences significantly increases their activity (Jurk et al., 2004).

Palindromic sequence, which is believed to allow duplex formation in an endosomal environment, is vital for the immunostimulatory activity of C-type ODN (Krieg, 2006). This structrure is illustrated in Figure 4. Immunostimulatory effect is severely reduced in similar ODNs lacking palindromic sequences, especially in the context of IFNα induction.

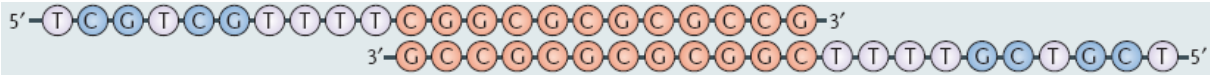

Figure 4. Duplex formation through palindromic sequences by two monomeric C-ODNs ODN2395 (Krieg, 2006).

These ODNs are reported to combine the immunostimulatory activity of D-type and K-type ODNs. They directly activate human B cells at a level comparable with K-ODNs. Furthermore, the production of IFNα from pDC is induced at a higher level compared to K-ODNs. They also induce also higher levels of IFNγ, IP-10 from PBMC and upregulate activation markers on NK cells better than K-ODN. B-cell activation with this type of ODN is pronounced in whole human PBMC stimulation which is not the case for K type CpG ODN. IFNα production from pDC seems to have an additive effect on B-cell activation in whole PBMC stimulation. Depleting pDC from PBMC lowers B-cell activation by C-type while this type of reduction does not occur upon K-ODN stimulation (Hartmann et al., 2003).

To sum up, C-ODNs are somewhere between D-ODNs and K-ODNs both structurally and immunologically. They induce lower levels of interferon than D-type and higher levels than K-type. They also directly activate B cells. Additionally, they form duplexes under physiological conditions unlike linear K-ODNs and multimeric D-ODNs.

1.3.2.4. Other Types of CpG-ODNs

Several ODNs that do not fit into the previously mentioned classes have also been designed. One of them is Y-shaped ODN, which is formed by 3 linear CpG ODNs with complementary regions. Its structure is given in Figure 5. This ODN has a phophodiester backbone and induces higher levels of IL6 and TNFα from RAW264.7 cells, a mouse

macrophage cell line, than single- and double-strands of same ODNs used at same concentrations. It is claimed that this structure increases the efficiency of uptake into cells (Nishikawa et al., 2008).

Another work reported that 3' extension of phophodiester linear (CpG or non-CpG) ODNs with 24 guanine nucleotides turns these sequences into an effective IFNα inducer. Whereas shorter ODNs have reduced activity, elongation of the ODNs does not result in increased activity. Addition of a CpG motif increases the activity of this ODN. It has been shown that polyG addition confers complexation and efficient uptake into immune cells similar to the utilization of a complexation agent such as DOTAP (Haas et al., 2009).

Previous research in our lab has led to the identification of a novel 70-mer dendrimeric ODN, which forms uniform-sized nanoparticles with an average size distribution of 35 ± 10 nm (Figure 6). It exhibits a higher immunostimulatory potential than its linear control. Furthermore, the substitution of CpG dinucleotide with a GpC flip completely abolishes its activity in mice (Mammadov, M.Sc. Thesis, 2009).

Figure 5. Y-shaped CpG ODN (Nishikawa et al., 2008).

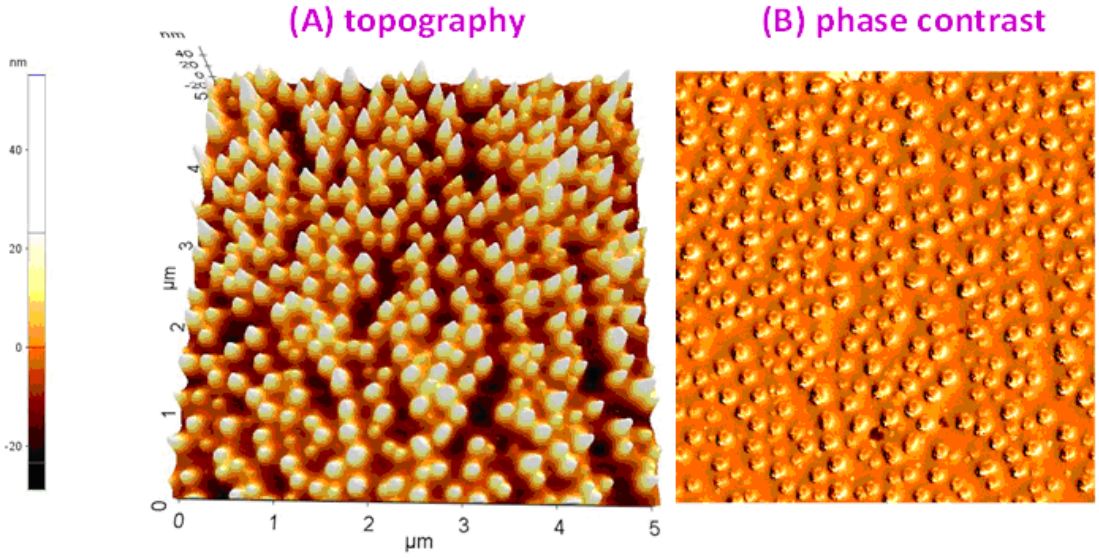

Figure 6. Formation of uniform-sized nanoparticles in a novel bifunctional dendrimeric ODN, designated as ODN420. (Mammadov, M.Sc. thesis, 2009)

1.3.3. Differential Immune Response Mediated by Particulate and Linear CpG ODN

Although both D-type and K-type ODNs contain CpG motifs and initiate their effect by signaling through TLR9, the immunologic pathways induced are unique in each class. First, D-ODNs have been reported to be localized in different vesicles than those of K-ODNs. Moreover, D-ODN is taken up four-fold more efficiently than K-ODN by PBMC, where excess concentration of either ODN does not inhibit binding or uptake of the other (Gursel et al., 2002a). Collectively, these data suggest that there are different mechanisms of uptake for each of these ODNs. Poly-G tail, which confers particulate structure in D-ODNs, is thought to be responsible for the more efficient uptake of D-ODNs in mouse cells (Anderson et al., 2008; de Jong et al., 2007) and human pDC (Kerkmann et al., 2006). Second, interferon regulatory factor (IRF)-7 is found to be critical for IFNα induction from pDC by D-ODN, as pDCs from IRF7$^{-/-}$ mice are unresponsive to D-ODN. D-ODN mediated cytokine production such as IL-12 and IL6 from cDC (conventional dendritic cells) and K-ODN mediated cDC and pDC activation are not affected in IRF7$^{-/-}$ mice (Honda et al., 2005b). The dichotomy of D-type and K-type ODNs is illustrated in Figure 7.

Two recent works have clarified the differential activities of D- and K-type ODNs. Honda et. al. have reported that induction of different cytokines from pDCs by two types of ODNs is caused by different localization patterns of K or D-type ODNs in pDCs. D-type ODNs are retained for longer periods in the early endosomal vesicles of pDCs, whereas K-type ODNs accumulate in vesicles with lysosomal markers (Honda et al., 2005a). According to this model, D-ODN interacts with MyD88–IRF-7 complex in early endosomes, which results in IRF7-mediated IFNα production. Meanwhile, K-ODN activates MyD88-IRAK4/1-TRAF6 complex which activate NF-κB and IRF-5-mediated pro-inflammatory cytokine production (Asselin-Paturel and Trinchieri, 2005). Retention of D-ODNs in early endosomes is facilitated by their higher-order structure. Artificial targeting of K-ODNs to early endosomes can be achieved through making their complexes with DOTAP (Honda et al., 2005a). These particulate forms of K-ODNs induce IFNα levels comparable with D-ODN (Kerkmann et al., 2005). Recruitment of D-ODN to early endosomes and its IFNα-inducing capacity are dependent on CXCL16, a scavenger receptor only expressed on pDCs but not on B-cells (Gursel et al., 2006). Moreover, D-ODNs lacking poly-G tail cannot interact with CXCL16. Identification of CXCL16 as a specific co-receptor for D-type ODN might also explain the higher efficiency of artificially multimerized ODNs regarding uptake and immune stimulation (Haas et al., 2009; Shirota et al., 2001). To date, there is no convincing evidence proving that particulate forms of K-ODNs depend on additional recognition by other receptors. However, high immunostimulatory potential of nanoparticle-forming CpG-ODNs at low concentrations, where free CpG-ODNs are not active, strengthens this hypothesis (Anderson et al., 2008; Gursel et al., 2001).

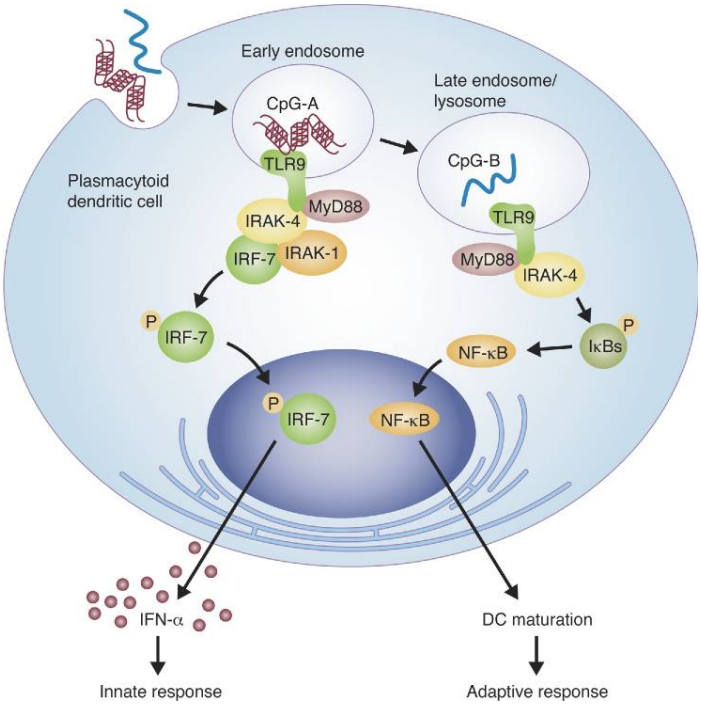

Figure 7. Dichotomy of different CpG ODN types delivered to early or late endosomes induce innate or adaptive immune responses, respectively, in pDCs. (Williams, 2006)

1.4. Utilization of CpG ODNs as Therapeutic Agents

Critical cellular target for CpG ODN therapy are pDCs. Moreover, pDCs from CpG-treated donors are able to mount protection in naive recipients. Another $TLR9^{+}$ cell type is B cells, where CpG-ODNs induce production polyclonal immunoglobulins that help to eradicate pathogen. NK cells and macrophages are indirectly activated by cytokines released from pDCs (Klinman, 2004).

In an attempt to define the most optimal sequences, several thousand sequences have been synthesized and tested on PBMCs isolated from over 100 donors. It has been observed that no single ODN is optimal for all tested individuals. Two strategies are suggested to overcome this problem. The first one is to synthesize single ODNs with different CpG motifs and the second one is to use mixtures of multiple ODNs with different CpG motifs (Leifer et al., 2003). This should be taken into consideration in therapeutic approaches with CpG ODNs, which are shown to be effective against infectious diseases, cancer, allergy/asthma.

Infectious diseases: CpG ODNs increase resistance of even immunosuppressed, newborn and pregnant animals to pathogenic infection. For example, in SIV (retrovirus like HIV)-infected macaques, D-type CpG ODN reduces parasitic (leishmania) load up to 1000-fold. However, CpG treatment increases SIV load in macaques, probably due to the activation of infected T cells. As HIV infection does not interfere with innate immunity until late stages of the disease, CpG ODN therapy may be used to protect patients from other infections (Klinman et al., 2004).

Moreover, induction of Th1 immunity by CpG ODN suggests that they can be used as vaccine adjuvants. CpG ODN + antigen immunization of mice has been shown to induce cellular and humoral immunity against antigens more powerfully than antigen alone. When K-ODN is adminstered together with AVA (the licensed vaccine against anthrax), antigen-specific response increases 6-fold with respect to injection of AVA alone (Klinman et al., 2006). Also, CPG 7909 plus vaccine has induced Hepatitis B surface antigen (HBsAg)-specific antibody responses (anti-HBs) at earlier time points starting from 2 weeks after the initial priming with respect to subjects who received vaccine alone. Thus, the development of antigen-specific response is also accelerated (Krieg, 2006).

Cancer: The combination of CpG ODN encapsulated in sterically stabilized cationic liposome and recombinant interleukin-13 Pseudomonas exotoxin (IL13-PE) is significantly effective against human neck and head cancer as xenografts in mice. CpG activity is dependent on NK cell activity and IL-13-PE augments its activity (Ishii et al., 2003). In another study, it has been shown that K-type CpG ODN effectively suppresses metastasis of cancer cells, especially if it is administered after surgical removal of the primary tumor (Kim et al., 2009). CpG ODN seems to be effective alone for small tumors, while CpG therapy should be combined with other therapies like chemotherapy for larger tumors (Krieg, 2006). For now, 4 different CpG ODNs are in clinical trials for treatment of 11 different cancers such as breast cancer and melanoma (Krieg, 2008). Possible mechanism of CpG-mediated anti-tumor activity is illustrated in Figure 7.

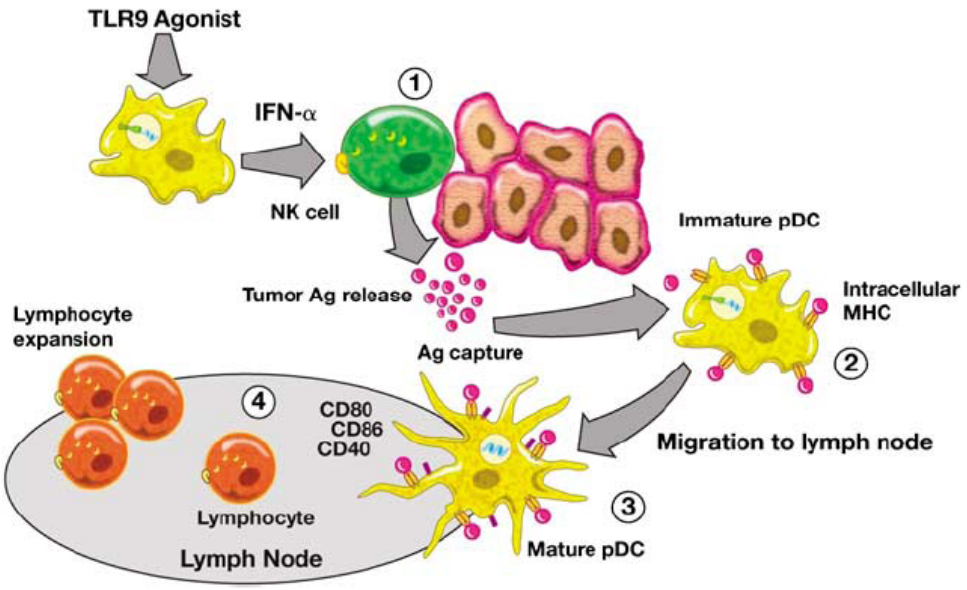

Figure 8. Proposed mechanism of CpG ODN-mediated anti-tumor activity (Krieg, 2008).

Allergy/Asthma: Exact mechanism for therapeutic effect of CpG ODN on asthma is not clear. Th1 cytokines are not necessary for treatment of allergy (Kline and Krieg, 2008). Yet, when CpG ODN is administered two days before challenge with ragweed in presensitized mice, allergic lung inflammation is inhibited for a prolonged time (Sur et al., 1999).

1.5. Synthetic DNA Containing Mammalian Telomeric Repeats with Immunosuppressive Activity as Another Class of Nanoparticle Forming ODNs

Although CpG ODN confers a selective advantage to the host by improving resistance to a variety of infectious microorganisms, uncontrolled immune activation can cause harm by exacerbating inflammatory tissue damage, inducing autoimmune disease or toxic shock. During infection or tissue damage, inflammation must be waned and terminated with wound healing. Thus, a negative feedback system of innate immune activation occurs via several inhibitory signals (Ishii and Akira, 2005).

Previous studies indicated that mammalian genome contain some elements antagonistic to the immunostimulatory effect of pathogen derived CpG rich DNA. Neutralizing or suppressive motifs can selectively block CpG-mediated immune

stimulation (Krieg et al., 1998). Optimal motifs for immunosuppressive ODN are surprisingly identical to the telomeric repeats (TTAGGG), which are found in high frequency in mammalian DNA but not in bacterial DNA (Gursel et al., 2003). The immunosuppressive activity of this motif correlates with its ability to form higher structures such as G-tetrads. Suppressive ODN does not interfere with binding or uptake of CpG ODN but blocks either TLR9 binding to CpG DNA or the signaling cascade upstream of NF-κB translocation to the nucleus (Gursel et al., 2003; Yamada et al., 2002). Several groups have identified other G-rich or GC-rich ODNs with immunosuppressive activity (Ho et al., 2003; Peter et al., 2008). Reported effects of treatment with immunosuppressive ODNs include reduction of Th1 cytokine expression and MHC class II expression.

The exact molecular mechanism as to how immunosuppressive ODN works is not clear. TLR9-dependent effects of immunosuppressive ODNs are proposed to be dependent on a putative target that is upstream of inhibitory kinase (IKK) activation (Lenert et al., 2001). It has been shown to inhibit Th1 differentiation by blocking IFN-γ and IL12-mediated signaling (Shirota et al., 2004). In one study, while Th1 responses are suppressed, it has been observed that Th2 responses are enhanced (Ho et al., 2003). Some immunosuppressive ODNs specifically inhibit TLR9 signaling (Peter et al., 2008). Meanwhile, several TLR9-independent effects have been observed upon treatment with other suppressive ODNs. It has been shown that treatment with an immunosuppressive ODN renders TLR9-deficient bone marrow derived macrophages more susceptible to *S. typhimurium* infection. This effect is attributed to the observation that immune responses to TLR2 ligand Pam_3Cys are also suppressed upon treatment with suppressive ODN (Trieu et al., 2009). While it can be suggested that these ODNs may compromise the immune system of the host, these agents pose great therapeutic potentials as anti-inflammatory agents in autoimmune diseases. Suppressive ODN treatment has caused protection of mice from LPS-induced endotoxic shock. Suppressive ODN does not inhibit LPS-induced cell activation or reduce LPS-dependent production of IL6, IL-12 and TGF-β. Yet, it acts at a later stage of LPS-induced immune activation and prevents phosphorylation of STAT1 and STAT4 by binding to it (Shirota et al., 2005).

1.6. Utilization of Immunosuppressive ODNs as Therapeutic Agents

Arthritis: Arthritis is the most common rheumatic disease and characterized by progressive destruction, deformity and disability of the joints. There are two experimental models of arthritis: CpG DNA-induced reactive arthritis and collagen-induced arthritis. Early administration of suppressive ODN reduces severity of arthritis in both models by reducing autoantibodies and IFNγ production by reactive T cells (Dong et al., 2004; Zeuner et al., 2002).

Systemic lupus erythematosus (SLE): Lupus is a systemic autoimmune disease characterized by the production of antinuclear autoantibodies, immune complex-mediated glomerulonephritis and various types of end-organ damage. Early administration of suppressive ODN controls a murine lupus model, in which female NZB x NZW mice progressively develop immunologic and clinical manifestations of disease that closely resemble SLE in humans (Dong et al., 2005).

Pulmonary inflammation: Silica-containing dust particles induce silicosis, an inflammatory disease of the lungs characterized by the infiltration of macrophages and neutrophils into the lungs and the production of proinflammatory cytokines, chemokines and reactive oxygen species (ROS). *In vivo* studies show that pretreatment with suppressive ODN improves the survival of mice exposed to silica as manifested by fewer infiltrating cells, less cytokine/chemokine production and lower levels of ROS (Sato et al., 2008).

Multiple sclerosis: Multiple sclerosis is an autoimmune disorder, in which components of the myelin sheath are targeted by the inflammatory strike resulting in demyelination and neurodegeneration. Paralysis, sensory disturbances, lack of coordination and visual impairment are common symptoms. Experimental autoimmune encephalomyelitis (EAE) is the animal model and can be induced by neuroantigens such as MOG or PLP. In an EAE model, combining a myelin cocktail plus IL-4-tolerizing DNA vaccine with a

suppressive G-rich ODN induces a shift of the autoreactive T cell response toward a protective Th2 cytokine pattern and reduces disease severity (Ho et al., 2005).

Uveitis: Uveitis is an autoimmune disease characterized by ocular inflammation. In a murine model, uveitis can be induced by interphotoreceptor retinoid-binding protein, a retinal antigen. Suppressive ODN treatment inhibits the retinal antigen-specific cytokine production and lymphocyte proliferation in mice immunized with IRBP (Fujimoto et al., 2009).

2. AIM OF STUDY

CpG ODNs are a promising class of DNA-based drug candidates. They directly stimulate human B cells and plasmocytoid dendritic cells, induce the production of Th1 and proinflammatory cytokines and trigger the maturation of antigen-presenting cells. Moreover, the synthesis of these drug candidates is cheaper with respect to conventional protein-based agents and well-established under GMP (good manufacturing practice) conditions. CpG ODNs are already in clinical trials for different diseases.

K-type CpG ODNs have phosphorothioate backbones and induce high levels of IL6, IL12, TNFα and IgM levels. They remain single-stranded in body fluid. On the other hand, D-type CpG ODNs have mixed backbones. The poly-G tails on 5' end and 3' end are made of phosphorothioate backbones while the central regions contain the natural phosphodiester backbone. D-type CpG ODNs are unique in the manner that they induce anti-viral type I IFN production and higher levels of monocyte maturation into DCs. Accumulating data indicate that these effects are at least partially attributed to their ability to be retained longer in the early endosomes by forming multimeric structures.

Previous studies in our lab have established the characterization of a novel CpG ODN. This ODN, designated as ODN420, is synthesized by linking seven ODN1466 sequences by two bifunctional linkers. ODN1466 is a K-type ODN. Yet, ODN420 spontaneously forms uniform nanoparticles like D-type ODNs and exhibits higher immunostimulatory activity like K-type ODNs. Only ODN420 with PS backbone has been used in these studies. Moreover, the effect of ODN420 has been tested only on primary cell culture obtained from mouse splenocytes. Its *in vivo* activity and its activity on human cells have not been studied yet. To date, the activity of K-ODN is assessed by PS backbones. When PO backbone is used, substantial loss in immunostimulatory potential has been observed. While PS linkage yield more nuclease resistant ODNs, it is very expensive than PO backbone. Considerable research efforts are being made to develop PO sequences displaying PS characteristics.

In this context, the first part of this study investigates the immunostimulatory potential of ODN420 with different (PS or PO) backbones in mouse splenocytes. These activities are compared to several ODN classes. The activity of nanoparticle ODNs on human PBMC is determined with various assays. Next, its immunostimulatory potential

is evaluated by an *in vivo* experiment. Finally, the potential of ODN420 as a vaccine adjuvant and as an anti-cancer agent are evaluated in two different *in vivo* studies. The mechanism and activity of another class of nanoparticle forming ODN, ODN-A151, which exhibits immunosuppressive activity, are also evaluated in the immunization experiment.

3. MATERIALS & METHODS

3.1. MATERIALS

3.1.1. Reagents

All oligodeoxynucleotides (ODNs) are synthesized at AlphaDNA (Canada) or kind gifts from Dennis Klinman (NCI/NIH, USA). ODNs are devoid of any detectable LPS contamination as judged by Limulus Ameobyte Lysate (LAL) assay. Bases written in lower case represent phosphodiester linkages whereas bases written in upper cases represent phosphorothioate linkages. Stimulatory CpG motifs and the control GpC motifs in the control ODNs are underlined. ODN sequences are given below:

A151 (24-mer) : 5`-TTAGGTTAGGTTAGGTTAGG-3`

C-A151 (24-mer) : 5`-TTCAAATTCAAATTCAAATTCAAA-3`

1466 (10-mer) : 5`-TCAACGTTGA-3`

1471 (10-mer) : 5`-TCAAGCTTGA-3`

K23 (12-mer) : 5`-TCGAGCGTTCTC-3`

D35 (20-mer) : 5`-GGtgcatcgatgcaggggGG-3`

D3(CG) (20-mer) : 5`-GGtcgatcgatcgaggggGG-3`

I-127 (20-mer) : 5`-GGtgcatgcatgcaggggGG-3`

Linear-7x-1466 (70-mer) : 7 x 1466 (linear sequence)

Linear-7x-1471 (70-mer) : 7 x 1471 (liner sequence)

420 (70-mer) : 7 x 1466 (dendrimeric sequence linked via two symmetric bifunctional linkers, please see Figure 9)

421 (70-mer) : 7 x 1471 (dendrimeric sequence linked via two symmetric bifunctional linkers, please see Figure 10)

422 (90-mer) : 9 x 1466 (dendrimeric sequence linked via a symmetric bifunctional linker and then via a trifunctional linker, please see Figure 11)

423 (90-mer) : 9 x 1471 (dendrimeric sequence linked via a symmetric bifunctional linker and then via a trifunctional linker, please see Figure 12)

Lipopolysachharide (LPS) isolated from *E. coli* is purchased from Sigma (USA) and R848 is purchased from Invivogen (USA). All primers for PCR are purchased from AlphaDNA (Montreal, Canada). ELISA reagents including paired antibodies for cytokines, recombinant antibodies, streptavidine-alkaline phosphatase (SA-AKP) and p-nitrophenyl phosphate disodium salt (PNPP)-substrate for alkaline phosphatase are purchased from Endogen/Perbio, Pierce (USA) unless otherwise stated.

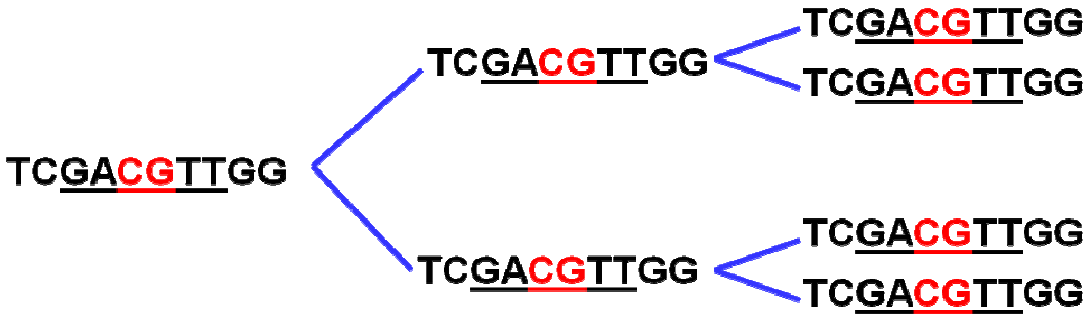

Figure 9. ODN420: Schematic representation of the ODN420 formation via the use of two bifunctional linkers at the 3`-end of ODN 1466 sequences.

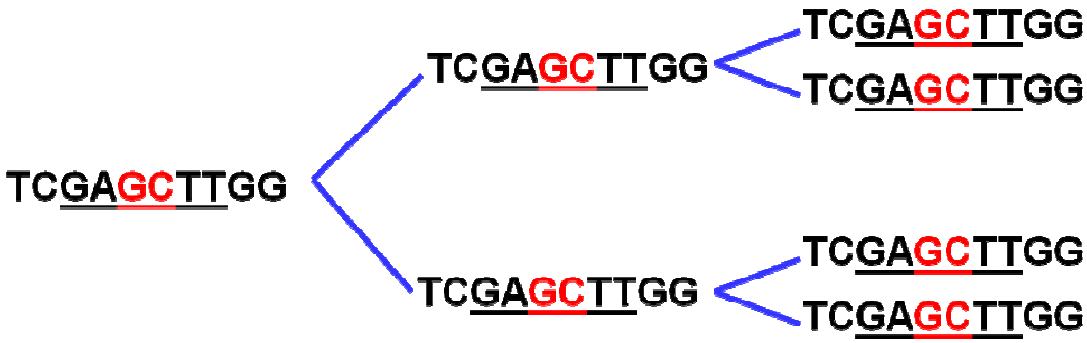

Figure 10. ODN421: Schematic representation of the ODN421 formation via the use of two bifunctional linkers at the 3`-end of ODN 1471 sequences.

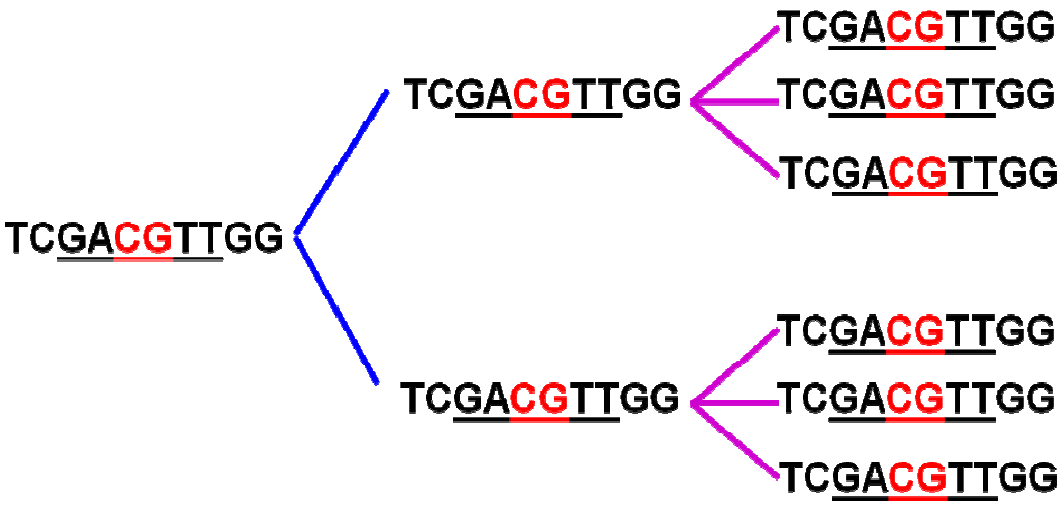

Figure 11. ODN422: Schematic representation of the ODN422 formation via the use of a bifunctional linker for G=2 and a trifunctional linker for G=3 at the 3`-ends of ODN 1466 sequences.

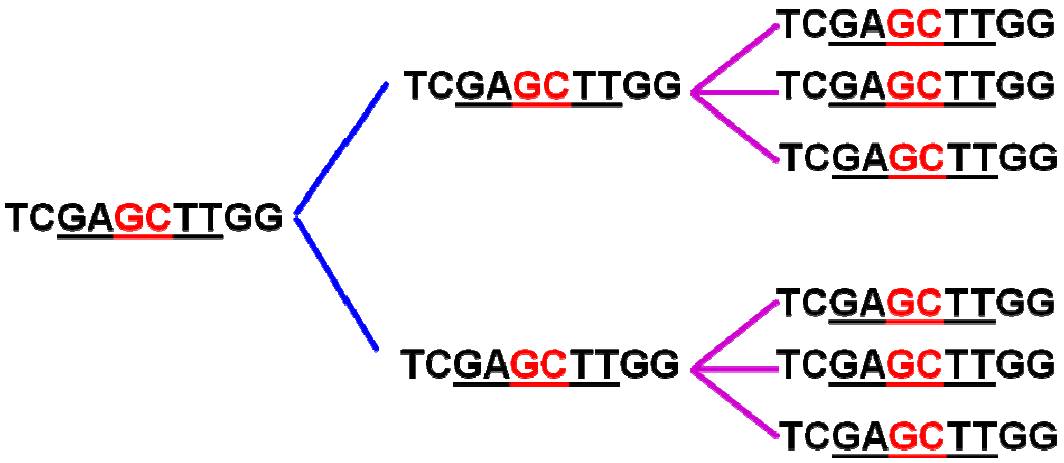

Figure 12. ODN423: Schematic representation of the ODN423 formation via the use of a bifunctional linker for G=2 and a trifunctional linker for G=3 at the 3` ends of ODN 1471 sequences.

3.1.2. Cell Culture Media, Buffers and Other Standard Solutions

DNAse/RNAse free water, RPMI1640 and low glucose DMEM media, Na-pyruvate, HEPES, L-glutamine, penicillin/streptomycin, non-essential amino acid solution, FBS are from Hyclone PerBio (USA).

Components of various culture media and different buffers are given in detail in the Appendix A.

3.2. METHODS

3.2.1. Cell Culture

3.2.1.1. Cell Lines

Human hepatocellular carcinoma cell line Huh7 (ATCC) is cultured with 10% FBS supplemented DMEM. Adherent cells are passaged when they reach 90% confluency with fresh media following trypsinization and washing.

3.2.1.2. Single Cell Splenocyte Preparation

Mice are euthanized by cervical dislocation. Spleens are removed with sterile instruments and put into 3 ml 2% FBS supplemented regular RPMI media in 6-well plates. In sterile cell culture conditions, single cell suspensions are obtained by smashing spleens with the back side of a sterile syringe in media with circular movements. Homogenous part of media is collected by using sterile plastic pasteur pipettes while cell clumps belonging to fibrous or connective tissue are left. Cells are centrifuged at 1500 rpm for 10 minutes at room temperature. Medium is sucked cell pellet is gently resuspended in 10 ml fresh media and centrifuged at the same conditions. These washing steps are repeated twice to remove remaining tissue debris. At the end of last washing step, cells are resuspended in 10 ml 5% FBS supplemented regular RPMI and counted.

3.2.1.3. Peripheral Blood Mononuclear Cell (PBMC) Isolation from Whole Blood

Blood samples from healthy donors are transferred to 50 ml tubes containing Naq-Citrate, EDTA or Heparin. New 50 ml tubes are filled with 15 ml Biocoll or Histopaque separating solution (Biochrom AG, Germany and Sigma USA respectively). 22.5 ml blood is slowly layered on top of Histopaque without disturbing layers. Samples are centrifuged at 1800 rpm for 30 minutes at break off setting. The cloudy buffy coat in the middle erythrocytes and basophils is taken with sterile Pasteur pipettes and transferred to a new tube. 2% FBS supplemented regular RPMI media is added until total volume reaches 50 ml. Samples are centrifuged at 1800 rpm for 10 minutes. Medium is sucked cell pellet is gently resuspended in 10 ml fresh media and centrifuged at the same conditions. These washing steps are repeated twice to remove remaining cell debris. At

the end of last washing step, cells are resuspended in 10 ml 5% FBS supplemented regular RPMI and counted.

3.2.1.4. Cell Counting and Distribution

After cells are resuspended in 10 fresh media as indicated above, 10 µl from these cell suspensions is taken and diluted 10 fold with 90 µl medium to reduce the cell number in the final 100 µl solution. 10 µl from diluted solution is placed on Neubaer cell counting chamber. Cells in 4 corners (composed of 16 small squares) with 1mm^2 area were counted under light microscope (Figure 13).

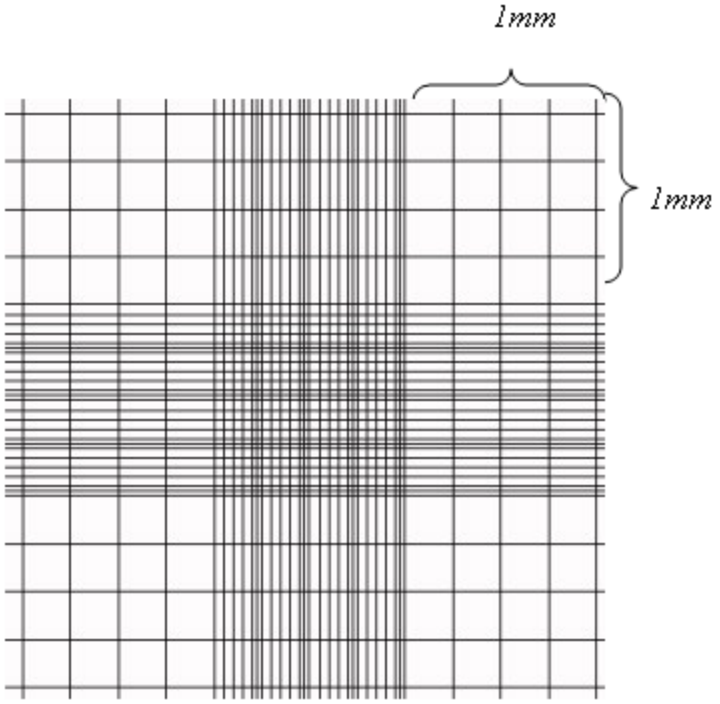

Figure 13. Neubaer cell counting chamber

The depth between coverslip and cell counting chamber is 0.1 mm. Thus, each 1 mm^2 area holds a volume of 0.1 mm^3. So, the number of cells/ml can be obtained from the equation given below:

$$\left[\frac{\text{Total cell number in 4 big squares}}{4}\right] \times 10 \times 10^4 = \text{number of cells per ml.}$$

number of cells per 0.1 mm^3

dilution factor

After total cell number is determined, original cell stock is centrifuged and resuspended in an appropriate volume of 5% FBS supplemented oligo medium if cells are to be stimulated with ODNs. If stimulation with ODNs is not to be performed, cells are resuspended in 5% FBS supplemented regular medium. Working cell concentration is adjusted to $4x10^6$ cells/ml for ELISA experiments, $1x10^7$cells/ml for RNA extraction and $2x10^6$ cells/ml for FACS analysis unless otherwise stated.

3.2.1.5. Stimulation Protocols

For stimulation in 96-well cell culture plates, 100 µl of $4x10^6$ cells/ml stock (400,000 cells/well) are transferred to 96-well plates. Total volume is adjusted to 200 µl with ODNs in 100 µl 5% FBS supplemented oligo medium. Unless otherwise stated, final concentration of ODNs is 1 µM. Stimulations are performed in triplicate wells for each indicated treatment (Gursel et al., 2001). Supernatants are collected after 24-48h for analysis of secretion of various cytokines. For gene expression studies and FACS analysis, 500 µl of original cell stock ($5x10^6$ cells for gene expression studies and $1x10^6$ cells for FACS analysis) is transferred to 15 ml tubes. Total volume is completed to 1 ml with specific ODNs in 500 µl 5% FBS supplemented oligo medium. Unless otherwise stated, final concentration of ODNs is 1 µM. For gene expression studies, incubation periods are 2-8 hours while incubation periods are 6-72 hours for FACS analysis depending on the marker to be examined. Tubes are left in tilted position with loosened caps to allow airflow and lids of 96-well plates are closed during the incubation period in CO_2 incubator.

3.2.2. Fluorescence Activated Cell Sorting (FACS)

3.2.2.1. Cell Surface Marker Staining

Cells are centrifuged at 1500 rpm for 7 minutes at the end of the incubation periods. Supernatant is sucked. The protocol is a slightly modified version of two previously published protocols (Gursel et al., 2006; Gursel et al., 2002b). Briefly, pellet is disturbed by applying mechanical force in one direction following centrifugation by using a pin rack. If cells are to be stained and analyzed later, cells are fixed in 100 μl fixation medium (Caltag, Austria) and transferred to 1.5 ml tubes. Cells are incubated in dark at room temperature for 15 minutes. 1 ml PBS-BSA-Na azide is added into each tube to wash cells. Cells are spun at 2000 rpm for 5 minutes in microcentrifuge. Supernatant is discarded and the washing step is repeated. At the end of the second washing step, PBS-BSA-Na azide is discarded and cells are incubated in 50 μl PBS-BSA-Na azide containing 4-6 μl of fluorochrome-associated cell surface marker. Antibodies against the following cell markers for human cells are used throughout this thesis: CD123-PE, CD86-PE/Cy5, CD19-PE/Cy5 (BD Pharmingen, USA), BDCA2-FITC (Miltenyi Biotech, USA) and CD83-PE (Caltag, Austria). If cells are to be stained and analyzed immediately, fixation is not required. The cells can be stained in 50 μl PBS-BSA-Na azide containing 4-6 μl of fluorochrome-associated cell surface marker. The remaining steps are similar but all steps are performed on ice if cells are not fixed. Cells are washed twice, resuspended in 500 μl PBS-BSA-Na azide, transferred to FACS tubes and analyzed in FACSCalibur (BD, USA).

3.2.2.2. Intracellular Cytokine Staining

Here, a modified version of a previously reported method is used (Gursel et al., 2002a). For TNFα staining, Brefeldin A is immediately added to tubes and tubes are incubated for 4.5 hours. Cells are centrifuged at 1500 rpm for 7 minutes at the end of the incubation periods. Supernatant is sucked. Pellet is disturbed by applying mechanical force in one direction. Cells are fixed in 100 μl fixation medium (Caltag, Austria) and transferred to 1.5 ml tubes. Cells are incubated in dark at room temperature for 15 minutes. 1 ml PBS-BSA-Na azide is added into each tube to wash cells. Cells are spun at

2000 rpm for 5 minutes. Supernatant is discarded and the washing step is repeated. At the end of the second washing step, PBS-BSA-Na azide is discarded and cells are incubated in 50 µl permeabilization medium (Caltag, Austria) containing 2-4 µl of fluorochrome-associated antibodies against human intracellular cytokines TNFα-PE and (BD Pharmingen). When TNFα-PE is not available, each tube is first incubated with 0.5 µg biotinylated antibody against TNFα (Pierce, USA) in 50 µl permeabilization medium in dark for 30 minutes. Then, after washing, cells are incubated with 1:200 diluted SA-PE (BD Pharmingen) in 50 µl permeabilization medium in dark for 30 minutes. Cells are washed twice, resuspended in 500 µl PBS-BSA-Na azide, transferred to FACS tubes and analyzed in FACSCalibur (BD, USA).

3.2.2.3. Carboxyfluorescein Diacetate Succinimidyl Ester (CFSE) Assay

The method is from a previously published protocol (Parish et al., 2009). After PBMC is isolated, 1.5 million cells/treatment groups are transferred to 50 ml tubes. Total volume is completed to 50 ml with warm PBS. Cells are spun at 1800 rpm for 10 minutes. Medium is sucked and cells are resuspended in warm PBS in a working concentration of $1x10^7$ cells/ml. Equal amount of warm PBS containing 2 µM CFSE is added on top of cells so that final concentration of CFSE is 1 µM for $5x10^6$ cells/ml. Cells are gently pipetted for equal distribution of CFSE and incubated at 37°C for 10 minutes. 30 ml 5% FBS supplemented regular medium is added for washing. Cells are spun at 1800 rpm for 10 minutes and medium is sucked. Cells are resuspended in 5% FBS supplemented oligo medium in a working concentration of $3x10^6$ cells/ml. 0.5 ml is transferred to 24-well plate and the regular stimulation protocol is performed by adding 0.5 ml oligo medium containing appropriate concentration of ODNs. Samples are incubated for 3 days and the cell surface marker staining protocol is performed with the surface marker of interest as mentioned above.

3.2.3. ELISA

3.2.3.1. Cytokine ELISA

At the end of the incubation periods of cells stimulated in 96-well tissue culture plates, plates are spun at 1500 rpm for 6 minutes and 170 μl supernatant is collected from each plate. The ELISA protocol is a modified version of a previously reported protocol (Gursel, 2003). Briefly, supernatants can be stored at -20^{o}C. 96-well PolySorp plates (F96 Nunc-Immunoplate, NUNC, Germany) or Immulon 2B plates (Thermo Labsystems, USA) are coated with monoclonal antibodies against mouse and human cytokines IFNγ and IL6. 50 μl from antibody solution (10 μg/ml for monoclonal antibodies against mouse IFNγ and IL6, 4 μg/ml for monoclonal antibody against human IL6, 10 μg/ml for monoclonal antibody against human IFNγ) is added to each well. Plates are incubated at room temperature for 5 hours or at 4°C for overnight. Coating antibody is spilled. Wells are blocked with 200 μl blocking buffer for 2 h at room temperature. Plates are washed with ELISA wash buffer 5 times with 5 minute incubation intervals after each wash and then rinsed with ddH_2O for 3 times. Plates are dried by tapping (same washing procedure is repeated in the subsequent steps). Supernatants of cultured cells and recombinant proteins are added (50 μl/well from both). Starting concentration for mouse IL6 and mouse IFNγ recombinant cytokines are 2000ng/ml and 500ng/ml, respectively. Starting concentrations for human IL6 and IFNγ recombinant cytokines are 1000 ng/ml and 500 ng/ml, respectively. Recombinant cytokines are serially two-fold diluted with 50 μl 1X PBS (for 11 times). Plates are incubated for 2-3 hours at room temperature or overnight at 4°C. Plates are washed as explained above. Then, 50 μl from 0.5 μg/ml biotinylated-secondary antibody solution (original biotinylated antibody stock is 1/1000 diluted in T-Cell Buffer, please see Appendix I for details) is added to each well. Plates are incubated with biotinylated antibodies overnight at 4°C. Plates are washed as previously explained. 50 μl from 1:5000 diluted streptavidin-alkaline phospahatase solution (SA-AP in T-cell buffer must be prepared one day prior to its use and kept at 4°C) is added to each well. SA-AP is further incubated for 1 hour at room temperature. The washing step is repeated. One PNPP tablet is added to 4 ml ddH_2O and 1 ml PNPP substrate for each plate and 50 μl of PNPP substrate is added to each well. Yellow color formation is followed and OD

at 405 nm is analyzed with ELISA reader for several readings until recombinant cytokine standards reach a four parameter saturation and S-shaped curve is obtained. Each sample should be triplicate in cytokine ELISA. Each cytokine level for the samples are calculated using corresponding standard curves.

3.2.3.2. IgG anti-OVA ELISA

IgG ELISA is very similar to cytokine ELISA protocol except for a few steps. The method is from a previously published report (Gursel et al., 2001). All incubation times and washing steps are similar with cytokine ELISA. Immulon 1B 96-well plates (Thermo Labsystems, USA) are used. Each well is coated with 50 µl of 10 µg/ml OVA (Pierce, USA) diluted in 1X PBS. Blocking and washing steps are same as cytokine ELISA please see above section for details). Instead of supernatants, serum for each animal is placed on the first row in 1/7 titration (10 µl serum is diluted with 60 µl 1X PBS). All wells except for the 1st row are filled with 52.5 µl 1X PBS and 4-fold serial dilution is performed on vertical axis by transferring 17.5 µl from above well to bottom well (total of 7 dilutions are carried out). Antibodies against mouse IgG, IgG1, IgG2a, IgG2b (Southern Biotech, USA) are directly linked with AP. So, SA-AP incubation step is not performed. AP-linked IgG antibodies (1 mg/ml) are 1:3000 diluted in T cell buffer and again prepared one day prior to their use. After the addition of PNPP, yellow color formation is followed and OD at 450 nm is analyzed with ELISA reader for several readings. Titrations at which similar ODs can be observed are used to compare the level of each IgG subclass titers between different treatment groups.

3.2.4. Determination of Gene Expression at mRNA Level

3.2.4.1. Total RNA Isolation

Cells are centrifuged at 1500 rpm for 7 minutes at 4°C. Supernatant is discarded and cells are lysed with 1 ml Trizol, a mono-phasic solution of phenol and guanidinium thiocyanate (Invitrogen). Cell lysates can be stored at -80°C or can be transferred into 1.5 ml tubes for further RNA purification steps. All subsequent steps are performed on ice and all centrifugation steps are done at 4°C. For each 1mL Trizol used, 200 µl chloroform

is added to each tube and tubes are shaken vigorously for 15 seconds. After they are incubated at room temperature for 3 minutes, samples are centrifuged at 13200 rpm for 15 minutes at 4°C. Following centrifugation, 550-600 µl of the clear upper aqueous phase is transferred to a new tube and 500 µl isopropanol is added to each tube and samples are mixed by gentle inversions to allow homogeneous mixing while avoiding uncontrolled RNA strand breaks. Then, tubes are incubated at room temperature for 10 minutes and centrifuged at 13200 rpm for 15 minutes. Supernatant is sucked and the pellet is gently washed with 1 ml of 75% ethanol. Samples are centrifuged at 8000 rpm for 7 minutes. Again, supernatant is discarded and pellet is gently washed with 1ml >99.9% ethanol. After centrifugation at 8000 rpm for 7 minutes, ethanol is discarded and pellet is dried under laminal flow hood in a tilted position. Dry pellets are dissolved in 20 µl RNase/DNase free ddH_2O. The OD measurements at 260 and 280 nm wavelengths are obtained with the spectrophotometer NanoDrop® ND-1000 (NanoDrop Technologies, USA). Purified total RNA samples are expected to have A_{260}/A_{280} value between 1.8 to 2.0 OD ratio which indicates minimal contamination with DNA, protein, polysaccharides or phenol. RNA samples are stored at -80°C for further use.

3.2.4.2. cDNA Synthesis

cDNAs are synthesized from total RNA samples with the cDNA synthesis kit (Finnzymes) according to the manufacturers' protocol. 1µg total RNA is mixed with 1 µl of Oligo(dT)15 primer (100 ng) primer and total volume is completed to 8 µl with RNase DNase free H_2O in 0.2 ml PCR tubes. Tubes are pre-denatured at 65°C for 5 minutes in MJ Mini thermocycler (BIO-RAD, USA) and then spun down. 10µl RT Buffer (includes dNTP mix and 10 mM $MgCl_2$) and 2µl M-MuLV RNase H^+ reverse transcriptase (includes RNase inhibitor) are added to the mixture. Tubes are incubated at 25°C for 10 minutes, 40°C for 45 minutes and 85°C for 5 minutes. cDNA samples are stored at -20°C for further use.

3.2.4.3. PCR

Designed primers are developed with Primer3 Input v.0.4.0 program (http://frodo.wi.mit.edu/primer3/input.htm) and Primer Designer Version 2.0 using the

cDNA sequences of human and mouse genes available at the Ensembl database. Each primer pair is blasted (http://www.ncbi.nlm.nih.gov/BLAST/) against the mouse or human genome. Detailed information on mouse and human primers are given in Table 6 and Table 7, respectively.

Table 6. Sequences and product sizes of the primers for mouse genes.

Primer		**Sequence**	**Product Size**
m β-actin	Forward Reverse	5'-GTATGCCTCGGTCGTACCA-3' 5'-CTTCTGCATCCTGTCAGCAA-3'	450 bp
m TLR-3	Forward Reverse	5'-GGGGCTGTCTCACCTCCAC-3' 5'-GCGGGCCCGAAAACATCCTT-3'	250 bp
m TLR-7	Forward Reverse	5'-TTAACCCACCAGACAAACCACAC-3' 5'-TAACAGCCACTATTTTCAAGCAGA-3'	700 bp
m TLR-9	Forward Reverse	5'- GATGCCCACCGCTCCCGCTATGT-3' 5'-TGGGGTGGAGGGGCAGAGAATGAA-3'	430 bp
m IFNg	Forward Reverse	5'-GCGTCATTGAATCACACCTG-3' 5'-ATCAGCAGCGACTCCTTTTC-3'	195 bp
m IL-15	Forward Reverse	5'-CATCCATCTCGTGCTACTTGTGTT-3' 5'-CATCTATCCAGTTGGCCTCTGT-3'	126 bp
m IP-10	Forward Reverse	5'-GCCGTCATTTTCTGCCTCAT-3' 5'-GCTTCCCTATGGCCCTCATT-3'	127 bp
m CD40	Forward Reverse	5'-GTCATCTGTGGTTTAAAGTCCCG-3' 5'-AGAGAAACACCCCGAAAATGG-3'	91 bp

Table 7. Sequences and product sizes of the primers for human genes.

Primer		Sequence	Product Size
h GAPDH	Forward	5'-ACCACCATGGAGAAGGCTGG-3'	532 bp
	Reverse	5'-CTCAGTGTAGCCCAGGATGC-3'	
h TLR-3	Forward	5'-TCGAGAGTGCCGTCTATTTG-3'	199 bp
	Reverse	5'-CAACTTCATGGCTAACAGTGC-3'	
h TLR-7	Forward	5'-ACGAACACCACGAACCTCAC -3'	725 bp
	Reverse	5'-GGCACATGCTGAAGAGAGTTAC- 3'	
h TLR-9	Forward	5'-GAAGGGACCTCGAGTGTGAA-3'	188 bp
	Reverse	5'-GTAGGAAGGCAGGCAAGGTA-3'	
h MxA-1	Forward	5'-TCGGCAACAGACTCTTCCAT-3'	191 bp
	Reverse	5'-TTCAGGAGCCAGCTGTAGGT-3'	
h MxA-2	Forward	5'-TGAAATAGGCATCCACCTGA-3'	169 bp
	Reverse	5'-TTGAAGCAGCCAGGAATAGC-3'	
h IFNα	Forward	5'-GGAGTTTGATGGCAACCAGT-3'	192 bp
	Reverse	5'-CTCTCCTCCTGCATCACACA-3'	
h IFNβ	Forward	GCTCTCCTGTTGTGCTTCTCCACTACAGC	476 bp
	Reverse	CTGACTATGGTCCAGGCACAGTGACTGT ACTCC	
h IFNγ	Forward	5'-TGGAGACCATCAAGGAAGACA-3'	156 bp
	Reverse	5'-GCGACAGTTCAGCCATCAC-3'	
h TNFα	Forward	5'-CCCGAGTGACAAGCCTGTAG-3'	271 bp
	Reverse	5'-GATGGCAGAGAGGAGGTTGAC-3'	

All reagents are mixed and subjected to optimal PCR conditions for specific primer set in MJ Mini thermocycler (Biorad). PCR mixtures are prepared according to the protocol in Table 8. Running conditions for mouse primers are given in Table 9 and those for human primers are given in Table 10. PCR products are kept at 4°C until they are loaded on agarose gel.

Table 8. PCR reactants

Reaction Ingredients	**Volume**
2x DyNAzyme™ II PCR Master Mix*	12,5 μl
DNAse/RNAse free H_2O	9 μl
Forward primer	1 μl (10pmol)
Reverse primer	1 μl (10pmol)
cDNA	1,5 μl
Total	**25 μl**

**2x DyNAzyme™ II PCR Master Mix* includes 0.04 U/μl DyNAzyme™ II DNA Polymerase, 20 mM Tris-HCI (pH 8.8 at 25°C), 3 mM MgCl2, 100 mM KCl, stabilizers and 400 μM of each dNTP.

Table 9. PCR conditions for mouse primers

PCR Step	**mβ-actin, mIP10, mTLR3, mTLR7**	**mTLR9**	**mIFNγ, mIL15**	**mCD40**
Initial Denaturation	-	94°C, 2'	-	95°C, 3'
Denaturation	94°C, 30''	94°C, 30''	94°C, 30''	95°C, 30''
Annealing	55°C, 30''	64°C, 30''	60°C, 30''	62°C, 30''
Extension	72°C, 30''	72°C, 1'	72°C, 30''	72°C, 45''
Number of cycles	35	35	35	35
Final Extension	72°C, 5'	72°C, 10'	72°C, 5'	72°C, 7'

Table 10. PCR conditions for human primers

PCR Step	**hIFNα, hIFNβ, hIFNγ, hMxA-1, hMxA-2**	**hTLR3, hTLR9**	**hTLR7, hGAPDH**	**hTNFα**
Initial Denaturation	95°C, 7'	95°C, 7'	-	-
Denaturation	95°C, 30''	95°C, 30''	94°C, 10''	94°C, 10''
Annealing	60°C, 30''	61°C, 30''	63°C, 20''	65°C, -0.2°C/cycle, 20''
Extension	72°C, 30''	72°C, 30''	-	-
Number of cycles	35	35	35	35
Final Extension	72°C, 3'	72°C, 3'	72°C, 1'	72°C, 1'

3.2.4.4. Agarose Gel Electrophoresis and Quantification of Band Intensities

1.5% agarose gel is prepared with 1X TAE buffer and final concentration of ethidium bromide is 1 μg/ml. 2 μl loading dye is mixed with 10 μl PCR product. 10 μl of mixture is loaded to each well. 3 μl of 105 ng/μl DNA ladder with 100-1000bp range or low range DNA ladder with 50-1000bp range (Jena Biosciences) is loaded on an empty well and used as a marker. 80V is applied for 45 minutes and the gel is visualized under UV transilluminator (Vilber Lourmat, France). The gel exposure time is kept fixed at 0.1 second for each run. Band intensity analysis is performed with BIO-PROFILE Bio-1D V11.9 sofware. Band intensity for each product is measured and background intensity is subtracted from this value. Blanked intensities for each product are divided by blanked house-keeping gene values (β-actin for mouse and GAPDH for human samples) to normalize resulting quantitative data or directly compared.

3.2.5. *In vivo* Experiments

3.2.5.1. Maintenance of the Animals

Adult male or female BALB/c, C57/BL6 or T-cell deficient nude mice (8-12 weeks old) are used for the *in vivo* experiments. The animals are kept in the animal holding facility of the Department of Molecular Biology and Genetics at Bilkent University under controlled ambient conditions (22°C ± 2) regulated with 12-hour light and 12-hour dark cycles. They are provided with unlimited access of food and water. All experimental procedures have been approved by the animal ethical committee of Bilkent University (Bil-AEC).

3.2.5.2. Immunization Protocol with Specific ODNs and OVA

Three to five adult male C57/BL6 mice per group are injected intraperitoneally with 15 μg of ODN-D35 or ODN-420 and 7.5 μg of OVA in combination with or without 15 μg A151. The protocol is given in detail in Figure 14. Fourteen days later, boosting injection is performed i.p. with the same ODN and OVA combinations. Animals are bled one day before each injection and on the twenty-seventh day. Mice blood is incubated at 37°C for 1.5 hours, the clot is discarded and then the remaining part is spun at 13200 rpm

for 1 minute. The mice sera for background, primary and secondary bleedings was collected in 96 well plates and stored at -20°C for further use. Animals are sacrificed on day twenty-eight and their spleens are removed. From the half of the spleen single cell splenocytes are prepared and incubated for 42h to assess IFNγ secretion between different treatment groups and from the rest of the spleens total RNA is extracted and is studied for the expression of several Th1, pro-inflammatory and inflammatory cytokines/chemokines by PCR.

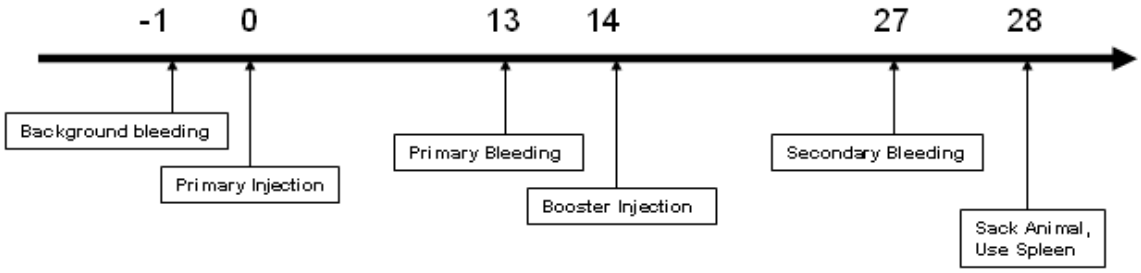

Figure 14. Immunization schedule for *in vivo* vaccination.

3.2.5.3. Tumor Xenograft Model

5 x 10^6 Huh7 cells in 250 µl sterile 1X PBS are injected subcutaneously to adult T-cell deficient nude mice (3-5/group). Since tumor formation is heterogeneous and some nude mice develop tumors later than 3 weeks, the day on which a palpable tumor forms is considered as day 0. Three doses of 100 µg of ODN-420 or ODN-A151 are injected intratumorally with one day-on and one day-off treatment starting from day 3 post-palpable tumor formation. Tumor dimensions are recorded daily as width, height and length by a caliper and calculated as mm^3.

3.2.6. Statistical Analysis

Statistical analysis is performed in SigmaSTAT 3.5 software. Students' t-test is used to understand if differences between untreated groups, groups treated with control-ODNs and ODN-treated groups are statistically significant.

4. RESULTS

4.1. *In vitro* Stimulatory Potential of Dendrimeric CpG-ODNs in Mouse Splenocytes

The structure of DNA backbone is an important factor in the activation of immune system by CpG-DNA. Most *in vitro* and *in vivo* studies utilize ODNs with phosphorothioate (PS) backbone due to their increased stability against nucleases and higher uptake rate. Yet, long-lasting effects such as lymphadenopathy, sustained local IFNγ and IL-12 production have been observed in PS-modified ODNs. Also, the PS modification brings another level of complexity and increases the cost of production for therapeutic purposes. Although ODNs with phosphodiester (PO) backbone have been shown to stimulate the immune system in a non-specific manner in one study (Yasuda et al., 2006), they can be superior in certain cases (Dalpke et al., 2002).

To understand the influence of different backbones, murine splenocytes are stimulated with various ODNs at 0.3 μM and 1 μM concentration for 42 hours. At the end of the incubation period, culture supernatants are collected and analyzed for IL6 levels by cytokine ELISA.

As seen in Figure 15, at 0.3 μM dose, ODN420 (70-mer) with PS backbone is by far the most active ODN. However, ODN420 with PO backbone performs even better than ODN420 with PS backbone at 1 μM concentration. In other words, there is a dose-dependent increase in IL6 secretion level for ODN420 with PO backbone while ODN420 with PS backbone is active at very low concentrations but its activity decreases when the concentration increases. The 70-mer linear control ODN, ODN1466, is a modest IL6 inducer. Additionally, ODNs 421 and 1471, in which the CG dinucleotide is flipped by GC, are not active. Thus, it can be concluded that this immune activation is strictly CpG-motif dependent and mediated by TLR9.

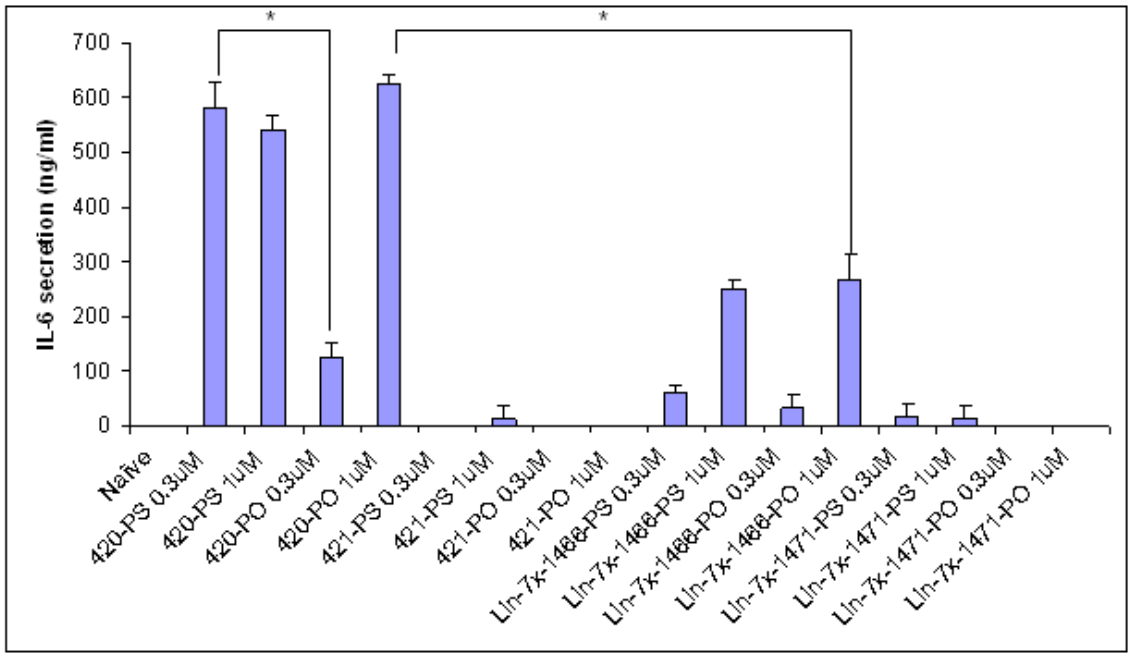

Figure 15. IL6 production by murine splenocytes in response to 0.3 μM and 1 μM concentrations of CpG-ODN stimulation (* $p<0.001$).

Mouse splenocytes contain a heterogeneous population of TLR9 responsive cells such as B cells, dendritic cells (DC) and monocytes/macrophages as well as T cells, which do not express TLR9. On the other hand, TLR9 expression is restricted to only B cells and plasmocytoid DCs in human blood. Since one of the goals of this thesis is to show the potential of an ODN that can be utilized for clinical trials, we next analyze the effect of ODN420 in human PBMC.

4.2. *In vitro* Stimulation Assays Using Human PBMC

4.2.1. Activation of Dendritic Cell markers and IL6 Secretion by Human PBMC as a Result of Stimulation with 1 μM NP-forming ODN Treatment

As a preliminary experiment, blood from 2 healthy donors is collected. PBMC is isolated and stimulated with various ODNs at 1 μM concentration. Supernatants are collected at the end of 36 hours and analyzed for IL6 secretion by cytokine ELISA (Figure 16). Cells are analyzed for activation of DC markers (CD83 and CD86) by FACS (Figure 17).

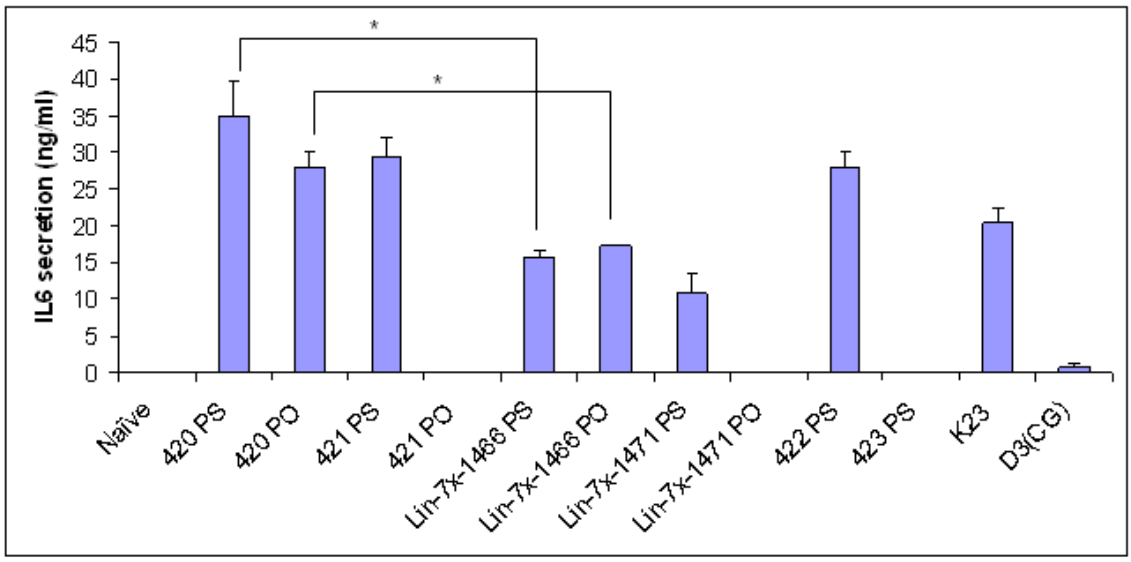

Figure 16. IL6 secretion by human PBMC in response to 1 μM concentration of CpG-ODN stimulation (* $p<0.002$).

Figure 16 clarifies the superiority of ODN420 with respect to its linear control ODN-1466. At 1 μM concentration, ODN420 with PO backbone is as active as PS backbone. K23 is used as a positive control and D3(CG) is used as a negative control in this experiment. ODN422 (90-mer) is also highly active. Again, the control ODNs with PO backbone, which contain GC flips instead of the CG motif, are not active in human PBMC. Of particular interest, 421-PS and 1471-PS, control ODNs which are not stimulatory in mouse splenocytes, are active in human PBMC. Similar results have been obtained for 2nd sample (data not shown).

In Figure 17, percentage of double positive cells ($CD83^+$ $CD86^+$) is 1.20, 1.58 and 2.02 in untreated, 420-PS and 420-PO treated cells, respectively. Percentage of $CD86^+$ cells is 2.46 in untreated cells. However this percentage increases to 17.69 in 420-PS treated cells and to 19.41 in 420-PO treated cells. Thus, DCs are shown to be activated upon treatment with ODN420. Although FACS analysis has been performed for cells treated with control ODNs, the results of those groups will be given in detail in another experiment in the subsequent sections of this chapter. Similar results have been obtained for 2nd sample (data not shown).

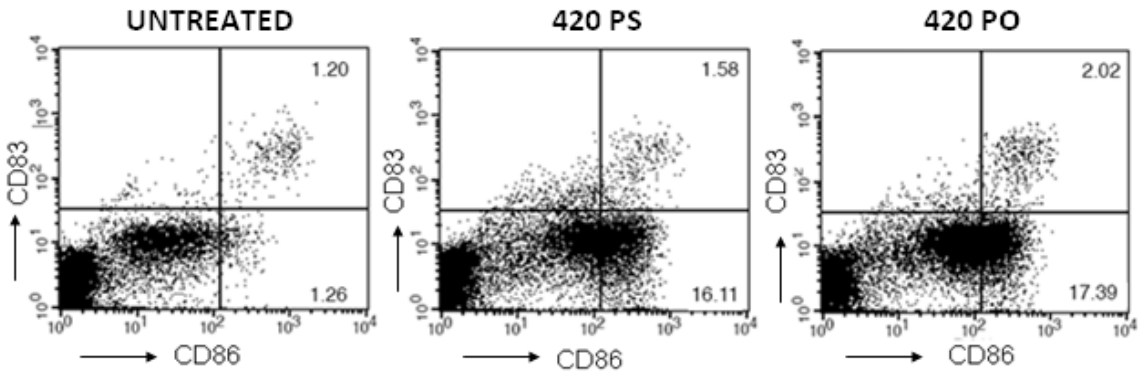

Figure 17. Activation of DC markers as a result of 1 μM CpG-ODN stimulation. CD83+ CD86+ cell percentage is given on the upper right corner. CD86+ cells, which are CD83- are given on the lower right corner of each dot plot.

4.2.2. Proliferation of Immune Cells Upon Stimulation with CpG-ODNs

With these encouraging data from preliminary studies, the next step is to analyze the effect of these ODNs on proliferation of immune cells and the production of tumor necrosis factor-alpha (TNFα).

CFSE (carboxyfluorescein succinimidyl ester) is a commonly used fluorescent dye that is utilized in monitoring lymphocyte proliferation. When cells divide, CFSE label is distributed equally between the daughter cells. As a result, halving of cellular fluorescence intensity points to successive generations in proliferating cells. When another marker specific for a certain cell population such as T cells or NK cells is used, the proliferation rate of the specific cell type can be monitored. In this study, PBMC is isolated and cells are labeled with CFSE. Then, they are incubated with various ODNs at 1 μM concentration for 72 hours. 10 μg/ml PHA is used as a positive control for the proliferation of immune cells. At the end of the incubation period, cells are stained with CD19. CD19 marker is expressed in all stages of B cell development until their maturation to plasma cells. The percentage of $CD19^+$ cells with reduced CFSE fluorescence is analyzed in B cells with FACS (Figure 18). According to these results ODN420 with PO backbone is as effective as ODN420 with PS backbone in induction of B cell proliferation. These ODNs are almost as potent as PHA. However control ODNs with PS backbone also induces B cell proliferation in correlation with the IL6 secretion level in previous cytokine ELISA on human PBMC (Figure 16). It can be suggested that

the optimal concentration of ODNs with PS backbone is much lower than 1 μM and the positive results obtained for control ODNs can be avoided when ODNs with PS backbone are used at lower concentrations. Among various ODNs with PO backbone, ODN420 is the most effective agent in induction of immune cell proliferation.

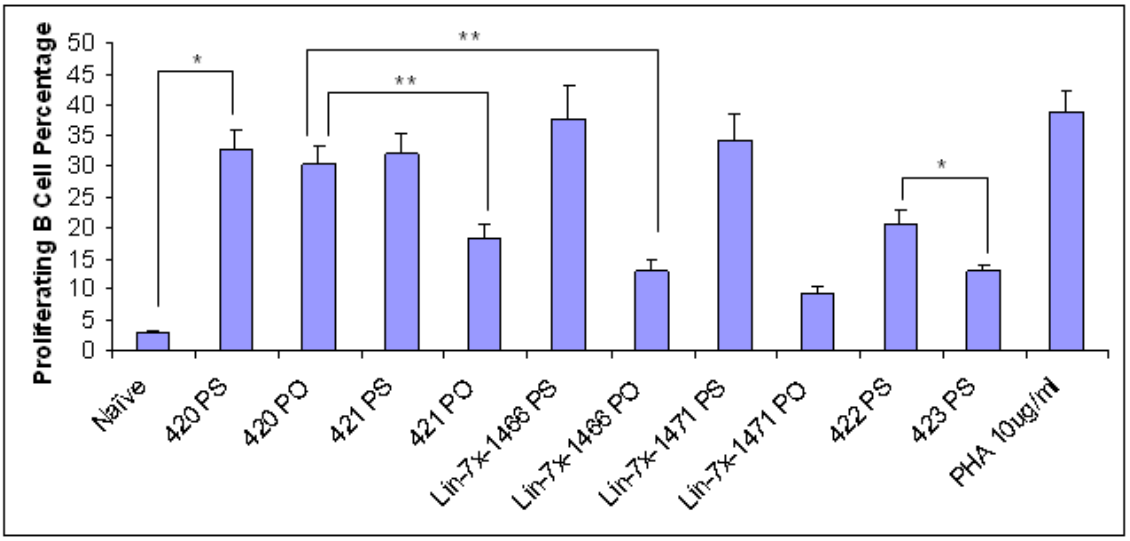

Figure 18. Proliferating B cell percentage determined by CFSE assay and CD19 staining after stimulation with various ODNs at 1 μM concentration for 72 hours. * indicates a p-value < 0.007 and ** indicates a p-value < 0.05.

4.2.3. TNFα Production by pDC After Stimulation with CpG-ODNs

In a similar experiment setup, intracellular cytokine staining is performed and TNFα production levels are compared in response to different ODNs. TNFα is a crucial cytokine involved in systemic inflammation and is a member of a group of cytokines that stimulate the acute phase reaction with IL6. For intracellular TNFα staining, cells are incubated with 1 μM of various ODNs. Brefeldin A is immediately added to tubes to prevent the secretion of TNFα from cells and incubation period is 4.5 hours. At the end of the incubation period, cells are fixed and stained with BDCA2, CD123 and TNFα antibodies in permeabilization medium. CD123 is expressed in pDC and basophils while BDCA2 is a pDC marker. Thus, $BDCA2^+$ $CD123^+$ cells represent pDC and TNFα levels are compared in $BDCA2^+$ $CD123^+$ cells (Figures 19 and 20). In Figure 19, the average TNFα+ cell percentage among BDCA2+ CD123+ cell pDC is 1.41, 25.13, 9.24, 3.56 and

5.00 in untreated cells, cells treated with ODN420-PS, ODN420-PO, ODN1466-PS and ODN1466-PO, respectively. These data suggest that ODN420 induces TNFα production by pDC much more effectively than the linear 70-mer control ODN1466. ODN420-PS induces 1.5-fold higher TNFα secretion than ODN420-PO. In general, if an agent induces high level of DC maturation and low level of TNFα production, it is a good candidate for IFNα induction. IFNα is a very critical cytokine for anti-viral immunity. Thus, it can be suggested that ODN420 with PO backbone is a better candidate for IFNα production than ODN420 with PS backbone. Although intracellular cytokine staining protocol for IFNα has been performed, a successful read-out could not be achieved (data not shown). IFNα is primarily produced by pDC, which constitute less than 0.1% of total cell population in human blood, in very low amounts. Type I IFNs (IFNα and IFNβ) and related genes have been analyzed by PCR in later experiments because of these challenges.

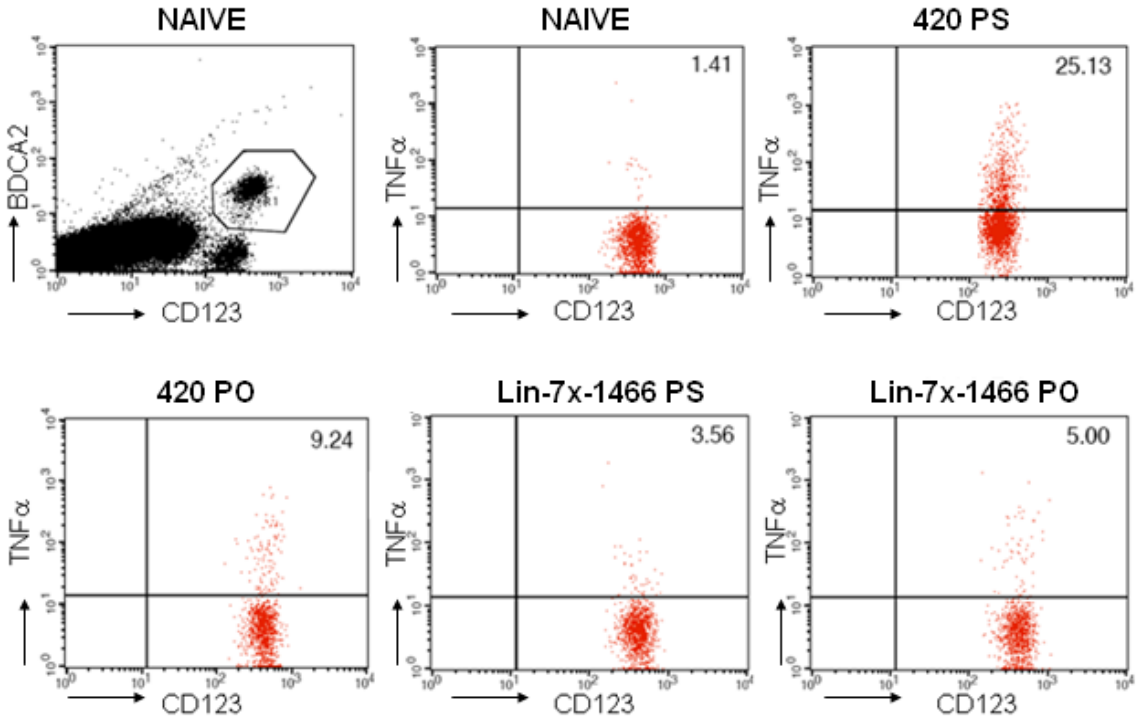

Figure 19. TNFα-positive cells in BDCA2+ CD123+ pDC stimulated with 1 μM CpG-ODN in selected groups. The dot plot on the upper left corner represents the gate used in this analysis. Percentage of triple-positive cells among BDCA2+ CD123+ pDC is given on the upper right corner of each dot plot.

Data regarding all control groups and ODN422 is given in Figure 20. ODNs with specific CpG sequences (ODN420, ODN1466 and ODN422) are more effective in inducing TNFa secretion by pDC compared to their control sequences (ODN421, ODN1471, ODN423, respectively) according to these data. ODN421-PS is the only active ODN with PS backbone in TNFα production, which is consistent with previous ELISA and FACS data regarding human PBMC. Again, the reason why ODN421 is not active in mice but active in human is unknown at this point and should be analyzed later.

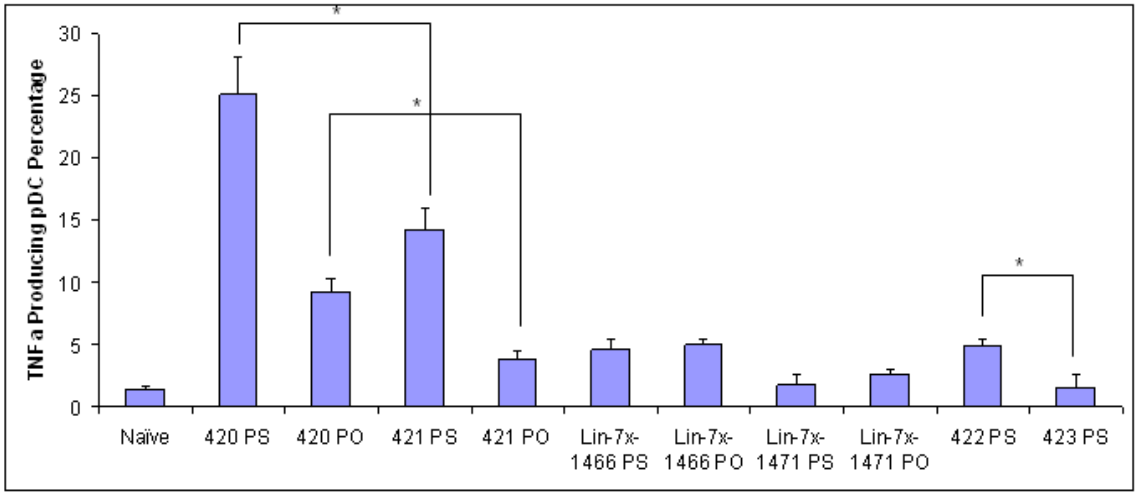

Figure 20. TNFα-positive cells in BDCA2+ CD123+ pDC stimulated with 1 μM CpG-ODN in all groups. (*p<0.05)

4.2.4. Dose-dependent Response of Human PBMC to NP-forming ODN Treatment

All previous data on human PBMC have been generated by treating the cells with 1 μM ODN concentration to differentiate the effect of ODNs at equimolar concentration. Next, it is of particular interest to identify the optimal dose of NP-forming ODN treatment in human PBMC for understanding the behavior of each ODN and for reducing the amount of human cells required in subsequent gene expression studies. Human blood is collected from two healthy donors, PBMC is isolated and stimulated with various ODNs at 3 different concentrations; 0.1 μM, 0.3 μM and 1 μM. Incubation period is 24 hours. Supernatants are collected and analyzed for IL6 and IFNg secretion by cytokine ELISA (Figures 21 and 22). Cells are collected and analyzed for activation of DC markers (CD83 and CD86) by FACS (Figures 23 and 24).

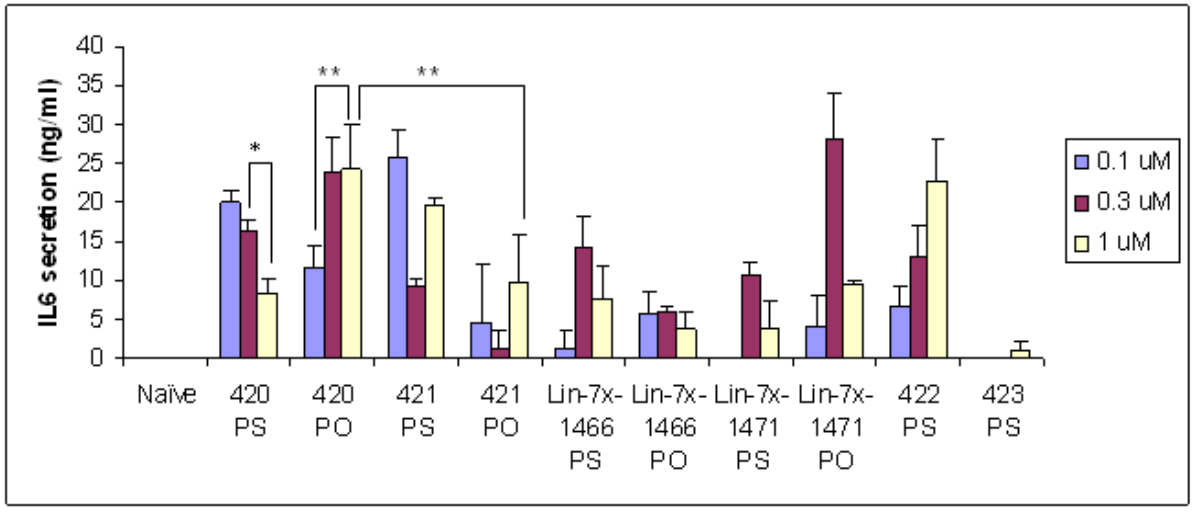

Figure 21. IL6 secretion by human PBMC in response to 0.1, 0.3 and 1 μM concentrations of CpG-ODN stimulation. * indicates a p-value < 0.01 and ** indicates a p-value < 0.05.

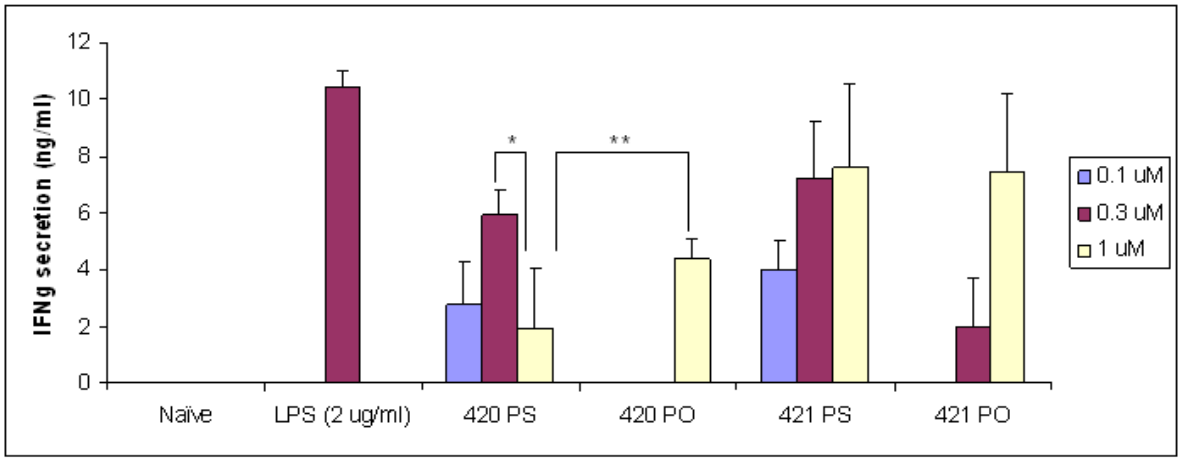

Figure 22. IFNγ secretion by human PBMC in response to different concentrations of CpG-ODN stimulation. * indicates a p-value < 0.01 and ** indicates a p-value < 0.03.

IFNγ secretion could be observed only in the groups treated with ODN420 and ODN421. This is why data regarding other groups are not shown in Figure 22. The fact that ODN421 lacks CpG motifs makes the immunostimulatory activity of ODN421 questionable. However, IFNγ secretion levels correlate with the IL6 secretion levels. Data in Figure 21 and Figure 22 further confirm that the activity of ODN420 with PS

backbone is quite high until 0.3 μM concentration. However, at higher concentrations its activity is reduced. At 0.1 μM, ODN420-PS induces 10-fold higher IL6 secretion than its linear control ODN1466-PS. The activity of ODN420 with PO backbone is enhanced as its concentration increases to 1 μM. These data are further validated by DC markers.

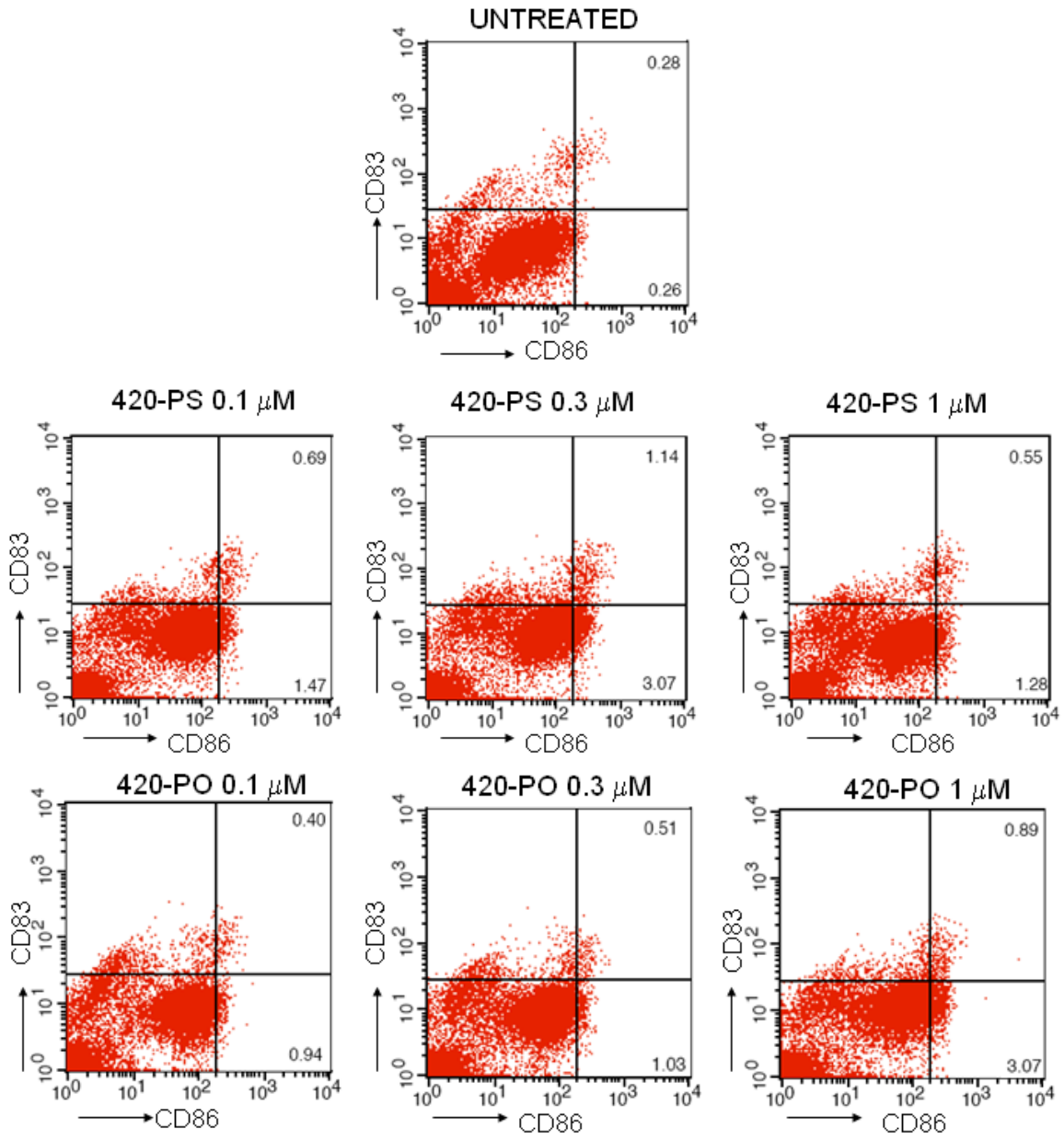

Figure 23. Activation of DC markers upon treatment with ODN420 at 0.1, 0.3 and 1 μM concentrations. CD83+ CD86+ cell percentage is given on the upper right corner. CD86+ cells, which are CD83- are given on the lower right corner of each dot plot.

According to Figure 23, CD86+ cell percentage is 0.54 in untreated cells. Upon treatment with ODN420-PS, it increases to 2.16, 4.21 and 1.83 at 0.1 μM, 0.3 μM and 1 μM concentrations, respectively. The CD86+ cells are 1.34%, 1.54% and 3.96% of the total live cell population in cells treated with ODN420-PO at 0.1 μM, 0.3 μM and 1 μM concentrations, respectively. These data again show that the optimal dose of ODN420 with PS backbone is around 0.3 μM while ODN420-PO activity is enhanced at higher concentrations. Data regarding all groups is given in Figure 24.

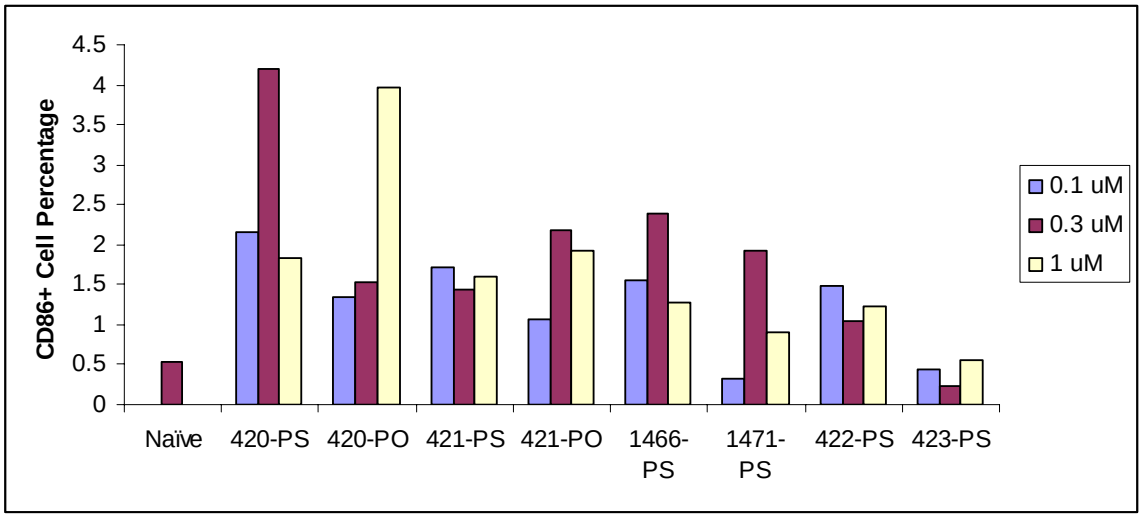

Figure 24. Dose-dependent activation of DC markers upon ODN treatment.

Similar results have been obtained for 2nd sample (data not shown). Next, we wanted to analyze if ODN420-PO activity would increase when it is used at 3 μM concentration. So, a similar assay has been performed and four different concentrations have been performed for human PBMC from two healthy donors (Figure 25). This time cells have been stimulated with 0.1, 0.3, 1 and 3 μM of various ODNs. Supernatants are collected and analyzed for IL6 secretion. According to these results, ODN420-PS activity is even lower at 3 μM than its activity at 1 μM concentration. Although the difference is not very significant, ODN420-PO activity increases when the concentration is increased from 1 μM to 3 μM. Therefore, the optimal dose for ODNs with PS backbone has been determined as 0.3 μM while the optimal dose of ODNs with PO backbone has been determined as 3 μM. These concentrations are used for the subsequent gene expression studies.

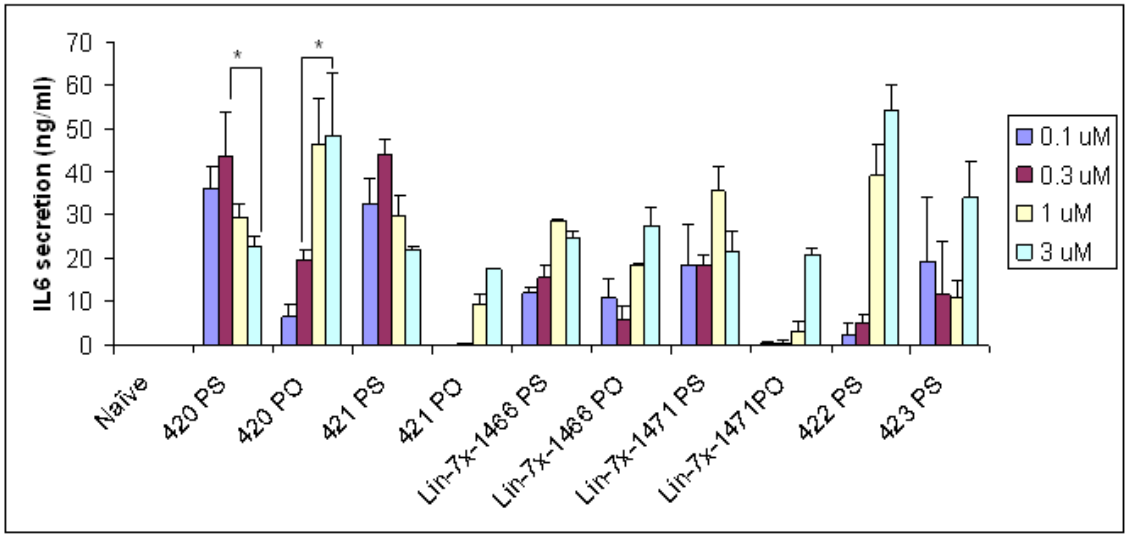

Figure 25. IL6 secretion by human PBMC in response to 0.1, 0.3, 1 and 3 μM concentrations of CpG-ODN stimulation. * indicates a p-value < 0.03.

4.2.5. Gene Expression Studies with Human PBMC After Stimulation with NP-forming ODNs at Optimal Doses

To determine the changes in endosomal TLRs and interferon-related genes upon stimulation with NP-forming ODNs, we have stimuled PBMC from two healthy donors with various ODNs for 4 hours. ODNs with PS backbone are used at 0.3 μM concentration and ODNs with PO backbone are used at 3 μM concentration since these concentrations have been previously identified as the optimal doses. Then, RNA is isolated and reverse transcriptase PCR is performed for *gapdh, ifna, ifnb, ifng, mxa-1, mxa-2, tnfa, tlr3, tlr7* and *tlr9* genes (Figure 26). Here, *gapdh* is a housekeeping gene and used as an internal control to show that cDNA levels of samples are in equal amounts. *Mxa-1* and *mxa-2* are critical interferon-inducible genes that function in anti-viral immunity. PCR products are run on agarose gel and the band intensities of stimulated groups are compared with untreated (naïve) group. The band intensity of naïve group is considered as "1" and band intensities of other groups are calculated according to this value. Comparison of band intensities for first sample is given in Figure 27. Similar results are obtained for second sample (please see Appendix). Band intensity values for

genes that are not expressed at basal level cannot be compared according to this method and the results of treatment groups are compared among each other.

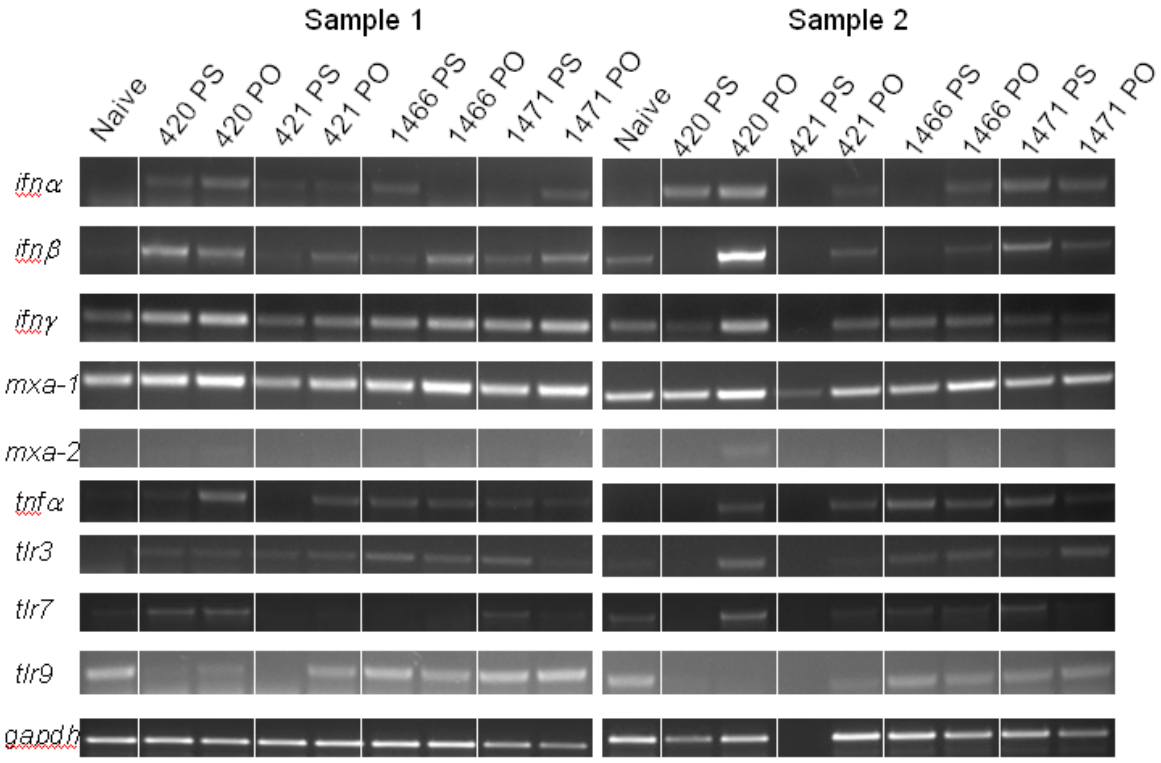

Figure 26. The agarose gel picture of the RT-PCR products of *tnfα*, *ifn*-related genes and endosomal *tlr* genes. PBMCs from two donors are stimulated with NP-forming ODNs at optimum doses for 4 hours.

Ifnα, *mxa-2*, *tnfα* and *tlr3* are not expressed at all in untreated groups (Figure 26). However, the expression of these genes is highly induced upon treatment with ODN420-PS and ODN420-PO. In both samples, there is a high level of induction of *ifnα*. The level of induction with control ODNs is much lower compared to ODN420-PS and ODN420-PO groups. In the comparison between PS and PO backbones, 420-PO induces higher levels of *ifnα*, *mxa-2* and *tlr3* in the first sample compared to ODN420-PS. In the second sample, *mxa-2*, *tnfα* and *tlr3* bands cannot be visualized in the ODN420-PS group emphasizing the efficacy of ODN420 with natural phosphodiester (PO) backbone. Also, *ifnb*, *ifng* and *tlr7* expression levels in ODN420-PS group are comparable with untreated group and expression of these genes increases 2-4 fold in ODN420-PO group in the

second sample (please see Appendix B). It can be argued that the superiority of ODN420-PO with respect to ODN420-PS can be caused by the concentrations used in the treatment. However, these concentrations have been determined as the optimal doses and it has been repeatedly shown that ODN420-PS activity decreases at concentrations higher than 0.3 μM. Thus, it can be suggested that the differences between mRNA levels between these two groups would become even higher if ODN420-PS were used at 3 μM, the concentration at which ODN420-PO has been used.

In the first sample, *ifnβ* expression significantly increases to almost 9-fold and 7-fold upon stimulation with ODN420-PS and ODN420-PO, respectively (Figure 27A). *Ifnγ* expression is 2-fold higher and 3-fold higher in ODN420-PS and ODN420-PO groups respectively than basal expression level in untreated group (Figure 27B). Although control ODNs induce the expression of these genes up to a point, the fold induction in *mxa-1* gene underlines the specificity of stimulation with ODN420. This critical interferon-inducible gene is only induced in ODN420 groups (Figure 27C). Again, ODN420-PO is more effective in *mxa-1* induction than ODN420-PS. The changes in the expression level of endosomal *tlr* genes are very important in this study. In addition to the upregulation of *tlr3* gene discussed above, *tlr7* is expressed at 3.5-fold higher level in ODN420-PS treated group and 5-fold higher in ODN420-PO group (Figure 27D). None of the control ODNs causes an increase in the expression level of *tlr7*. The down-regulation of *tlr9* gene, whose product is considered to play the central role in the effect of CpG-ODNs, is not surprising (Figure 27E). It has been well-established that there is a control mechanism in the cell. When TLR9 signaling pathway is activated, its expression level is reduced for 8 hours to check that the danger signal really exists. If the signal persists after this time point, its expression is up-regulated. In this experiment, incubation period is 4 hours. According to these data, *tlr9* expression is 90% and 60% reduced in ODN420-PS and ODN420-PO treated groups, respectively. Among control ODNs, down-regulation of *tlr9* is observed only in ODN421-PS, which is again consistent with previous data regarding ODN421-PS activity in human cells. Therefore, the down-regulation of *tlr9* gene implies that TLR9 signaling pathway is active in groups treated with ODN420. Also, these data suggest that ODN420-PS is as at least as active as ODN420-PO and possibly even more when it is used at its optimal concentration, 3 μM.

A)

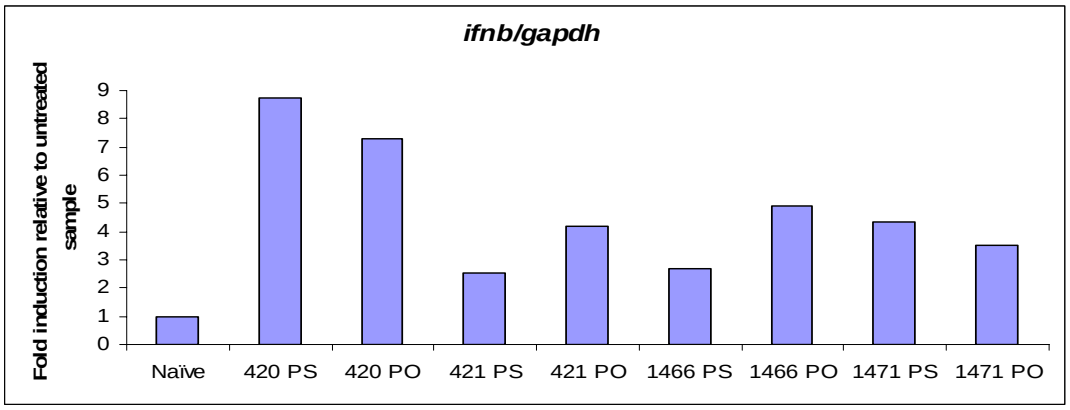
ifnb/gapdh
Fold induction relative to untreated sample
0
1
2
3
4
5
6
7
8
9
Naïve
420 PS
420 PO
421 PS
421 PO
1466 PS
1466 PO
1471 PS
1471 PO

B)

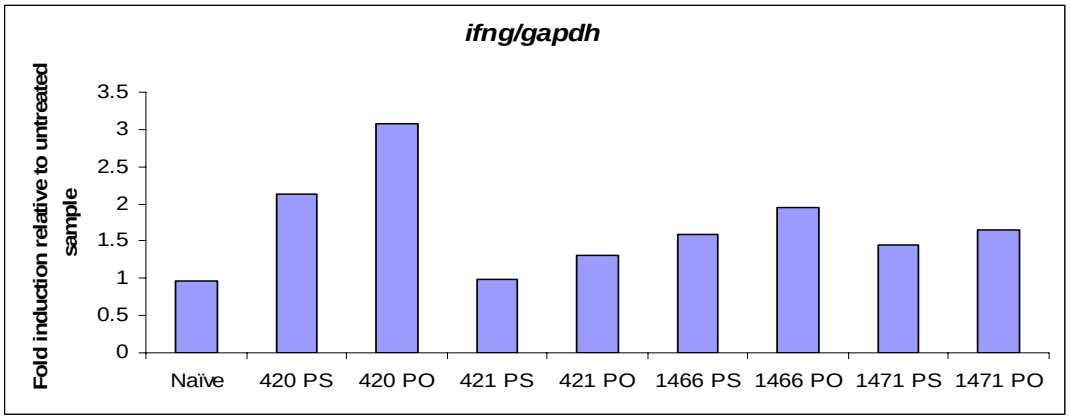
ifng/gapdh
Fold induction relative to untreated sample
0
0.5
1
1.5
2
2.5
3
3.5
Naïve
420 PS
420 PO
421 PS
421 PO
1466 PS
1466 PO
1471 PS
1471 PO

C)

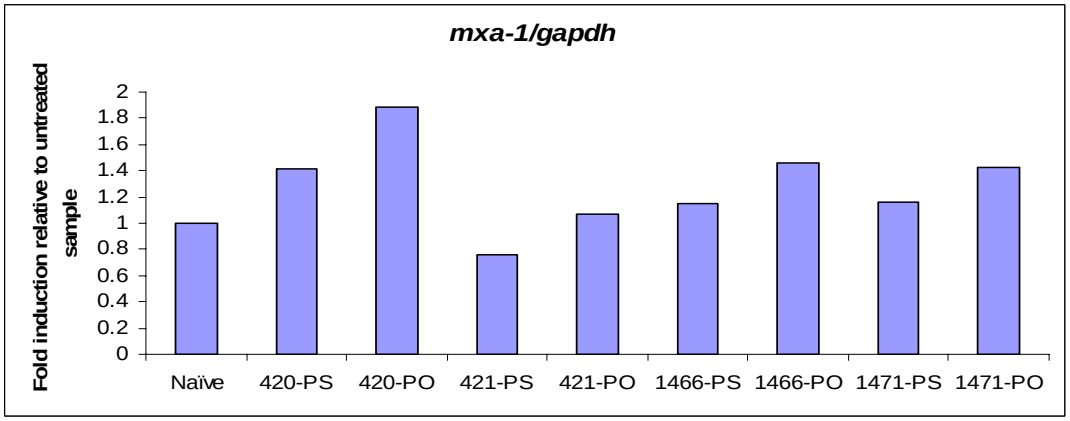
mxa-1/gapdh
Fold induction relative to untreated sample
0
0.2
0.4
0.6
0.8
1
1.2
1.4
1.6
1.8
2
Naïve
420-PS
420-PO
421-PS
421-PO
1466-PS
1466-PO
1471-PS
1471-PO

D)

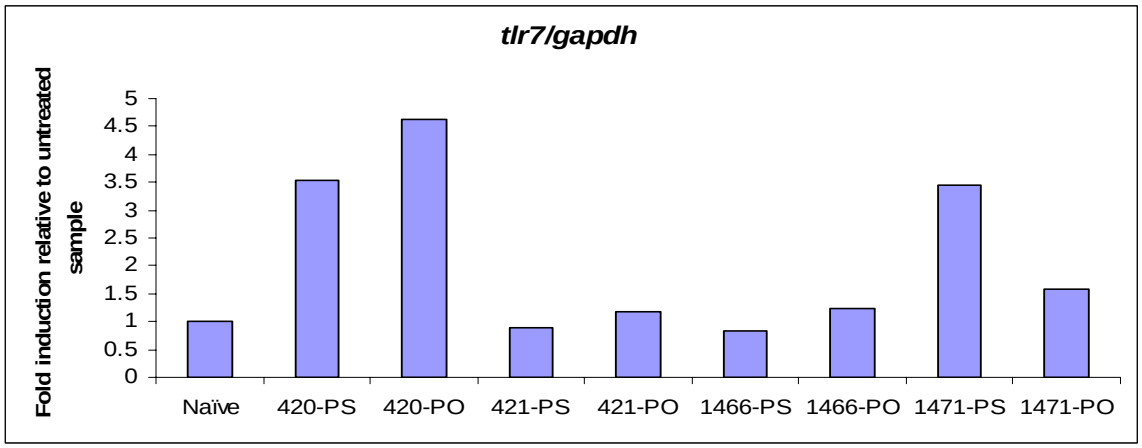

E)

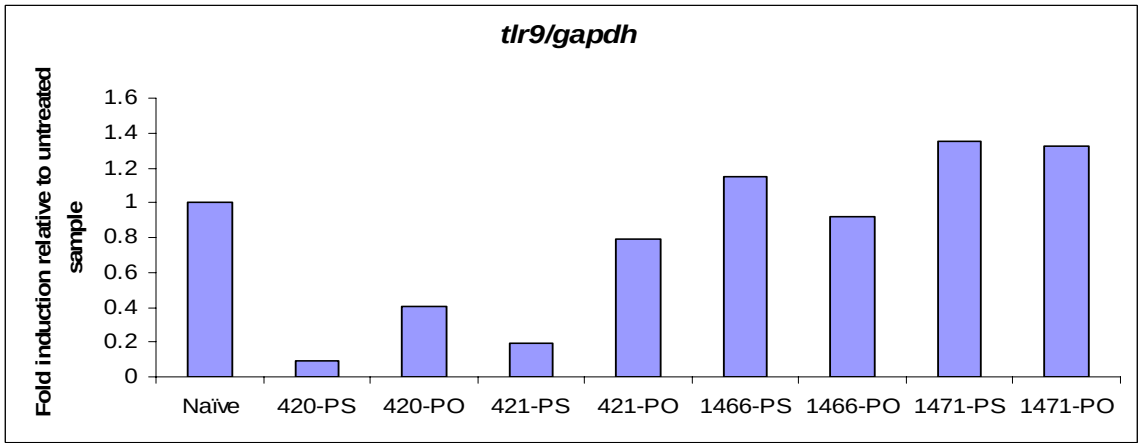

Figure 27. Fold induction graphs of various interferon related genes and endosomal tlr genes at mRNA level for the first sample. The expression profiles of *ifnb* (A), *ifng* (B), *mxa-1* (C), *tlr7* (D) and *tlr9* (E) in untreated and treated groups are compared by band intensities in the gel pictures in Figure 26.

4.3. *In vivo* Studies Utilizing Nanoparticle Forming Immunostimulatory and Immunosuppressive ODNs

4.3.1. *In vivo* Stimulatory Potential of Nanoparticle Forming ODNs

So far, *in vitro* data suggested that dendrimeric novel CpG-ODNs pose a higher immunostimulatory potential than the linear control ODNs and this effect is specific since control ODNs with GC flip sequences are not stimulatory except for ODN421-PS in human cells. After the promising *in vitro* studies, next step is naturally to test the effect of

these ODNs upon injection into C57BL/6 mice. To test the *in vivo* effect of dendrimeric CpG-ODNs, they are injected intraperitoneally to mice along with conventional A-type ODN D35. The injected dose is 20 μg for ODNs with PS backbone and 60 for ODNs with PO backbone and D35. Five hours after *in vivo* i.p. injection, animals are euthanized. Spleens are removed, single cell splenocytes are prepared, RNA is isolated and the expression profiles of various cytokines, chemokines and *tlr* genes are compared by RT-PCR. PCR products are run on agarose gel (Figure 28) and the band intensities of stimulated groups are compared with untreated (naive) group (Figure 29).

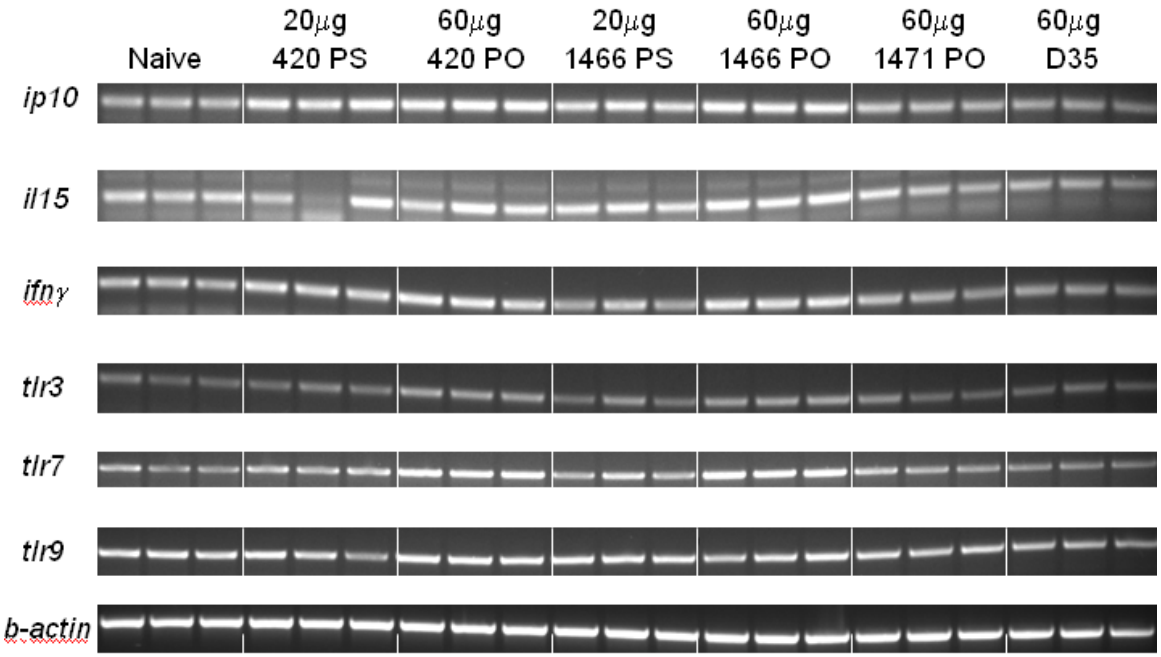

Figure 28. The agarose gel picture of the RT-PCR products of ip10, il15, ifnγ and endosomal tlr genes in splenocytes of mice injected with 20 μg of ODN with PS backbone or 60 μg of ODN with PO backbone.

A)

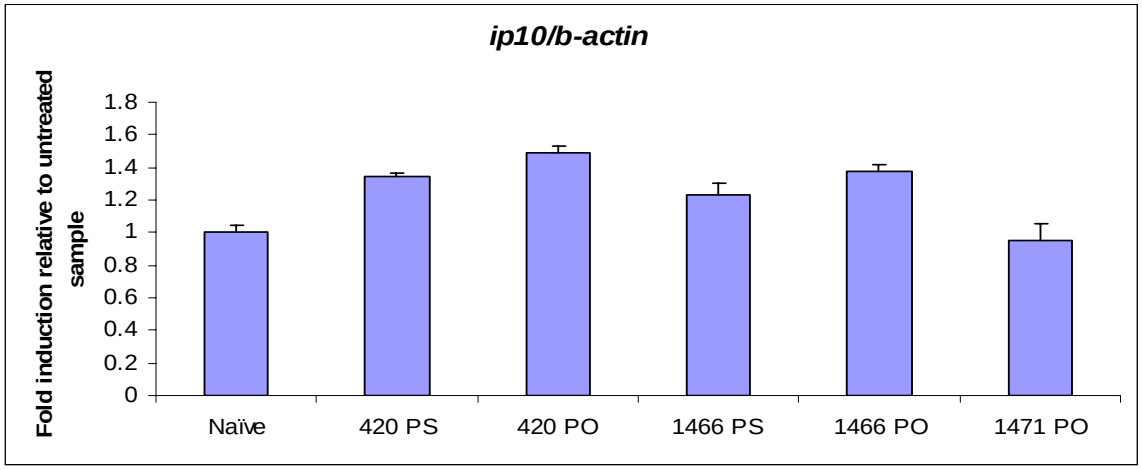
ip10/b-actin
Fold induction relative to untreated sample
1.8
1.6
1.4
1.2
1
0.8
0.6
0.4
0.2
0
Naïve
420 PS
420 PO
1466 PS
1466 PO
1471 PO

B)

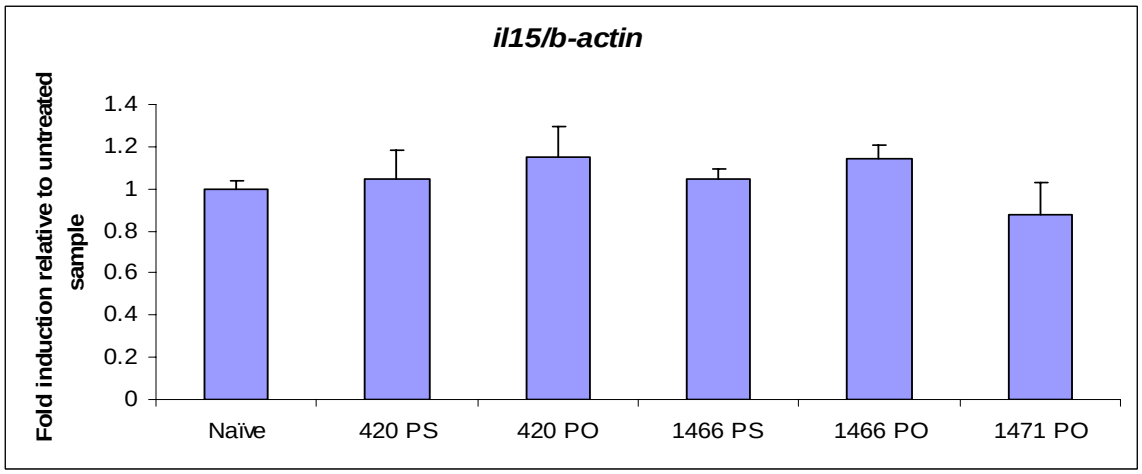
il15/b-actin
Fold induction relative to untreated sample
1.4
1.2
1
0.8
0.6
0.4
0.2
0
Naïve
420 PS
420 PO
1466 PS
1466 PO
1471 PO

C)

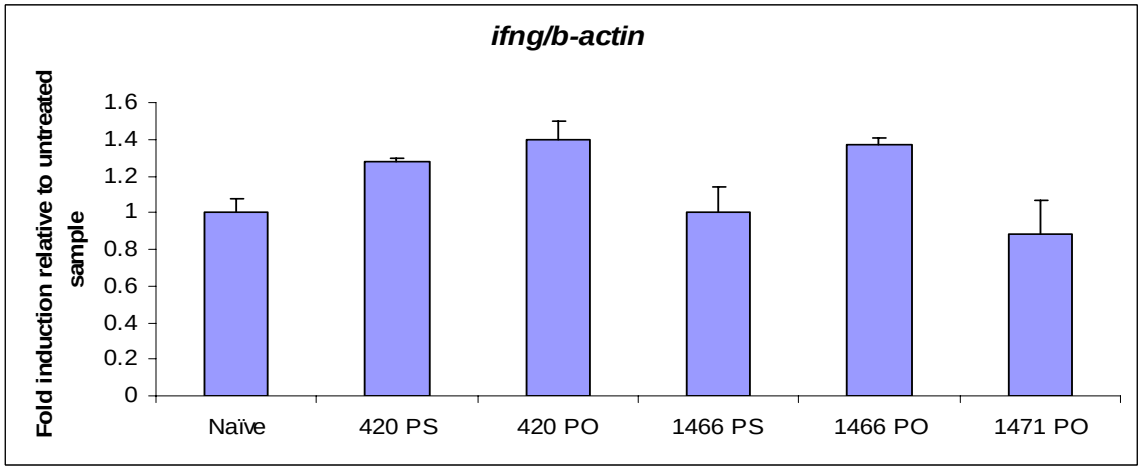
ifng/b-actin
Fold induction relative to untreated sample
1.6
1.4
1.2
1
0.8
0.6
0.4
0.2
0
Naïve
420 PS
420 PO
1466 PS
1466 PO
1471 PO

D)

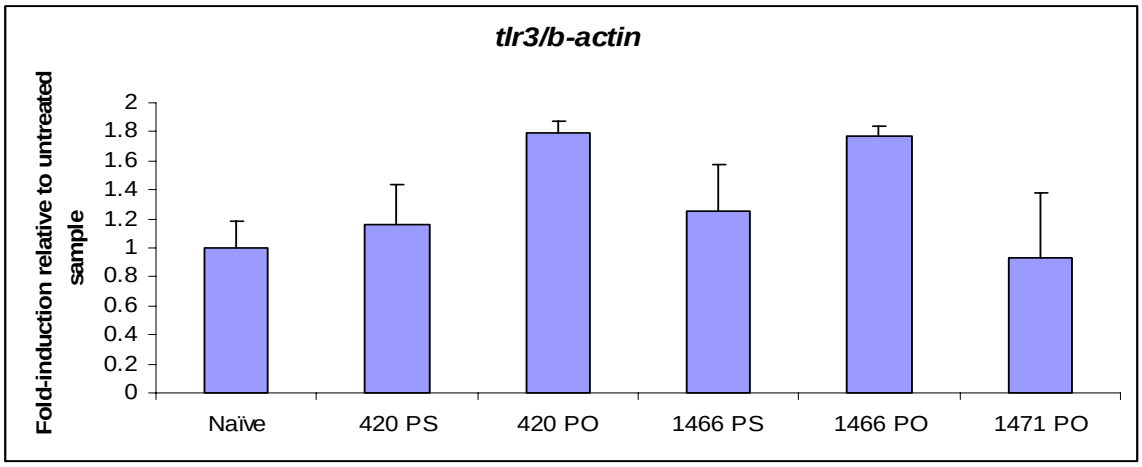

E)

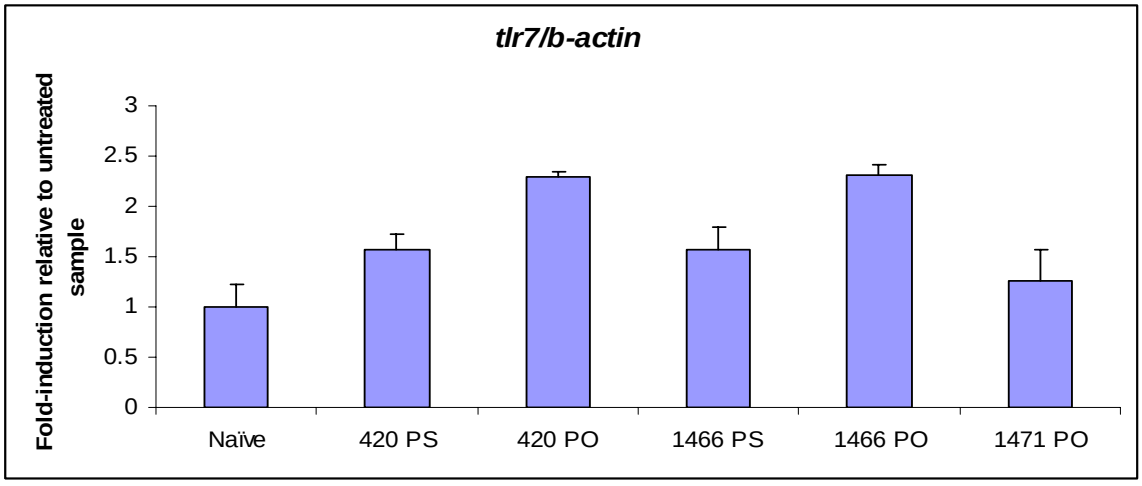

F)

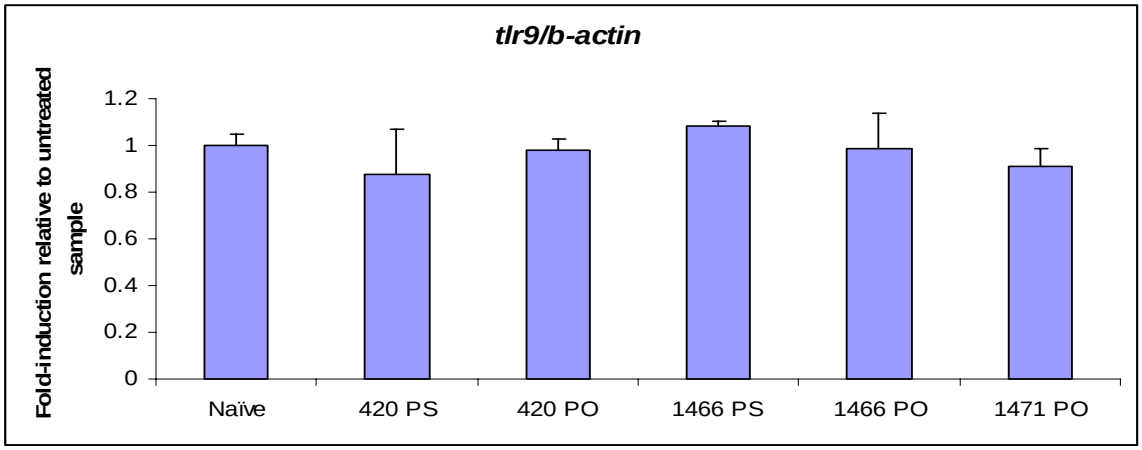

Figure 29. Relative band intensities of various critical genes. The expression profiles of *ip10* (A), *il15* (B), *ifnγ* (C), *tlr3* (D), *tlr7* (E) and *tlr9* (F) in untreated and treated groups are compared by band intensities in the gel pictures in Figure 28.

This study reveals that dendrimeric ODNs are also active in *in vivo* conditions. The fold-induction levels are smaller with respect to *in vitro* studies. Yet, this is quite expectable because of the distribution of the agent in the organism. With respect to untreated group, ODN420-PS and ODN420-PO cause a 40% increase in *ip10* expression in mouse splenocytes (Figure 29A). IP10 is a chemokine that has a critical role in recruitment of immune cells to sites of inflammation and its expression is inducible by IFNs (both type I and II). The increase of *il15* expression is around 20% (Figure 29B) and that of *ifnγ* expression is around 30% (Figure 29C) in ODN420 treated groups with respect to untreated group. The increase in the expression of these critical genes suggests that the immune system is activated upon treatment with dendrimeric ODNs. ODN1466, the linear control of ODN420, is also quite active but it is relatively less stimulatory than ODN420. Meanwhile, ODN1471, the control of ODN1466 with the GC flip dinucleotide sequence, exhibits no stimulatory potential and the genes are expressed at a level similar to untreated group. The expression levels of *tlr3* and *tlr7* are enhanced and that of *tlr9* is reduced upon treatment with ODN420 (Figures 29D, 29E and 29F). In all cases except for reduction of *tlr9* expression, ODN420-PO is around 10%-40% more active in *in vivo* conditions. These results suggest that ODN420 with the natural phosphodiester backbone is at least as potent as its counterpart with the modified phosphorothioate backbone *in vivo* when it is used at its optimal concentration.

4.3.2. Immunization of C57BL/6 Mice with Dendrimeric ODNs and OVA in Combination With or Without Nanoparticle Forming Suppressive ODN

Having established the *in vivo* immunostimulatory activity of ODN420, we wanted to investigate whether we could use this ODN as a vaccine adjuvant. In spite of the high potential of ODN420 with PO backbone, we decided to use ODN420-PS in this study because of its higher resistance against nucleases. Additionally, we wanted to find out if the immunosuppressive NP-forming ODN, ODNA151, would inhibit this Th1-mediated response in the immunization protocol by increasing Th2 activity. The protocol is discussed in detail in the Materials and Methods section. Briefly, three adult male C57/BL6 mice per group are injected intraperitoneally with 15 μg of ODN-D35, ODN-D35 or ODN-420 and 7.5 μg of OVA in combination with or without 15 μg A151.

Fourteen days later, boosting injection is performed i.p. with the same ODN and OVA combinations. Animals are bled one day before each injection and on the twenty-seventh day. Animals are sacrificed on day twenty-eight and their spleens are removed. Background, primary and secondary sera are analyzed for the level of specific IgG subtypes by IgG anti-OVA ELISA (Table 11 and Table 12). Single cell splenocytes are studied for the expression of certain cytokines at mRNA level (Figure 30). Anti-OVA IgG ELISA for sera from background bleeding has revealed that all groups are positive at 1 / 7±4 titer (data not shown). Thus, all changes in IgG levels are caused by the specific activity of ODNs.

Table 11. IgG anti-OVA ELISA for total IgG, IgG1, IgG2a and IgG2b subtypes in sera from primary bleeding.

	TITER 1/N AT WHICH SERA FROM PRIMARY BLEEDING IS POSITIVE			
Treatment group	**Total IgG**	**IgG1**	**IgG2a**	**IgG2b**
Untreated	7 ± 4	7 ± 4	7 ± 4	7 ± 4
A151+OVA	7 ± 4	7 ± 4	7 ± 4	7 ± 4
D35+OVA	28 ± 14	7 + 14	14 ± 2	7 ± 2
D35+A151+OVA	7 ± 4	7 ± 4	7 ± 2	7 ± 2
420-PS+OVA	112 ± 20	7 ± 4	7 ± 2	7 ± 2
420-PS+A151+OVA	7 ± 4	7 ± 4	7 ± 2	7 ± 2

First number represents the average of sera titer at which IgG can be detected from three mice and the second number represents the standard deviation.

Table 11 reveals that primary bleeding sera from D35-treated group is positive for IgG at a titer of 1/28. On the other hand, ODN420-treated group is positive for total IgG at a titer of 1/112 even before boosting injection, which is lower than that of D35. Meanwhile, NP-forming immunosuppressive ODN, ODNA151, in general reduces the total IgG, IgG2a and IgG2b titers when it is used in combination with stimulatory ODNs that are used as adjuvants. ODN420 in combination with A151 treated group is positive for total IgG at a titer of 1/7.

Table 12. IgG anti-OVA ELISA for IgG, IgG1, IgG2a, IgG2b subtypes in sera from secondary bleeding.

	TITER 1/N AT WHICH SERA FROM SECONDARY BLEEDING IS POSITIVE			
Treatment group	**Total IgG**	**IgG1**	**IgG2a**	**IgG2b**
Untreated	7 ± 4	7 ± 4	7 ± 4	7 ± 4
A151+OVA	7 ± 4	7 ± 4	7 ± 4	7 ± 4
D35+OVA	1792 ± 500	1300 ± 450	112 ± 12	112 ± 12
D35+A151+OVA	28 ± 14	28 ± 12	7 ± 2	7 ± 2
420-PS+OVA	4000 ± 800	1500 ± 300	448 ± 50	28 ± 4
420-PS+A151+OVA	792 ± 480	500 ± 25	7 ± 4	7 ± 4

First number represents the average of sera titer at which IgG can be detected from three mice and the second number represents the standard deviation.

Data from secondary bleeding (Table 12) is even more informative because high IgG values are expected to be seen after the boosting injection in immunization protocols. Untreated and A151-treated groups are not positive for any IgG at titers lower than 1/7, as expected. In the comparison between the efficacy of D35 and ODN420 as vaccine adjuvants, D35-treated group is positive for total IgG, IgG1, IgG2a and IgG2b at titers of 1/1792, 1/1300, 1/112 and 1/112, respectively. However, ODN420-treated group is positive for this IgGs at titers of 1/4000, 1/1500, 1/448 and 1/28, respectively. Thus, ODN420 induces higher levels of IgGs than ODN-D35 except for only IgG2b. The 1/448 titer at which IgG2a is positive suggests that ODN420 induces a strong Th1 response. In correlation with the data from primary bleeding, A151-treatment down-regulates the Th1 response in the immunization protocol. In ODN420 in combination with A151 treated group, positive titers are 1/792, 1/500, 1/7 and 1/7 for total IgG, IgG1, IgG2a and IgG2b, respectively. Thus, the efficacy of ODN420 is lowered as an adjuvant. In general, the IgG2a/IgG1 ratio implies the strength of Th1 response. The higher the IgG2a and the lower the IgG1, the more effective the Th1 response. Significantly, the 1/500 titer and the 1/7 titer at which ODN420 and A151-treated group is positive for IgG1 and IgG2a indicate that the Th1 response is strongly suppressed. We cannot reach to the conclusion that this is achieved by enhancing Th2 response with these data. Further studies such as IL4 ELISA are required to show that ODN-A151 increases Th2 response.

These data imply that ODN420 can be successfully used as a vaccine adjuvant and is a strong inducer of Th1 response. Meanwhile, ODN-A151 lowers the Th1 response that is caused by various ODN adjuvants and OVA. ODN-A151 treatment has no effect by itself. Yet, if a strong Th1 response is generated, ODN-A151 fine-tunes and reduces the Th1 response possibly by causing a shift to Th2 response, according to these data. These results are also validated by RT-PCR of critical genes involved in immune system. Both up-regulation of critical genes involved in immune system upon dendrimeric ODN-treatment and the fine-tuning, which results in down-regulation of these genes, upon ODN-A151 treatment are further confirmed by RT-PCR results (Figure 30). Band intensity analysis reveals that ODN420 induces 50% higher *ifnγ* expression with respect to untreated group (data not shown). D35 and ODN-420 cause a general increase in transcription of *cd40*, *il15* and *ifnγ*. The up-regulation effect is hindered when these stimulatory ODNs are used in combination with ODN-A151.

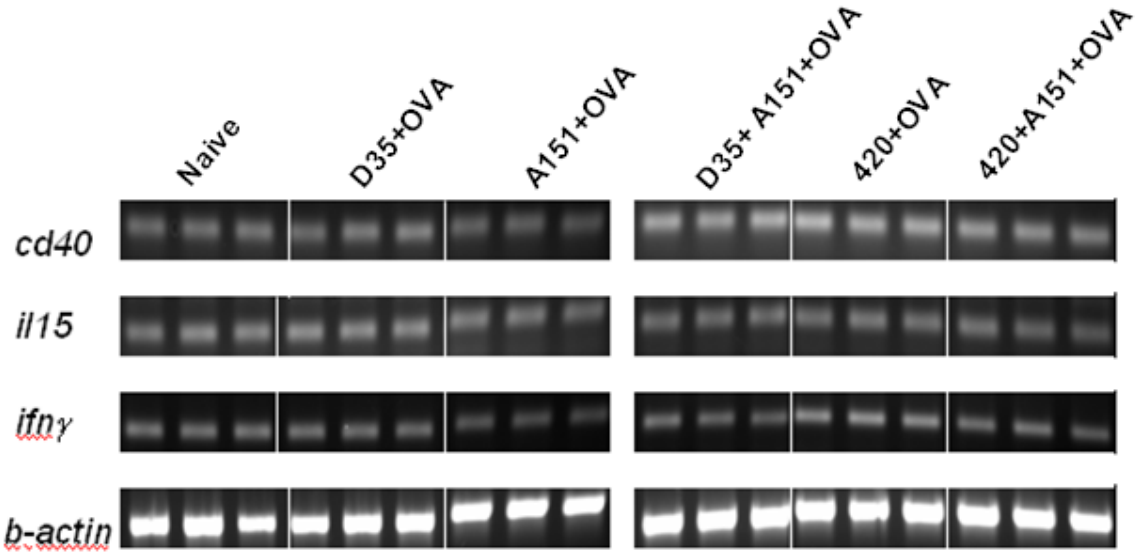

Figure 30. The agarose gel picture of the RT-PCR products of ip10, il15, ifnγ and endosomal tlr genes in splenocytes of mice immunized with two doses of 15 µg ODN and 7.5 µg OVA.

4.3.3. Use of Nanoparticle Forming ODNs as Anti-Cancer Agents

CpG-ODNs are known to induce anti-tumor immunity by a variety of mechanisms including induction of CD8+ cytotoxic T cells, up-regulation of MHC molecules by tumor cells as well as antigen-presenting cells and interfering with the immunosuppressive microenvironment generated by tumors. Approximately 30% of cancer cases are caused by an inflammatory background and details of the relationship between cancer and inflammation are being recently discovered. For example, NF-kB is a central transcription factor in inflammatory response. Yet, it also causes production of angiogenic factors and growth signals that can promote malignant progression. With these data in literature, we wanted to test the effect of ODN-420 and ODNA151 in tumor xenografts. Details of this experiment are given in the Materials and Methods section. Briefly, Huh7 cells, a human hepatocellular carcinoma cell line, are xenografted into T-cell deficient nude mice. Since tumor formation is heterogeneous and some nude mice develop tumors later than 3 weeks, the day on which a palpable tumor forms is considered as day 0. Three doses of 100 µg of ODN-420 or ODN-A151 are injected intratumorally with one day-on and one day-off treatment starting from day 3 post-palpable tumor formation. Tumor dimensions are recorded daily as width, height and length by a caliper and calculated as mm^3 (Figure 31A and Figure 31B). Pictures of tumor xenografts in untreated and ODN420-treated mice are given in Figure 32.

A)

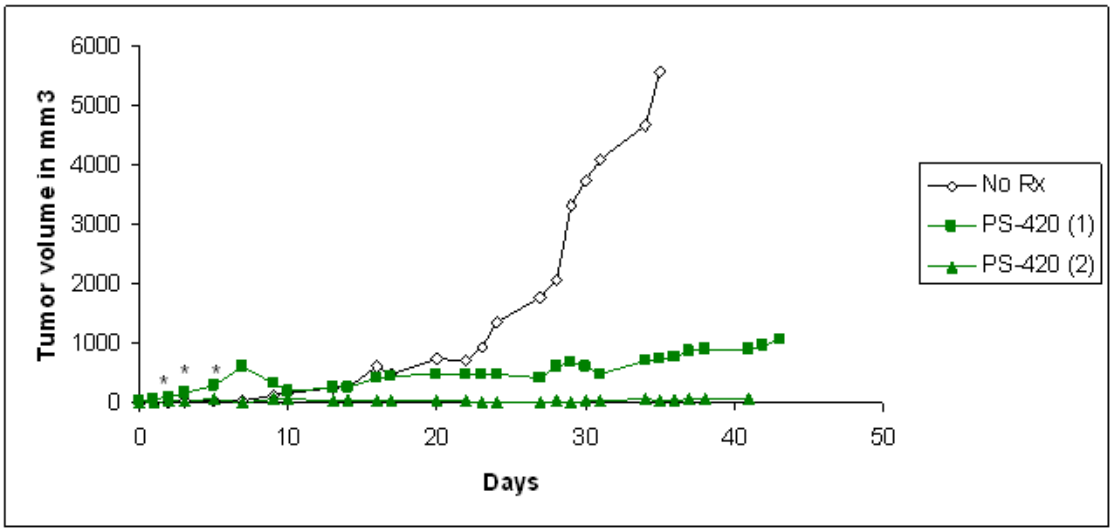

B)

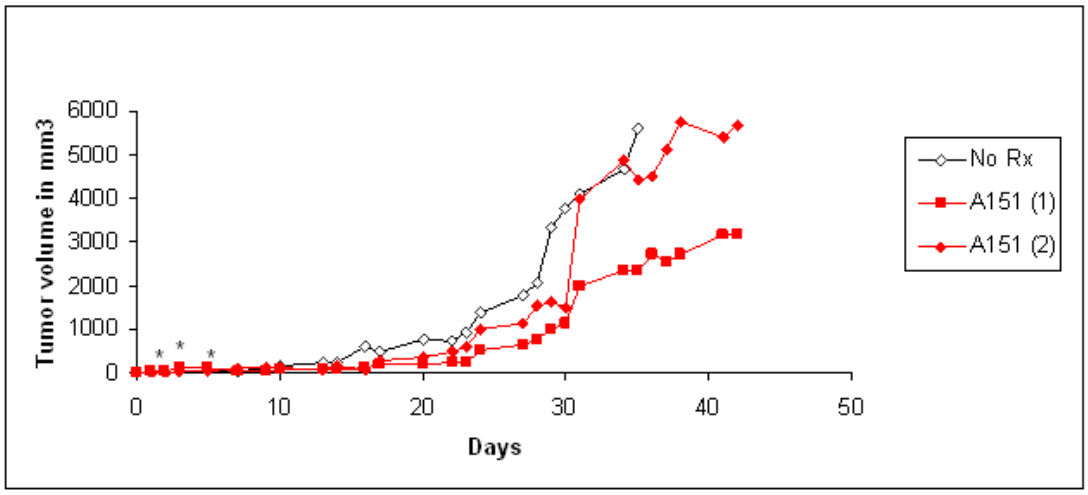

Figure 31. The effect of nanoparticle forming ODNs as anti-cancer agents. Tumor volumes of untreated mice and mice treated with ODN-420 are given in (A). Tumor volumes of untreated mice and mice treated with ODN-A151 are given in (B).

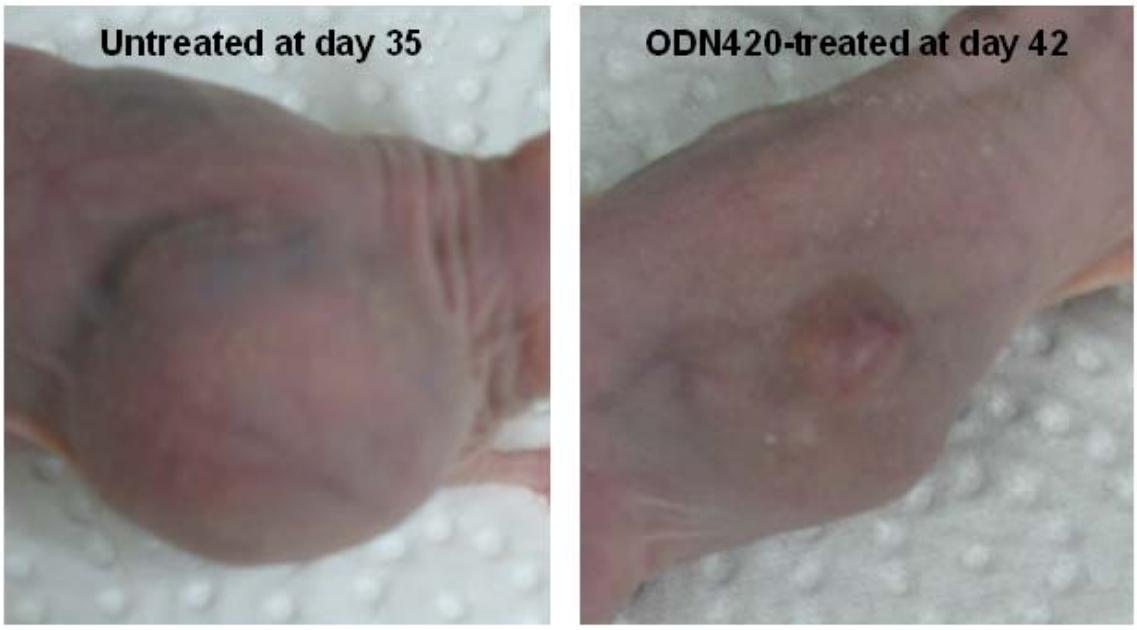

Figure 32. Tumor xenografts in untreated and ODN420-treated mice at days 35 and 42 post palpable tumor formation, respectively.

Although it might seem confusing to study both immunostimulatory and immunosuppressive ODNs as anti-cancer agents, cancer is a very complex disease. While an anti-tumor immunity is critical for the organism's response against cancer, an

inflammatory micro-environment can support the growth of tumor. At day thirty-five tumor volume is 5586 mm^3 in untreated mice. At the same day, tumor volumes are 900 mm^3 and 72 mm^3 in mice treated with ODN-420 (Figure 32). According to these data, ODN-420 treatment can cause partial remission of the tumor. This effect is observed in one mouse treated with ODN-420. The growth of tumor is delayed in the other animal in the same group. In the comparison between ODN-A151 treated tumor xenografts and untreated xenograft, ODN-A151 cannot induce remission of the tumor but only delay the tumor growth (~d=30). Therefore, ODN-420 is a more promising candidate as an anti-cancer agent than ODN-A151. Certainly, sample size should be increased in the future experiments for statistical significance of these data.

5. DISCUSSION

CpG ODNs are of great importance for the regulation of the immune system. While K-type ODNs induce higher levels of IL12 and TNFα, D-type ODNs stimulate higher levels of anti-viral type I IFNs and induce maturation of monocytes into DCs. While each class of CpG ODN (D-type, K-type, C-type), results in different activities, these differences are also brought forth by several factors. These factors are the number of CpG motifs on one strand, backbone chemistry (PS vs. PO), flanking sequences (Pu-Pu-C-G-Py-Py or Pu-Py-C-G-Pu-Py), presence of poly-G runs at terminal end and the physical structure of the ODN (linear single-strands vs. multimeric structures that form nanoparticles). One challenge in the identification of optimal CpG sequences for human studies is that many ODNs that are active in mice, do not exhibit similar immunostimulatory potentials in human cells.

ODNs that are able to form multimeric structures and are of nanoparticulate nature are superior in their immunostimulatory potentials than those that remain as single-stranded linear structures for several reasons. First, they are retained in early endosomes for a longer period and able to promote type I IFN production. Second, they pose higher activity under physiological conditions. Because of premature serum protein binding and exonuclease activity, most of the administered ODNs are degraded/eliminated before they reach the relevant target immune cells. Finally, they are superior to their linear counterparts in terms of effective internalization. A scavenger receptor, CXCL16, is used as a co-receptor in the uptake of ODNs with nanoparticulate nature (Gursel et al., 2006). This scavenger receptor does not promote the uptake of ODNs that remain as linear structures in the body.

During various attempts to manipulate the physical structure of ODNs and increase its resistance to nucleases, CpG ODN has been previously loaded into nanoparticulate phospholipid carriers such as liposomes. ODNs loaded into sterically stabilized cationic liposomes are more effectively internalized by immune cells and exhibit immunostimulatory activity at low concentrations (Gursel et al., 2001). Additionally, linear ODNs complexed with particulate carriers such as DOTAP liposomes or polymyxin have been also shown to exhibit IFNα production (Guiducci et al., 2006; Honda et al., 2005a). This shows that the primary determinant of immune

activation is not ODN type or the sequence but the endosomal localization of ODNs. Another group has taken a different approach to construct ODNs with multimeric structures and has shown that addition of poly-G tails to ODNs with PO backbone can enable multimerization and thus sequence independent IFNα production (Haas et al., 2009).

We have designed a novel dendrimeric ODN, ODN-420, which spontaneously folds into a multimeric structure and exhibits high immunostimulatory potential (Mammadov, M.Sc. thesis). It contains 7 CG motifs and has the potency to exhibit more resistance against nucleases because of its nanoparticulate nature without the use of an additional carrier system (Karatepe, Mammadov and Gursel, *unpublished data*). To date, there is no reported dendrimeric ODN in the literature. Previous studies have focused on the activity of this ODN with the more nuclease resistant PS backbone on mouse splenocytes. However, this modification brings another level of complexity and increases the cost of production in large scale synthesis. We have analyzed whether ODN420 with the natural PO backbone would be as active as ODN420 with the PS backbone and whether ODN420 would be a potent type I IFN inducer. For a preliminary *in vitro* study, we have incubated mouse splenocytes with different concentrations of dendrimeric ODNs and the control ODNs. As shown in Figure 15, at low dose (0.3 μM), ODN420-PS exhibits a much higher activity in comparison to ODN420-PO, as expected. However, this difference is not observed at 1 μM concentration, where ODN420-PO is even more immunostimulatory than ODN420-PS. In control ODNs (ODN421 and ODN1471), where the CpG motif is fliped by a GpC motif, there was no activity. This shows that the immune activation is CpG-motif dependent and mediated by TLR9, rather than the sequence-independent effects of these long ODNs. Additionally, the linear 70-mer ODN1466 is a less potent inducer of IL6 than the dendrimeric ODNs. This clarifies that the level of immune activation is dependent on the multimeric structure formed by dendrimeric ODNs.

After establishing that ODN420-PO is as active as ODN420-PS at 1 μM in mice splenocytes, we next analyzed the activity of these ODNs on human peripheral blood mononuclear cells (PBMC) with various assays. As previously mentioned, sequences with high immunostimulatory potential in mouse cells, are rarely active at comparable

levels in human cells because of the differences in the optimal sequences in human and mice cells. For this assay, human PBMC have been incubated with 1 μM of various ODNs. IL6 secretion levels have been compared by ELISA and DC activation marker levels have been assessed by flow cytometry. In Figure 16, it is observed that ODN420 with PO backbone is as active as PS backbone at 1 μM. These results correlate with data from mice splenocytes. Again, the control ODNs with PO backbone, which contain flipped motifs of GC instead of the CG motif, are not active in human PBMC. Of particular interest, 421-PS and 1471-PS control ODNs which are not stimulatory in mouse splenocytes, are found to be active in human PBMC albeit, there is a donor to donor variation. Analysis of relevant DC activation markers, which gives information on the maturation/activation of antigen presenting cells, has been performed in Figure 17. These results have revealed that ODN420 both with the PS backbone and PO backbone trigger the activation of antigen presenting cells.

In another experiment, the effect of dendrimeric ODNs on proliferation of B cells has been analyzed. Figure 18 shows that ODN420-PO is as effective as ODN420 with PS backbone in the induction of B cell proliferation at 1 μM. It is important to note that, 1μM ODNs were used in this experiment, PS backbone ODNs were known to induce sequence non-specific B-cell proliferation (Liang et al., 1996). To distinguish CpG specific cell proliferation a dose titration experiment between control and CpG ODN is needed. In our case PS ODNs (independent of CpG motifs) are as potent as the positive control PHA. Of note, ODN420PO gave CpG specific proliferation higher than the linear CpG counterpart at 1 μM. In a similar experimental setup, intracellular cytokine staining is performed and TNFα production levels by pDC are compared in response to different ODNs. According to Figure 19, ODN420-PS and ODN420-PO induce high levels of TNFα production in comparison to their linear controls, ODN1466-PS and ODN1466-PO. Figure 20 shows that other control ODNs are not active and do not induce TNFα production except for ODN421-PS.

Next, we have performed an assay to understand the optimal doses in NP-forming ODN treatment in human PBMC in order to understand the behavior of each ODN. Figures 21 and 22 show that IL6 and IFNγ secretion levels increase in ODN420-PO treatment as the concentration increases from 0.1 μM to 1 μM while the secretion levels

are reduced in ODN420-PS treatment at concentrations higher than 0.3 μM. DC activation markers have correlated well with these results (Figures 23 and 24). Another assay has been performed to study the 3 μM concentration. As can been seen in Figure 25, ODN420-PO activity is further improved at 3 μM. Thus, these results have shown that ODNs with PS backbone are optimally active at 0.3 μM while ODNs with PO backbone are optimally active at 3 μM.

It has been previously established that immune cells differentially respond to different types of CpG ODNs. D-type ODNs preferentially stimulate IFNγ production by NK cells, whereas the K-type ODNs stimulate cell proliferation and the production of IL6 and IgM by monocytes and B cells (Verthelyi et al., 2001). Another study has further characterized the differential response to different CpG ODNs. Krug et. al. has identified certain CpG ODNs, which are referred as D-type ODNs, induce high levels of IFNα/β in human pDC in contrast to K-type ODNs, which strongly activate human B cells and blood DCs (Krug et al., 2001). We wanted to identify whether ODN420 would also induce type I IFNs (IFNα/β). As mentioned earlier, this cytokine is critical against viral infections. Moreover, throughout this work one of the most important goals is to demonstrate the breadth of activation of this novel NP-ODN both in mice and man. So, human PBMC have been treated with various ODNs at optimal doses and various interferon-related genes have been analyzed. Data from Figures 26 and 27 suggest that the expression levels of *ifnα*, *ifnβ*, *ifnγ* and other interferon-relate genes such as *mxa-1* and *mxa-2* are greatly induced upon treatment with ODN420. Type I IFN induction ability of ODN420-PO is higher than that of ODN420-PS. While it can be argued that this difference is caused by the fact that the concentration of ODN420-PO is 3 μM and ODN420-PS is 0.3 μM, we would suggest that the differences would become even higher if ODN420-PS were used at 3 μM, the concentration at which ODN420-PO has been used. Although it was not possible to study the secreted protein by ELISA, the gene transcript findings of *mxa-1* and *mxa-2* in addition to *ifnα*, *ifnβ*, strongly suggest that our sequences are potentially type I IFN producers. The literature findings suggested that MxA proteins were IFNα/β induced GTPases that inhibits the multiplication of several

RNA viruses by interacting with the viral nucleocapsid (Peltekian et al., 2005; Schwemmle et al., 1995).

Up to this point, various immunostimulatory activities of ODN420 have been analyzed by *in vitro* studies. Induction of high levels of IL6, TNFα, B cell proliferation and activation of pDC maturation markers are superior properties of K-type ODNs. Meanwhile, induction of type I IFNs (IFNα/β), that are critical in anti-viral immunity, is a property of D-type ODNs. Therefore, our dendrimeric ODN, '420' is a novel DNA-based agent and possesses the superior characteristics of both K-type and D-type ODNs. Another interesting point is the optimal concentrations of ODN420-PS and ODN420-PO. K-type ODNs are active at an optimal dose of 1 μM and maximal activity of D-type ODNs is reached at 3 μM. Interestingly, ODN420-PS is active at 0.3 μM and ODN420-PO is most active at 3 μM. Therefore, at this point, it would not be possible to classify this novel ODN as D-type or K-type. It can be suggested that this novel ODN combines useful properties of both types. This is a novel class of CpG ODNs. Since it is devoid of poly-G runs and conforms to a nanoparticle structure, we can regard this ODN as a new class. It also possesses more than one CpG motifs attached to a single sequence, and it is equally active in mice and humans. Furthermore, the PO forms are as potent as the PS backbone forms.

As previously mentioned, ODNs with PS backbone are more resistant to nucleases under physiological conditions. At this point, we have hypothesized that ODN420-PO would be stable *in vivo* and exhibit immunostimulatory activity at a level comparable with ODN420-PS due to it increased resistance conferred by the formation of nanoparticulate structure. We have then injected mice with various ODNs intraperitoneally and removed their spleens five hours after injection. Upon analysis of various cytokines and chemokines, it has been shown that ODN420 with the natural PO backbone is at least as potent as its counterpart with the modified PS backbone *in vivo* when used at its optimal concentration (Figures 28 and 29). Although a higher dose is used for ODN420-PO, these results still show that ODN420-PO is stable under physiological conditions and at least a sufficient amount of ODNs is able reach the targeted immune cells and activate TLR9 signaling before undergoing degradation by nucleases.

Having established the potentials of ODN420-PO, we have decided to use ODN420-PS for the subsequent animal experiments. The overall response to CpG ODNs is Th1-mediated. Here we have assessed whether this ODN could be used as a vaccine adjuvant in following mouse experiments. ODN420 and OVA-treated group is positive for total IgG at a titer of 1/112 even before booster injection (Table 11). This effect is more pronounced after booster injection. D35-treated group is positive for total IgG, IgG1, IgG2a and IgG2b at titers of 1/28, 1/1300, 1/112 and 1/112, respectively. However, ODN420-treated group is positive for these IgGs at titers of 1/4000, 1/1500, 1/448 and 1/28, respectively (Table 12). Thus, ODN420 induces higher levels of IgGs than ODN-D35 except for IgG2b. These results have shown that ODN420 induces a Th1-mediated immunity and can be effectively used as a vaccine adjuvant. In this experiment, the potential of another class of NP-forming ODN with immunosuppressive activity has also been analyzed. In the case of tissue injury, necrosis may occur and host DNA, which is rich in telomeric TTAGGG repeats, may be released into the surrounding tissue. It has been previously shown that ODNs with these repetitive elements can suppress the immune system by forming G-tetrads (Dong et al., 2004; Zeuner et al., 2002). The ability of these ODNs to suppress the immune system is dependent on their ability to form nanoparticles. We have analyzed whether this immunosuppressive ODN, ODN-A151, would interfere with the immune response generated during immunization. In secondary bleeding, positive titers are 1/792, 1/500, 1/7 and 1/7 for total IgG, IgG1, IgG2a and IgG2b, respectively, for ODN420 in combination with A151-treament group. Thus, treatment with ODN-A151 has decreased total IgG and IgG subtype levels generated by immunization with various adjuvants and OVA and reduced the Th1 response. Analysis of various Th1-related cytokines has confirmed these results (Figure 30).

Finally, we next asked whether both ODN420 and ODN-A151 could be utilized as anti-cancer agents. We have hypothesized that both immunostimulatory and immunosuppressive nanoparticle-forming ODNs could be utilized against cancer due to the complexity of the molecular mechanisms underlying cancer. While ODN420 can promote anti-tumor immunity, ODN-A151 can suppress the inflammatory response, which may provide favorable conditions for tumor growth. Tumor xenografts are established in nude mice by injection of Huh7 cells. Animals are treated with 100 μg of

either ODN420 or ODN-A151 starting from 3 days after the formation of a palpable tumor with one day-on one day-off treatment for three doses. According to Figure 31A, ODN-420 treatment can achieve partial remission of the tumor. This effect is observed in one mouse treated with ODN-420. The growth of tumor is delayed in the other animal in the same group. Meanwhile, ODN-A151 cannot induce remission of the tumor; it is able to delay its growth (Figure 31B). Therefore, ODN-420 is a more promising candidate as an anti-cancer agent than ODN-A151. Definitely, this experiment should be repeated and sample size should be increased in the following experiment for generation of more reliable and statistically significant data. However, this preliminary data suggests that ODN420 can be a promising candidate as an anti-cancer agent. The mechanism of ODN420 as an anti-cancer agent can be attributed to activation of NK cells and granulocytes in nude mice. These parameters should also be subject for further analysis.

To sum up, we have shown that ODN420 exhibits high immunostimulatory potential with respect to conventional linear or multimeric ODNs. ODN420-PS exhibits immunomodulatory activity at concentrations such as 0.1 μM, where other ODNs are not active. ODN420-PO is not active at such low concentrations but it is even more potent than ODN420-PS at concentrations such as 1 μM. The activity of the natural phosphodiester (PO) backbone is very promising because PS-modification of the backbone structure adds another level of complexity to the system and increases the cost of production in large scale synthesis. While conventional ODNs with PO backbone are easily degraded by nucleases *in vivo*, we have shown that ODN420-PO is also active under physiological conditions possibly due to its ability to form nanoparticles. The immunostimulatory potential of these ODNs in human PBMC has been analyzed by various assays and it has become clear that this ODN exhibits superior characteristics of both D-type ODNs and K-type ODNs. While ODN420 induces high levels of IL6, IL12, TNFα, B cell proliferation and activation of pDC maturation markers, it also induces production of type I IFNs (IFNα/β). Finally, it has been shown that this ODN can be used as a Th1-promoting vaccine adjuvant as well as an anti-cancer agent.

6. FUTURE STUDIES

While animal experiments are critical for designing CpG ODNs for immunotherapeutic purposes, optimal sequences for mice and human share only 75% homology. Therefore, many sequences, which are active in mice, do not exhibit correlating immunostimulatory potentials in human trials. We have identified a unique nanoparticle-forming CpG ODN that exhibits high immunostimulatory activity in mice and reproduced these results in human peripheral blood cells.

While ODN420 treatment has up-regulated type I IFNs and various interferon-related genes in human cells, these results should be reproduced in mice studies. Additionally, these data have been obtained at mRNA level and should be confirmed in protein level with FACS or ELISA. Additionally, tumor xenograft experiment should be repeated with a larger sample size and the immunization experiment should be repeated with disease-specific antigens instead of OVA.

Previous studies have identified that pre-treatment of mouse splenocytes with dextran sulfate, which is a ligand for scavenger receptors, completely abrogates the immunostimulatory activity of ODN420 (Mammadov, M.Sc. thesis). These data indicate that a scavenger receptor such as CXCL16, which is a co-receptor for D-type ODNs (Gursel et al., 2006), is responsible for the more efficient uptake mechanism of ODN420. To explain the underlying mechanism of NP-forming ODN uptake and efficiency, antibodies against individual scavenger receptors should be used in both *in vitro* and *in vivo* studies.

Also, several discrepancies have been observed in human donors in response to stimulation with NP-forming ODN treatment. It is well-established in the literature that the efficacy of CpG ODNs is highly deviant between patients. Thus, the number of donors in human studies should be increased to gain a better understanding on the action of ODN420 and to show that it is effective in large populations.

Another set of experiments should utilize specific cell types. For example, D-type ODNs are known to exhibit low stimulatory potential on B cells. We have worked on either human PBMC or mice splenocytes to identify the effects of ODN420. These samples contain heterogenous populations of cells. Similar experiments should be

performed on specific cell subsets such as B cells or pDC to further characterize the immunomodulatory activity of ODN420 on distinct cell types.

Finally, shorter dendrimeric ODNs can be designed and their immunostimulatory potentials can be analyzed. Current literature suggests that the minimum length of a CpG-ODN sequence is 8 bases for a single strand. However, it is possible that even shorter sequences may be immunostimulatory when they are used in dendrimeric ODNs.

7. REFERENCES

Ahmad-Nejad, P., Hacker, H., Rutz, M., Bauer, S., Vabulas, R.M., and Wagner, H. (2002). Bacterial CpG-DNA and lipopolysaccharides activate Toll-like receptors at distinct cellular compartments. Eur J Immunol *32*, 1958-1968.

Akira, S., Takeda, K., and Kaisho, T. (2001). Toll-like receptors: critical proteins linking innate and acquired immunity. Nat Immunol *2*, 675-680.

Akira, S., Uematsu, S., and Takeuchi, O. (2006). Pathogen recognition and innate immunity. Cell *124*, 783-801.

Akira, S., Yamamoto, M., and Takeda, K. (2003). Role of adapters in Toll-like receptor signalling. Biochem Soc Trans *31*, 637-642.

Alberts, B. (2008). Molecular biology of the cell, 5th edn (New York, Garland Science).

Alexopoulou, L., Holt, A.C., Medzhitov, R., and Flavell, R.A. (2001). Recognition of double-stranded RNA and activation of NF-kappaB by Toll-like receptor 3. Nature *413*, 732-738.

Anderson, R.B., Cianciolo, G.J., Kennedy, M.N., and Pizzo, S.V. (2008). Alpha 2-macroglobulin binds CpG oligodeoxynucleotides and enhances their immunostimulatory properties by a receptor-dependent mechanism. J Leukoc Biol *83*, 381-392.

Asagiri, M., Hirai, T., Kunigami, T., Kamano, S., Gober, H.J., Okamoto, K., Nishikawa, K., Latz, E., Golenbock, D.T., Aoki, K.*, et al.* (2008). Cathepsin K-dependent toll-like receptor 9 signaling revealed in experimental arthritis. Science *319*, 624-627.

Asselin-Paturel, C., and Trinchieri, G. (2005). Production of type I interferons: plasmacytoid dendritic cells and beyond. J Exp Med *202*, 461-465.

Banchereau, J., and Steinman, R.M. (1998). Dendritic cells and the control of immunity. Nature *392*, 245-252.

Barton, G.M., and Kagan, J.C. (2009). A cell biological view of Toll-like receptor function: regulation through compartmentalization. Nat Rev Immunol *9*, 535-542.

Barton, G.M., Kagan, J.C., and Medzhitov, R. (2006). Intracellular localization of Toll-like receptor 9 prevents recognition of self DNA but facilitates access to viral DNA. Nat Immunol *7*, 49-56.

Bauer, M., Heeg, K., Wagner, H., and Lipford, G.B. (1999). DNA activates human immune cells through a CpG sequence-dependent manner. Immunology *97*, 699-705.

Bauer, S., Kirschning, C.J., Hacker, H., Redecke, V., Hausmann, S., Akira, S., Wagner, H., and Lipford, G.B. (2001). Human TLR9 confers responsiveness to bacterial DNA via species-specific CpG motif recognition. Proc Natl Acad Sci U S A *98*, 9237-9242.

Bernasconi, N.L., Traggiai, E., and Lanzavecchia, A. (2002). Maintenance of serological memory by polyclonal activation of human memory B cells. Science *298*, 2199-2202.

Boule, M.W., Broughton, C., Mackay, F., Akira, S., Marshak-Rothstein, A., and Rifkin, I.R. (2004). Toll-like receptor 9-dependent and -independent dendritic cell activation by chromatin-immunoglobulin G complexes. J Exp Med *199*, 1631-1640.

Chockalingam, A., Brooks, J.C., Cameron, J.L., Blum, L.K., and Leifer, C.A. (2009). TLR9 traffics through the Golgi complex to localize to endolysosomes and respond to CpG DNA. Immunol Cell Biol *87*, 209-217.

Chu, R.S., Targoni, O.S., Krieg, A.M., Lehmann, P.V., and Harding, C.V. (1997). CpG oligodeoxynucleotides act as adjuvants that switch on T helper 1 (Th1) immunity. J Exp Med *186*, 1623-1631.

Costa, L.T., Kerkmann, M., Hartmann, G., Endres, S., Bisch, P.M., Heckl, W.M., and Thalhammer, S. (2004). Structural studies of oligonucleotides containing G-quadruplex motifs using AFM. Biochem Biophys Res Commun *313*, 1065-1072.

Dalpke, A.H., Zimmermann, S., Albrecht, I., and Heeg, K. (2002). Phosphodiester CpG oligonucleotides as adjuvants: polyguanosine runs enhance cellular uptake and improve immunostimulative activity of phosphodiester CpG oligonucleotides in vitro and in vivo. Immunology *106*, 102-112.

de Jong, S., Chikh, G., Sekirov, L., Raney, S., Semple, S., Klimuk, S., Yuan, N., Hope, M., Cullis, P., and Tam, Y. (2007). Encapsulation in liposomal nanoparticles enhances the immunostimulatory, adjuvant and anti-tumor activity of subcutaneously administered CpG ODN. Cancer Immunol Immunother *56*, 1251-1264.

Dong, L., Ito, S., Ishii, K.J., and Klinman, D.M. (2004). Suppressive oligonucleotides protect against collagen-induced arthritis in mice. Arthritis Rheum *50*, 1686-1689.

Dong, L., Ito, S., Ishii, K.J., and Klinman, D.M. (2005). Suppressive oligodeoxynucleotides delay the onset of glomerulonephritis and prolong survival in lupus-prone NZB x NZW mice. Arthritis Rheum *52*, 651-658.

Doyle, S., Vaidya, S., O'Connell, R., Dadgostar, H., Dempsey, P., Wu, T., Rao, G., Sun, R., Haberland, M., Modlin, R., *et al.* (2002). IRF3 mediates a TLR3/TLR4-specific antiviral gene program. Immunity *17*, 251-263.

Ewald, S.E., Lee, B.L., Lau, L., Wickliffe, K.E., Shi, G.P., Chapman, H.A., and Barton, G.M. (2008). The ectodomain of Toll-like receptor 9 is cleaved to generate a functional receptor. Nature *456*, 658-662.

Fitzgerald, K.A., McWhirter, S.M., Faia, K.L., Rowe, D.C., Latz, E., Golenbock, D.T., Coyle, A.J., Liao, S.M., and Maniatis, T. (2003). IKKepsilon and TBK1 are essential components of the IRF3 signaling pathway. Nat Immunol *4*, 491-496.

Fujimoto, C., Klinman, D.M., Shi, G., Yin, H., Vistica, B.P., Lovaas, J.D., Wawrousek, E.F., Igarashi, T., Chan, C.C., and Gery, I. (2009). A suppressive oligodeoxynucleotide inhibits ocular inflammation. Clin Exp Immunol *156*, 528-534.

Gohda, J., Matsumura, T., and Inoue, J. (2004). Cutting edge: TNFR-associated factor (TRAF) 6 is essential for MyD88-dependent pathway but not toll/IL-1 receptor domain-containing adaptor-inducing IFN-beta (TRIF)-dependent pathway in TLR signaling. J Immunol *173*, 2913-2917.

Gray, R.C., Kuchtey, J., and Harding, C.V. (2007). CpG-B ODNs potently induce low levels of IFN-alphabeta and induce IFN-alphabeta-dependent MHC-I cross-presentation in DCs as effectively as CpG-A and CpG-C ODNs. J Leukoc Biol *81*, 1075-1085.

Guiducci, C., Ott, G., Chan, J.H., Damon, E., Calacsan, C., Matray, T., Lee, K.D., Coffman, R.L., and Barrat, F.J. (2006). Properties regulating the nature of the plasmacytoid dendritic cell response to Toll-like receptor 9 activation. J Exp Med *203*, 1999-2008.

Gursel, I., Gursel, M., Ishii, K.J., and Klinman, D.M. (2001). Sterically stabilized cationic liposomes improve the uptake and immunostimulatory activity of CpG oligonucleotides. J Immunol *167*, 3324-3328.

Gursel, I., Gursel, M., Yamada, H., Ishii, K.J., Takeshita, F., and Klinman, D.M. (2003). Repetitive elements in mammalian telomeres suppress bacterial DNA-induced immune activation. J Immunol *171*, 1393-1400.

Gursel, M., Gursel, I., Mostowski, H.S., and Klinman, D.M. (2006). CXCL16 influences the nature and specificity of CpG-induced immune activation. J Immunol *177*, 1575-1580.

Gursel, M., Verthelyi, D., Gursel, I., Ishii, K.J., and Klinman, D.M. (2002a). Differential and competitive activation of human immune cells by distinct classes of CpG oligodeoxynucleotide. J Leukoc Biol *71*, 813-820.

Gursel, M., Verthelyi, D., and Klinman, D.M. (2002b). CpG oligodeoxynucleotides induce human monocytes to mature into functional dendritic cells. Eur J Immunol *32*, 2617-2622.

Haas, T., Metzger, J., Schmitz, F., Heit, A., Muller, T., Latz, E., and Wagner, H. (2008). The DNA sugar backbone 2' deoxyribose determines toll-like receptor 9 activation. Immunity *28*, 315-323.

Haas, T., Schmitz, F., Heit, A., and Wagner, H. (2009). Sequence independent interferon-alpha induction by multimerized phosphodiester DNA depends on spatial regulation of Toll-like receptor-9 activation in plasmacytoid dendritic cells. Immunology *126*, 290-298.

Hartmann, G., Battiany, J., Poeck, H., Wagner, M., Kerkmann, M., Lubenow, N., Rothenfusser, S., and Endres, S. (2003). Rational design of new CpG oligonucleotides that combine B cell activation with high IFN-alpha induction in plasmacytoid dendritic cells. Eur J Immunol *33*, 1633-1641.

Hartmann, G., Weiner, G.J., and Krieg, A.M. (1999). CpG DNA: a potent signal for growth, activation, and maturation of human dendritic cells. Proc Natl Acad Sci U S A *96*, 9305-9310.

Hawn, T.R., Verbon, A., Lettinga, K.D., Zhao, L.P., Li, S.S., Laws, R.J., Skerrett, S.J., Beutler, B., Schroeder, L., Nachman, A., *et al.* (2003). A common dominant TLR5 stop codon polymorphism abolishes flagellin signaling and is associated with susceptibility to legionnaires' disease. J Exp Med *198*, 1563-1572.

Hemmi, H., Kaisho, T., Takeuchi, O., Sato, S., Sanjo, H., Hoshino, K., Horiuchi, T., Tomizawa, H., Takeda, K., and Akira, S. (2002). Small anti-viral compounds activate immune cells via the TLR7 MyD88-dependent signaling pathway. Nat Immunol *3*, 196-200.

Hemmi, H., Takeuchi, O., Kawai, T., Kaisho, T., Sato, S., Sanjo, H., Matsumoto, M., Hoshino, K., Wagner, H., Takeda, K., *et al.* (2000). A Toll-like receptor recognizes bacterial DNA. Nature *408*, 740-745.

Ho, P.P., Fontoura, P., Platten, M., Sobel, R.A., DeVoss, J.J., Lee, L.Y., Kidd, B.A., Tomooka, B.H., Capers, J., Agrawal, A., *et al.* (2005). A suppressive oligodeoxynucleotide enhances the efficacy of myelin cocktail/IL-4-tolerizing DNA vaccination and treats autoimmune disease. J Immunol *175*, 6226-6234.

Ho, P.P., Fontoura, P., Ruiz, P.J., Steinman, L., and Garren, H. (2003). An immunomodulatory GpG oligonucleotide for the treatment of autoimmunity via the innate and adaptive immune systems. J Immunol *171*, 4920-4926.

Honda, K., Ohba, Y., Yanai, H., Negishi, H., Mizutani, T., Takaoka, A., Taya, C., and Taniguchi, T. (2005a). Spatiotemporal regulation of MyD88-IRF-7 signalling for robust type-I interferon induction. Nature *434*, 1035-1040.

Honda, K., Yanai, H., Negishi, H., Asagiri, M., Sato, M., Mizutani, T., Shimada, N., Ohba, Y., Takaoka, A., Yoshida, N., *et al.* (2005b). IRF-7 is the master regulator of type-I interferon-dependent immune responses. Nature *434*, 772-777.

Hoshino, K., Kaisho, T., Iwabe, T., Takeuchi, O., and Akira, S. (2002). Differential involvement of IFN-beta in Toll-like receptor-stimulated dendritic cell activation. Int Immunol *14*, 1225-1231.

Hoshino, K., Takeuchi, O., Kawai, T., Sanjo, H., Ogawa, T., Takeda, Y., Takeda, K., and Akira, S. (1999). Cutting edge: Toll-like receptor 4 (TLR4)-deficient mice are hyporesponsive to lipopolysaccharide: evidence for TLR4 as the Lps gene product. J Immunol *162*, 3749-3752.

Ishii, K.J., and Akira, S. (2005). Innate immune recognition of nucleic acids: beyond toll-like receptors. Int J Cancer *117*, 517-523.

Ishii, K.J., Kawakami, K., Gursel, I., Conover, J., Joshi, B.H., Klinman, D.M., and Puri, R.K. (2003). Antitumor therapy with bacterial DNA and toxin: complete regression of established tumor induced by liposomal CpG oligodeoxynucleotides plus interleukin-13 cytotoxin. Clin Cancer Res *9*, 6516-6522.

Ito, T., Amakawa, R., and Fukuhara, S. (2002a). Roles of toll-like receptors in natural interferon-producing cells as sensors in immune surveillance. Hum Immunol *63*, 1120-1125.

Ito, T., Amakawa, R., Kaisho, T., Hemmi, H., Tajima, K., Uehira, K., Ozaki, Y., Tomizawa, H., Akira, S., and Fukuhara, S. (2002b). Interferon-alpha and interleukin-12 are induced differentially by Toll-like receptor 7 ligands in human blood dendritic cell subsets. J Exp Med *195*, 1507-1512.

Ivanov, S., Dragoi, A.M., Wang, X., Dallacosta, C., Louten, J., Musco, G., Sitia, G., Yap, G.S., Wan, Y., Biron, C.A., *et al.* (2007). A novel role for HMGB1 in TLR9-mediated inflammatory responses to CpG-DNA. Blood *110*, 1970-1981.

Iwasaki, A., and Medzhitov, R. (2004). Toll-like receptor control of the adaptive immune responses. Nat Immunol *5*, 987-995.

Janeway, C. (2005). Immunobiology : the immune system in health and disease, 6th edn (New York, Garland Science).

Janeway, C.A., Jr. (2001). How the immune system protects the host from infection. Microbes Infect *3*, 1167-1171.

Janeway, C.A., Jr., and Medzhitov, R. (2002). Innate immune recognition. Annu Rev Immunol *20*, 197-216.

Jurk, M., Schulte, B., Kritzler, A., Noll, B., Uhlmann, E., Wader, T., Schetter, C., Krieg, A.M., and Vollmer, J. (2004). C-Class CpG ODN: sequence requirements and characterization of immunostimulatory activities on mRNA level. Immunobiology *209*, 141-154.

Kaisho, T., Hoshino, K., Iwabe, T., Takeuchi, O., Yasui, T., and Akira, S. (2002). Endotoxin can induce MyD88-deficient dendritic cells to support T(h)2 cell differentiation. Int Immunol *14*, 695-700.

Kerkmann, M., Costa, L.T., Richter, C., Rothenfusser, S., Battiany, J., Hornung, V., Johnson, J., Englert, S., Ketterer, T., Heckl, W.*, et al.* (2005). Spontaneous formation of nucleic acid-based nanoparticles is responsible for high interferon-alpha induction by CpG-A in plasmacytoid dendritic cells. J Biol Chem *280*, 8086-8093.

Kerkmann, M., Lochmann, D., Weyermann, J., Marschner, A., Poeck, H., Wagner, M., Battiany, J., Zimmer, A., Endres, S., and Hartmann, G. (2006).

Immunostimulatory properties of CpG-oligonucleotides are enhanced by the use of protamine nanoparticles. Oligonucleotides *16*, 313-322.

Kim, H.A., Ko, H.M., Ju, H.W., Kim, K.J., Roh, S.G., Lee, H.K., and Im, S.Y. (2009). CpG-ODN-based immunotherapy is effective in controlling the growth of metastasized tumor cells. Cancer Lett *274*, 160-164.

Kim, Y.M., Brinkmann, M.M., Paquet, M.E., and Ploegh, H.L. (2008). UNC93B1 delivers nucleotide-sensing toll-like receptors to endolysosomes. Nature *452*, 234-238.

Kline, J.N., and Krieg, A.M. (2008). Toll-like receptor 9 activation with CpG oligodeoxynucleotides for asthma therapy. Drug News Perspect *21*, 434-439.

Klinman, D.M. (2004). Immunotherapeutic uses of CpG oligodeoxynucleotides. Nat Rev Immunol *4*, 249-258.

Klinman, D.M., Currie, D., Gursel, I., and Verthelyi, D. (2004). Use of CpG oligodeoxynucleotides as immune adjuvants. Immunol Rev *199*, 201-216.

Klinman, D.M., Xie, H., and Ivins, B.E. (2006). CpG oligonucleotides improve the protective immune response induced by the licensed anthrax vaccine. Ann N Y Acad Sci *1082*, 137-150.

Klinman, D.M., Yi, A.K., Beaucage, S.L., Conover, J., and Krieg, A.M. (1996). CpG motifs present in bacteria DNA rapidly induce lymphocytes to secrete interleukin 6, interleukin 12, and interferon gamma. Proc Natl Acad Sci U S A *93*, 2879-2883.

Krieg, A.M. (2006). Therapeutic potential of Toll-like receptor 9 activation. Nat Rev Drug Discov *5*, 471-484.

Krieg, A.M. (2008). Toll-like receptor 9 (TLR9) agonists in the treatment of cancer. Oncogene *27*, 161-167.

Krieg, A.M., Wu, T., Weeratna, R., Efler, S.M., Love-Homan, L., Yang, L., Yi, A.K., Short, D., and Davis, H.L. (1998). Sequence motifs in adenoviral DNA block immune activation by stimulatory CpG motifs. Proc Natl Acad Sci U S A *95*, 12631-12636.

Krieg, A.M., Yi, A.K., Matson, S., Waldschmidt, T.J., Bishop, G.A., Teasdale, R., Koretzky, G.A., and Klinman, D.M. (1995). CpG motifs in bacterial DNA trigger direct B-cell activation. Nature *374*, 546-549.

Krug, A., Rothenfusser, S., Hornung, V., Jahrsdorfer, B., Blackwell, S., Ballas, Z.K., Endres, S., Krieg, A.M., and Hartmann, G. (2001). Identification of CpG oligonucleotide sequences with high induction of IFN-alpha/beta in plasmacytoid dendritic cells. Eur J Immunol *31*, 2154-2163.

Lande, R., Gregorio, J., Facchinetti, V., Chatterjee, B., Wang, Y.H., Homey, B., Cao, W., Su, B., Nestle, F.O., Zal, T., *et al.* (2007). Plasmacytoid dendritic cells sense self-DNA coupled with antimicrobial peptide. Nature *449*, 564-569.

Latz, E., Schoenemeyer, A., Visintin, A., Fitzgerald, K.A., Monks, B.G., Knetter, C.F., Lien, E., Nilsen, N.J., Espevik, T., and Golenbock, D.T. (2004). TLR9 signals after translocating from the ER to CpG DNA in the lysosome. Nat Immunol *5*, 190-198.

Latz, E., Verma, A., Visintin, A., Gong, M., Sirois, C.M., Klein, D.C., Monks, B.G., McKnight, C.J., Lamphier, M.S., Duprex, W.P., *et al.* (2007). Ligand-induced conformational changes allosterically activate Toll-like receptor 9. Nat Immunol *8*, 772-779.

Lee, H.K., and Iwasaki, A. (2007). Innate control of adaptive immunity: dendritic cells and beyond. Semin Immunol *19*, 48-55.

Lee, M.S., and Kim, Y.J. (2007). Pattern-recognition receptor signaling initiated from extracellular, membrane, and cytoplasmic space. Mol Cells *23*, 1-10.

Leifer, C.A., Brooks, J.C., Hoelzer, K., Lopez, J., Kennedy, M.N., Mazzoni, A., and Segal, D.M. (2006). Cytoplasmic targeting motifs control localization of toll-like receptor 9. J Biol Chem *281*, 35585-35592.

Leifer, C.A., Verthelyi, D., and Klinman, D.M. (2003). Heterogeneity in the human response to immunostimulatory CpG oligodeoxynucleotides. J Immunother *26*, 313-319.

Lenert, P., Stunz, L., Yi, A.K., Krieg, A.M., and Ashman, R.F. (2001). CpG stimulation of primary mouse B cells is blocked by inhibitory oligodeoxyribonucleotides at a site proximal to NF-kappaB activation. Antisense Nucleic Acid Drug Dev *11*, 247-256.

Liang, H., Nishioka, Y., Reich, C.F., Pisetsky, D.S., and Lipsky, P.E. (1996). Activation of human B cells by phosphorothioate oligodeoxynucleotides. J Clin Invest *98*, 1119-1129.

Lien, E., and Golenbock, D.T. (2003). Adjuvants and their signaling pathways: beyond TLRs. Nat Immunol *4*, 1162-1164.

Lund, J.M., Alexopoulou, L., Sato, A., Karow, M., Adams, N.C., Gale, N.W., Iwasaki, A., and Flavell, R.A. (2004). Recognition of single-stranded RNA viruses by Toll-like receptor 7. Proc Natl Acad Sci U S A *101*, 5598-5603.

Macfarlane, A.J., Kon, O.M., Smith, S.J., Zeibecoglou, K., Khan, L.N., Barata, L.T., McEuen, A.R., Buckley, M.G., Walls, A.F., Meng, Q., *et al.* (2000). Basophils, eosinophils, and mast cells in atopic and nonatopic asthma and in late-phase allergic reactions in the lung and skin. J Allergy Clin Immunol *105*, 99-107.

Medzhitov, R. (2001). Toll-like receptors and innate immunity. Nat Rev Immunol *1*, 135-145.

Medzhitov, R., Preston-Hurlburt, P., and Janeway, C.A., Jr. (1997). A human homologue of the Drosophila Toll protein signals activation of adaptive immunity. Nature *388*, 394-397.

Meylan, E., Burns, K., Hofmann, K., Blancheteau, V., Martinon, F., Kelliher, M., and Tschopp, J. (2004). RIP1 is an essential mediator of Toll-like receptor 3-induced NF-kappa B activation. Nat Immunol *5*, 503-507.

Meylan, E., Tschopp, J., and Karin, M. (2006). Intracellular pattern recognition receptors in the host response. Nature *442*, 39-44.

Murphy, K.P., Travers, P., Walport, M., and Janeway, C. (2008). Janeway's immunobiology, 7th edn (New York, Garland Science).

Nishikawa, M., Matono, M., Rattanakiat, S., Matsuoka, N., and Takakura, Y. (2008). Enhanced immunostimulatory activity of oligodeoxynucleotides by Y-shape formation. Immunology *124*, 247-255.

Ouyang, X., Negishi, H., Takeda, R., Fujita, Y., Taniguchi, T., and Honda, K. (2007). Cooperation between MyD88 and TRIF pathways in TLR synergy via IRF5 activation. Biochem Biophys Res Commun *354*, 1045-1051.

Parish, C.R., Glidden, M.H., Quah, B.J., and Warren, H.S. (2009). Use of the intracellular fluorescent dye CFSE to monitor lymphocyte migration and proliferation. Curr Protoc Immunol *Chapter 4*, Unit4 9.

Park, B., Brinkmann, M.M., Spooner, E., Lee, C.C., Kim, Y.M., and Ploegh, H.L. (2008). Proteolytic cleavage in an endolysosomal compartment is required for activation of Toll-like receptor 9. Nat Immunol *9*, 1407-1414.

Peltekian, C., Gordien, E., Garreau, F., Meas-Yedid, V., Soussan, P., Willams, V., Chaix, M.L., Olivo-Marin, J.C., Brechot, C., and Kremsdorf, D. (2005). Human MxA protein participates to the interferon-related inhibition of hepatitis B virus replication in female transgenic mice. J Hepatol *43*, 965-972.

Peter, M., Bode, K., Lipford, G.B., Eberle, F., Heeg, K., and Dalpke, A.H. (2008). Characterization of suppressive oligodeoxynucleotides that inhibit Toll-like receptor-9-mediated activation of innate immunity. Immunology *123*, 118-128.

Rahman, A.H., and Eisenberg, R.A. (2006). The role of toll-like receptors in systemic lupus erythematosus. Springer Semin Immunopathol *28*, 131-143.

Raulet, D.H., and Guerra, N. (2009). Oncogenic stress sensed by the immune system: role of natural killer cell receptors. Nat Rev Immunol *9*, 568-580.

Sato, S., Nomura, F., Kawai, T., Takeuchi, O., Muhlradt, P.F., Takeda, K., and Akira, S. (2000). Synergy and cross-tolerance between toll-like receptor (TLR) 2- and TLR4-mediated signaling pathways. J Immunol *165*, 7096-7101.

Sato, T., Shimosato, T., Alvord, W.G., and Klinman, D.M. (2008). Suppressive oligodeoxynucleotides inhibit silica-induced pulmonary inflammation. J Immunol *180*, 7648-7654.

Schmidt, K.N., Leung, B., Kwong, M., Zarember, K.A., Satyal, S., Navas, T.A., Wang, F., and Godowski, P.J. (2004). APC-independent activation of NK cells by the Toll-like receptor 3 agonist double-stranded RNA. J Immunol *172*, 138-143.

Schromm, A.B., Lien, E., Henneke, P., Chow, J.C., Yoshimura, A., Heine, H., Latz, E., Monks, B.G., Schwartz, D.A., Miyake, K., *et al.* (2001). Molecular genetic analysis of an endotoxin nonresponder mutant cell line: a point mutation in a conserved region of MD-2 abolishes endotoxin-induced signaling. J Exp Med *194*, 79-88.

Schwemmle, M., Richter, M.F., Herrmann, C., Nassar, N., and Staeheli, P. (1995). Unexpected structural requirements for GTPase activity of the interferon-induced MxA protein. J Biol Chem *270*, 13518-13523.

Shimazu, R., Akashi, S., Ogata, H., Nagai, Y., Fukudome, K., Miyake, K., and Kimoto, M. (1999). MD-2, a molecule that confers lipopolysaccharide responsiveness on Toll-like receptor 4. J Exp Med *189*, 1777-1782.

Shirota, H., Gursel, I., Gursel, M., and Klinman, D.M. (2005). Suppressive oligodeoxynucleotides protect mice from lethal endotoxic shock. J Immunol *174*, 4579-4583.

Shirota, H., Gursel, M., and Klinman, D.M. (2004). Suppressive oligodeoxynucleotides inhibit Th1 differentiation by blocking IFN-gamma- and IL-12-mediated signaling. J Immunol *173*, 5002-5007.

Shirota, H., Sano, K., Hirasawa, N., Terui, T., Ohuchi, K., Hattori, T., Shirato, K., and Tamura, G. (2001). Novel roles of CpG oligodeoxynucleotides as a leader for the sampling and presentation of CpG-tagged antigen by dendritic cells. J Immunol *167*, 66-74.

Sur, S., Wild, J.S., Choudhury, B.K., Sur, N., Alam, R., and Klinman, D.M. (1999). Long term prevention of allergic lung inflammation in a mouse model of asthma by CpG oligodeoxynucleotides. J Immunol *162*, 6284-6293.

Tabeta, K., Hoebe, K., Janssen, E.M., Du, X., Georgel, P., Crozat, K., Mudd, S., Mann, N., Sovath, S., Goode, J.*, et al.* (2006). The Unc93b1 mutation 3d disrupts exogenous antigen presentation and signaling via Toll-like receptors 3, 7 and 9. Nat Immunol *7*, 156-164.

Takeda, K., and Akira, S. (2004). TLR signaling pathways. Semin Immunol *16*, 3-9.

Takeda, K., and Akira, S. (2005). Toll-like receptors in innate immunity. Int Immunol *17*, 1-14.

Takeda, K., Kaisho, T., and Akira, S. (2003). Toll-like receptors. Annu Rev Immunol *21*, 335-376.

Takeshita, F., Leifer, C.A., Gursel, I., Ishii, K.J., Takeshita, S., Gursel, M., and Klinman, D.M. (2001). Cutting edge: Role of Toll-like receptor 9 in CpG DNA-induced activation of human cells. J Immunol *167*, 3555-3558.

Takeuchi, O., Takeda, K., Hoshino, K., Adachi, O., Ogawa, T., and Akira, S. (2000). Cellular responses to bacterial cell wall components are mediated through MyD88-dependent signaling cascades. Int Immunol *12*, 113-117.

Tian, J., Avalos, A.M., Mao, S.Y., Chen, B., Senthil, K., Wu, H., Parroche, P., Drabic, S., Golenbock, D., Sirois, C.*, et al.* (2007). Toll-like receptor 9-dependent activation by DNA-containing immune complexes is mediated by HMGB1 and RAGE. Nat Immunol *8*, 487-496.

Trieu, A., Bokil, N., Dunn, J.A., Roberts, T.L., Xu, D., Liew, F.Y., Hume, D.A., Stacey, K.J., and Sweet, M.J. (2009). TLR9-independent effects of inhibitory oligonucleotides on macrophage responses to S. typhimurium. Immunol Cell Biol *87*, 218-225.

Utaisincharoen, P., Anuntagool, N., Chaisuriya, P., Pichyangkul, S., and Sirisinha, S. (2002). CpG ODN activates NO and iNOS production in mouse macrophage cell line (RAW 264.7). Clin Exp Immunol *128*, 467-473.

Verthelyi, D., Ishii, K.J., Gursel, M., Takeshita, F., and Klinman, D.M. (2001). Human peripheral blood cells differentially recognize and respond to two distinct CPG motifs. J Immunol *166*, 2372-2377.

Vollmer, J., Weeratna, R., Payette, P., Jurk, M., Schetter, C., Laucht, M., Wader, T., Tluk, S., Liu, M., Davis, H.L.*, et al.* (2004). Characterization of three CpG oligodeoxynucleotide classes with distinct immunostimulatory activities. Eur J Immunol *34*, 251-262.

Wang, D., Bhagat, L., Yu, D., Zhu, F.G., Tang, J.X., Kandimalla, E.R., and Agrawal, S. (2009). Oligodeoxyribonucleotide-based antagonists for Toll-like receptors 7 and 9. J Med Chem *52*, 551-558.

Williams, R. (2006). The endosome effect. Journal of Experimental Medicine *203*, 1834-1834.

Wright, S.D., Tobias, P.S., Ulevitch, R.J., and Ramos, R.A. (1989). Lipopolysaccharide (LPS) binding protein opsonizes LPS-bearing particles for recognition by a novel receptor on macrophages. J Exp Med *170*, 1231-1241.

Wu, C.C., Lee, J., Raz, E., Corr, M., and Carson, D.A. (2004). Necessity of oligonucleotide aggregation for toll-like receptor 9 activation. J Biol Chem *279*, 33071-33078.

Yamada, H., Gursel, I., Takeshita, F., Conover, J., Ishii, K.J., Gursel, M., Takeshita, S., and Klinman, D.M. (2002). Effect of suppressive DNA on CpG-induced immune activation. J Immunol *169*, 5590-5594.

Yamamoto, M., Sato, S., Hemmi, H., Sanjo, H., Uematsu, S., Kaisho, T., Hoshino, K., Takeuchi, O., Kobayashi, M., Fujita, T.*, et al.* (2002a). Essential role for TIRAP in activation of the signalling cascade shared by TLR2 and TLR4. Nature *420*, 324-329.

Yamamoto, M., Sato, S., Hemmi, H., Uematsu, S., Hoshino, K., Kaisho, T., Takeuchi, O., Takeda, K., and Akira, S. (2003). TRAM is specifically involved in the Toll-like receptor 4-mediated MyD88-independent signaling pathway. Nat Immunol *4*, 1144-1150.

Yamamoto, M., Sato, S., Mori, K., Hoshino, K., Takeuchi, O., Takeda, K., and Akira, S. (2002b). Cutting edge: a novel Toll/IL-1 receptor domain-containing adapter that preferentially activates the IFN-beta promoter in the Toll-like receptor signaling. J Immunol *169*, 6668-6672.

Yamamoto, S., Yamamoto, T., Kataoka, T., Kuramoto, E., Yano, O., and Tokunaga, T. (1992). Unique palindromic sequences in synthetic oligonucleotides are required to induce IFN and augment IFN-mediated natural killer activity. J Immunol *148*, 4072-4076.

Yasuda, K., Rutz, M., Schlatter, B., Metzger, J., Luppa, P.B., Schmitz, F., Haas, T., Heit, A., Bauer, S., and Wagner, H. (2006). CpG motif-independent activation of TLR9 upon endosomal translocation of "natural" phosphodiester DNA. Eur J Immunol *36*, 431-436.

Yoneyama, M., Suhara, W., Fukuhara, Y., Fukuda, M., Nishida, E., and Fujita, T. (1998). Direct triggering of the type I interferon system by virus infection: activation of a transcription factor complex containing IRF-3 and CBP/p300. EMBO J *17*, 1087-1095.

Zeuner, R.A., Ishii, K.J., Lizak, M.J., Gursel, I., Yamada, H., Klinman, D.M., and Verthelyi, D. (2002). Reduction of CpG-induced arthritis by suppressive oligodeoxynucleotides. Arthritis Rheum *46*, 2219-2224.

8. APPENDICES

8.1. Appendix A

Buffers, Solutions, Culture media

Blocking Buffer (ELISA)

- 500 ml 1x PBS
- 25 grams BSA (5%)
- 250 µl Tween20 (0,025%)

Crystal particles of BSA should be dissolved very well, with magnetic-heating stirrer for 20-30 min. The buffer should be stored at -20°C.

Loading Dye (Agarose gel)

- 0,009 grams Bromofenol blue
- 0,009 grams Xylen cyanol
- 2,8 ml ddH_2O
- 1,2 ml 0,5M EDTA
- 11 ml glycerol

After preparing, just vortex it.

PBS (Phosphate Buffered Saline) [10x]

- 80 grams NaCl
- 2 grams KCl
- 8,01 grams $Na_2HPO_4 . 2H_2O$
- 2 grams KH_2PO_4

complete into 1 lt with ddH_2O (pH= 6,8).

For 1X PBS's pH should be ≈ 7,2-7,4 and should be autoclaved prior to use.

TAE (Tris-Acetate-EDTA) [50x]

- 242 grams Tris ($C_4H_{11}NO_3$)
- 37,2 grams Tritiplex 3 (EDTA= $C_{10}H_{14}N_2Na_2O_2 . 2H_2O$)
- 57,1 ml Glacial acetic acid

Complete to 1 lt final volume with ddH_2O. Autoclaved and diluted to 1X prior to use.

PBS-BSA-Na azide

- 500 ml 1x PBS
- 5g BSA (1%)
- 125mg (0,25%)

T-cell Buffer [ELISA]

- 500 ml 1x PBS
- 25 ml FBS (5%)
- 250 µl Tween20 (0,025%)

The buffer should be stored at -20°C.

Wash Buffer [ELISA]

- 500 ml 10x PBS
- 2,5 ml Tween20
- 4,5 lt ddH_2O

RPMI-1640 (Hyclone)

- 2 % : 10 ml FBS (Oligo FBS = inactivated at 65°C, Regular FBS = inactivated at 55°C)
- 5 % : 25 ml FBS
- 10 % : 50 ml FBS
- 5 ml Penicillin/Streptomycin (50 µg/ml final concentration from 10 mg/ml stock)
- 5 ml HEPES (Biological Industries), (10 mM final concentration from 1M stock)
- 5 ml Na Pyruvate, (0,11 mg/ml final concentration from 100mM, 11 mg/ml stock)
- 5 ml Non-Essential Amino Acids Solution, (diluted into 1x from 100x concentrate stock)
- 5 ml L-Glutamine, (2 mM final concentration from 200 mM, 29.2 mg/ml stock)

In 500 ml media

8.2. Appendix B

Fold induction graphs of various interferon related genes and endosomal tlr genes at mRNA level for stimulations from the second donor. The picture of agarose gel electrophoresis is given in Figure 26.

A)

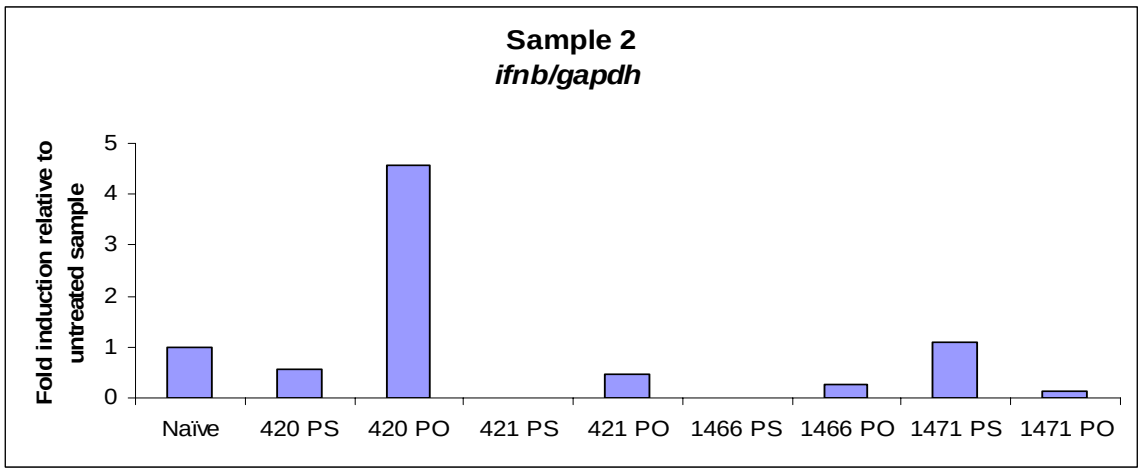

B)

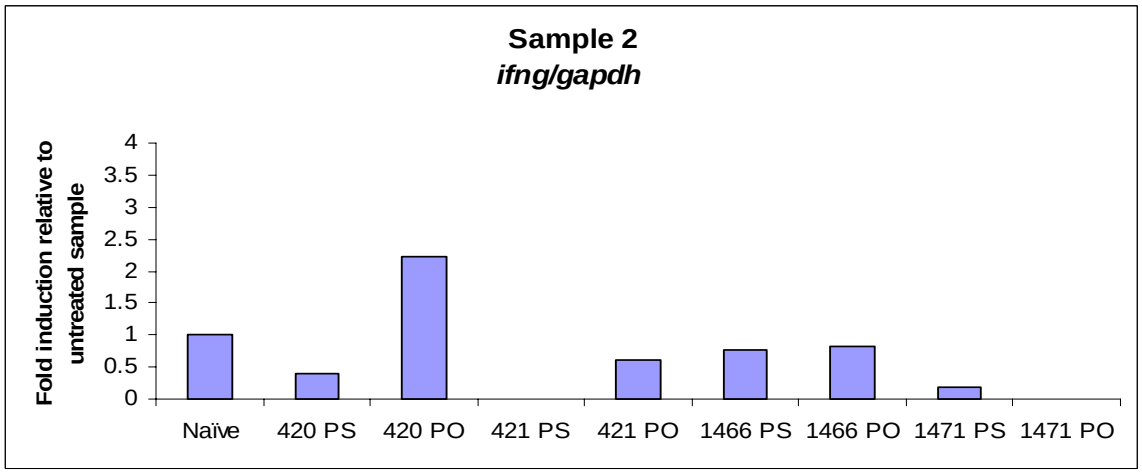

C)

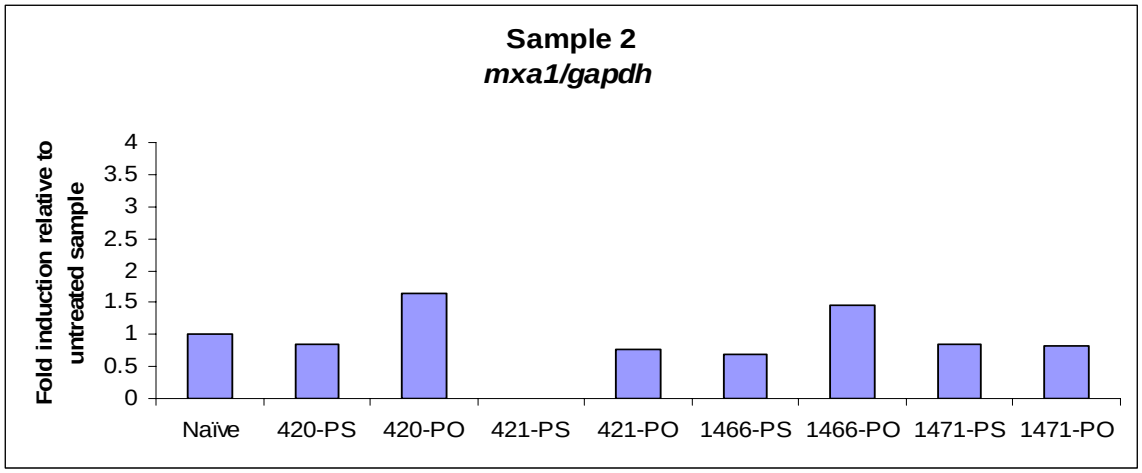
Sample 2
mxa1/gapdh
Fold induction relative to untreated sample
4
3.5
3
2.5
2
1.5
1
0.5
0
Naïve
420-PS
420-PO
421-PS
421-PO
1466-PS
1466-PO
1471-PS
1471-PO

D)

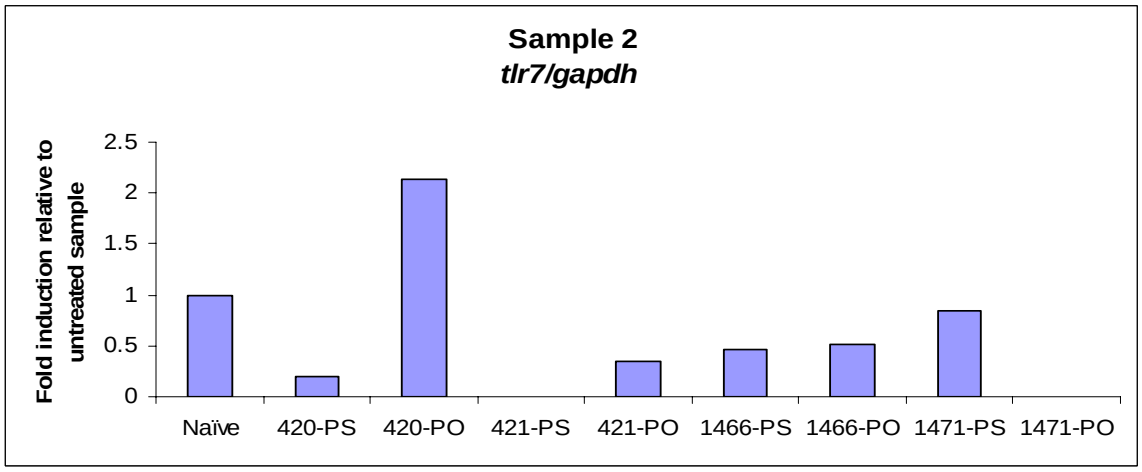
Sample 2
tlr7/gapdh
Fold induction relative to untreated sample
2.5
2
1.5
1
0.5
0
Naïve
420-PS
420-PO
421-PS
421-PO
1466-PS
1466-PO
1471-PS
1471-PO

E)

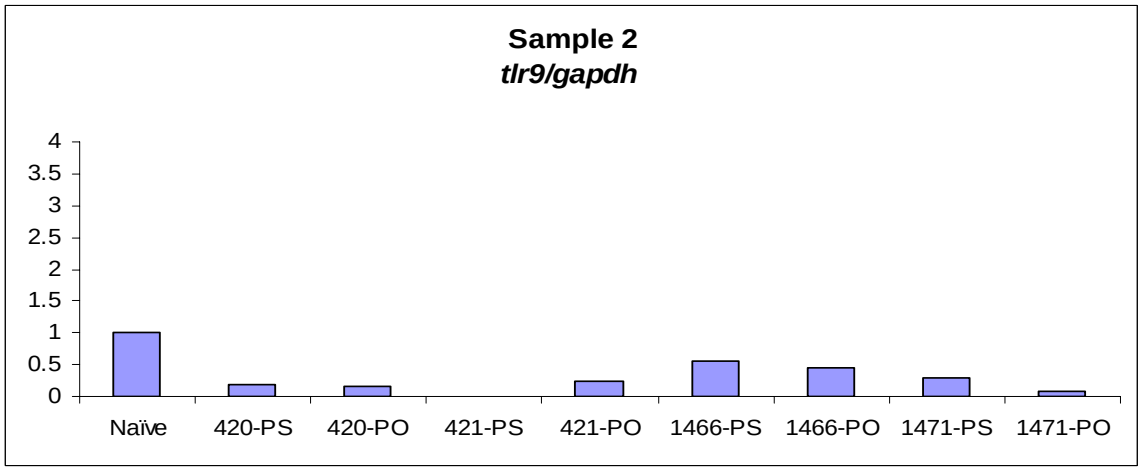
Sample 2
tlr9/gapdh
4
3.5
3
2.5
2
1.5
1
0.5
0
Naïve
420-PS
420-PO
421-PS
421-PO
1466-PS
1466-PO
1471-PS
1471-PO